

**Identification of Woodchuck Toll-like Receptors and Their Expression  
During the Course of Hepadnaviral Infection in the Woodchuck Model of  
Hepatitis B**

by

© John Bradley Williams

A thesis submitted to the School of Graduate Studies  
in partial fulfillment of the requirements for the  
degree of Master of Science in Medicine

Faculty of Medicine  
Memorial University of Newfoundland

May 2017

St. Johns

Newfoundland

## Abstract

The woodchuck hepatitis virus (WHV) is closely related to human hepatitis B virus (HBV), the prototypic member of the *Hepadnaviridae* family. Toll-like receptors (TLRs) may play an important role in the pathogenesis of hepadnaviral hepatitis, however, little is known about their expression during the course of hepadnaviral infection. In this study, woodchuck TLRs1-10 gene exon fragments were identified and their transcriptional profiles investigated in livers, hepatocytes isolated from these livers, and peripheral blood mononuclear cells (PBMCs) from healthy woodchucks and animals with different stages of experimental WHV infection. Overall expression analysis revealed that livers from woodchucks with acute hepatitis (AH) and chronic hepatitis (CH) had significantly upregulated expression of TLRs2-10 when compared to the livers of healthy animals and those with self-limited acute hepatitis (SLAH) and primary occult infection (POI). This was likely due to intrahepatic immune cell infiltration. In contrast, a significant downregulation of TLR3, TLR5, TLR7, TLR8, and TLR10 expression was identified in hepatocytes of woodchucks with CH when compared to hepatocytes from healthy animals and those with pre-acute hepatitis (PreAH), SLAH and POI. This may suggest WHV active suppression of the innate immune response in these cells. Upregulated transcription of the majority of TLRs was found in PBMCs during CH but not in other stages of infection. In summary, this study uncovered that TLR expression is significantly modulated depending on the stage of WHV infection and form of hepatitis. Treatments designed to restore hepatocyte TLR expression may allow for better control of the virus through activation of a stronger intrahepatocyte immune response during CH.

## **Acknowledgements**

During my Master's degree I have had the opportunity to work with many knowledgeable and supporting individuals. First and foremost, I would like to thank Dr. Thomas Michalak for providing me with the opportunity to pursue my graduate studies in his laboratory. His patience and guidance throughout my graduate degree has been nothing less than exceptional. I can honestly say that I am privileged to have had the opportunity to work under such a great scientific mentor.

I would also like to thank Dr. Patricia Mulrooney-Cousins for always being there. She has provided me with a support system that hasn't gone unnoticed. Whenever I have had a question about research, or life in general, she has always answered with honesty and positivity. I truly thank her for her friendship and mentorship during my time in the Michalak lab.

I would also like to thank my supervisory committee members Dr. Rodney Russell, Dr. Vernon Richardson, and Dr. Kensuke Hirasawa. They have provided me with guidance and encouragement during my Master's degree, and for that, I thank them.

Additionally, I would like to thank all the people who worked in the Michalak lab during my time there. Whenever I needed assistance they were there to lend a helping hand. My experiences in this laboratory have provided me with crucial knowledge that will assist me in my future endeavors.

I would also like to extend a big thank you to my family for their support throughout this program. Their encouragement and guidance was an important part of my success.

In closing, I would like to thank the Canadian Institute of Health Research for their generous support during this project. I would also like to thank the School of Graduate Studies at Memorial University for a student fellowship received.

## Table of Contents

Abstract .....	i
Acknowledgements .....	ii
List of Tables .....	viii
List of Figures .....	ix
List of Abbreviations .....	xi
List of Appendices .....	xiv
Chapter 1 – Introduction .....	15
1.1. Brief History of Studies on Hepatitis B Virus Identification .....	15
1.2. Epidemiology of HBV Infection .....	16
1.3. Hepatitis B Virus .....	17
1.3.1. Molecular Organization and Viral Proteins .....	17
1.3.2. HBV Replication Cycle .....	18
1.4. Categories of HBV Infection .....	19
1.5. Hepadnaviral Family .....	23
1.5.1. Duck Hepatitis B Virus .....	23
1.5.2. Ground Squirrel Hepatitis Virus .....	24
1.5.3. Woodchuck Model of HBV infection .....	24
1.5.3.1. Woodchuck Hepatitis Virus .....	24
1.5.3.2. Categories of WHV Infection .....	25
1.6. Immune System Organization .....	27
1.6.1. Innate Immunity .....	29
1.6.1.1. Cells of the Innate Immune System .....	29
1.6.1.2. Pattern Recognition Receptors (PRRs) .....	29
1.6.2. Adaptive Immunity .....	30
1.6.2.1. Humoral Immune Response .....	30
1.6.2.2. T Cell-Mediated Immune Response .....	31
1.7. Toll-like Receptors .....	32
1.7.1. Background .....	32
1.7.2. Structure and Cellular Localization .....	33
1.7.3. Ligand Recognition .....	34
1.7.3.1. Extracellular TLRs .....	34
1.7.3.1.1. TLR1, 2 and 6 .....	34
1.7.3.1.2. TLR4 .....	35
1.7.3.1.3. TLR5 .....	36
1.7.3.1.4. TLR10 .....	36
1.7.3.2. Intracellular TLRs .....	37

1.7.3.2.1. TLR3 .....	37
1.7.3.2.2. TLR7 and 8 .....	38
1.7.3.2.3. TLR9 .....	38
1.7.3.2.4. TLR11 and 12 .....	39
1.7.3.2.5. TLR13 .....	40
1.7.4. TLR Signaling .....	40
1.8. TLRs and Antiviral Immunity .....	41
1.8.1. TLRs and Hepadnaviruses .....	42
1.8.2. Targeting TLRs in HBV Antiviral Therapy .....	45
1.8.3. TLRs as Vaccine Adjuvants .....	46
1.9. TLRs and the Woodchuck Model of HBV Infection .....	48
1.10. Objectives .....	49
Chapter 2 - Methods and Materials .....	51
2.1. Collection of Woodchuck Tissue Samples .....	51
2.1.1. Liver Biopsies .....	51
2.1.2. Autopsy Liver and Spleen Tissues .....	51
2.1.3. Preparation of Primary Hepatocytes and PBMCs .....	52
2.2. RNA Extraction .....	52
2.2.1. DNase Treatment of RNA .....	53
2.2.2. RNA Concentration, Purity, and Integrity Assessment .....	53
2.3. Reverse Transcription (RT) of RNA .....	55
2.4. Sense and Anti-Sense Primer Design for Detection of Woodchuck TLRs .....	55
2.5. End-Point PCR Conditions for Initial Amplification of Woodchuck TLRs .....	56
2.5.1. Agarose Gel Electrophoresis .....	58
2.6. Plasmid Construction .....	58
2.6.1. DNA Purification from Agarose Gel .....	58
2.6.2. Cloning of Purified TLR DNA Fragments .....	59
2.6.3. Mini-scale Preparations of Plasmid DNA .....	59
2.6.4. Restriction Enzyme Digestion of Miniprep .....	60
2.6.5. Automated DNA Sequencing .....	60
2.6.6. Maxi-scale Preparation of Plasmid DNA .....	61
2.7. Real-Time RT-qPCR for Quantification of Woodchuck TLRs .....	62
2.7.1. Primer Optimization .....	62
2.7.2. Determination of Sensitivity of Detection .....	63
2.7.3. Absolute Quantification .....	63
2.8. Real Time RT-qPCR for Quantification of Expression of Individual Woodchuck TLRs .....	65
2.8.1. Plate Layout and Controls .....	65
2.9. Multiplex Real-Time RT-qPCR for Simultaneous Quantification of Woodchuck TLRs1-10 .....	68

2.9.1. Plate Layout and Controls .....	68
2.10. Animals and Categories of WHV Infection .....	71
2.10.1. Categories of WHV Infection .....	71
2.10.2. Animals and Samples Examined .....	72
2.11. Calculation of Relative Expression.....	74
2.12. Statistical analyses.....	74
Chapter 3 - Results .....	75
3.1. General Study Design .....	75
3.2. Woodchuck TLR1-10 Gene Fragment Identification and Their Sequence Confirmation .....	76
3.3. Optimization of Real-time RT-qPCR Conditions for Absolute Quantification of Woodchuck TLRs1-10.....	108
3.3.1. Primer Specificity .....	108
3.3.2. Quantification Standard Curve Optimization.....	115
3.4. Housekeeping Gene Expression Profiles in Liver, Hepatocytes and PBMCs from Healthy and WHV-Infected Woodchucks .....	116
3.5. TLR Expression Levels in Normal Woodchuck Livers, Hepatocytes and PBMCs .....	119
3.6. Transcription of Individual TLRs in Livers and Hepatocytes Isolated from These Livers of Healthy Woodchucks and Animals with Different Stages of WHV Infection .....	119
3.7. Expression Profiles of TLRs1-10 in Sequential Liver Biopsies Obtained Prior to and During WHV Infection.....	125
3.8. Expression of TLRs1-10 in Sequential PBMC Samples of Healthy Animals and Those with Different Stages of Experimental WHV Infection .....	129
Chapter 4 - Discussion .....	132
4.1. Summary of Findings .....	132
4.2. Timeline of Woodchuck TLRs1-10 Identification.....	133
4.3. Woodchuck TLR1-10 mRNA Protein Coding Sequence Compatibility with Human TLRs1-10 .....	134
4.4. Amplification Techniques Utilized in This Study.....	135
4.5. TLRs1-10 Expression Profiles in Normal Woodchuck Livers and Isolated Hepatocytes Were Comparable, While PBMCs Displayed Different Patterns of TLRs1-10 Expression than in Hepatic Tissue.....	137
4.6. There Are Significant Differences in TLR Expression Profiles in the Liver and Isolated Hepatocytes During the Course of WHV Infection .....	138
4.7. Selective TLRs are Upregulated in PBMCs Isolated from Woodchucks with CH .....	142
Chapter 5 – Conclusions and Significance.....	145

5.1. Summary and Conclusions .....	145
5.1.1. Comments .....	148
5.2. Significance of Findings .....	149
Chapter 6 – Future Directions .....	150
References Cited.....	151
Appendices.....	167

## List of Tables

Table 2.1. Oligonucleotide Primer Sequences and PCR Conditions Used for Initial Amplification of Woodchuck TLRs1-10 .....	57
Table 2.2. Woodchuck TLR-Specific and Housekeeping Primer Sequences Used for Expression Analysis of Woodchuck TLRs1-10 by Real-Time RT-qPCR .....	64
Table 2.3. Woodchuck Samples from Different Categories of WHV Infection Used in This Study .....	73

## List of Figures

Figure 2.1. Plate layout for RT-qPCR quantification of individual TLRs in woodchuck samples. ....	66
Figure 2.2. Plate layout for multiplex RT-qPCR quantification of woodchuck TLRs1-10. ....	69
Figure 3.1. Initial PCR amplification of woodchuck-specific TLR1, analysis of minipreps of TLR1 plasmid DNA, and sequence confirmation. ....	77
Figure 3.2. Initial PCR amplification of woodchuck-specific TLR2, analysis of minipreps of TLR2 plasmid DNA, and sequence confirmation. ....	80
Figure 3.3. Initial PCR amplification of woodchuck-specific TLR3, analysis of minipreps of TLR3 plasmid DNA, and sequence confirmation. ....	83
Figure 3.4. Initial PCR amplification of woodchuck-specific TLR4, analysis of minipreps of TLR4 plasmid DNA, and sequence confirmation. ....	86
Figure 3.5. Initial PCR amplification of woodchuck-specific TLR5, analysis of minipreps of TLR5 plasmid DNA, and sequence confirmation. ....	89
Figure 3.6. Initial PCR amplification of woodchuck-specific TLR6, analysis of minipreps of TLR6 plasmid DNA, and sequence confirmation. ....	92
Figure 3.7. Initial PCR amplification of woodchuck-specific TLR7, analysis of minipreps of TLR7 plasmid DNA, and sequence confirmation. ....	95
Figure 3.8. Initial PCR amplification of woodchuck-specific TLR8, analysis of minipreps of TLR8 plasmid DNA, and sequence confirmation. ....	98
Figure 3.9. Initial PCR amplification of woodchuck-specific TLR9, analysis of minipreps of TLR9 plasmid DNA, and sequence confirmation. ....	101
Figure 3.10. Initial PCR amplification of woodchuck-specific TLR10, analysis of minipreps of TLR10 plasmid DNA, and sequence confirmation. ....	104
Figure 3.11. An example of real-time RT-qPCR optimization and determination of the assay sensitivity for detection of woodchuck TLR4. ....	109

Figure 3.12. An example of real-time RT-qPCR optimization and determination of the assay sensitivity for detection of woodchuck TLR10. .... 112

Figure 3.13. HPRT is a more reliable housekeeping gene than  $\beta$ -actin when comparing gene expression in woodchuck livers and hepatocytes derived from these livers. 117

Figure 3.14. Baseline expression levels of TLRs1-10 in healthy woodchuck livers, hepatocytes and PBMCs. .... 120

Figure 3.15. TLRs1-10 expression profiles in livers and hepatocytes purified from these livers from healthy and WHV-infected woodchucks..... 123

Figure 3.16. Transcription levels of TLRs1-10 in sequential liver biopsy samples collected from woodchucks with different forms of WHV infection. .... 126

Figure 3.17. Profiles of TLRs1-10 expression in sequential PBMC Samples isolated from healthy woodchucks and those with different forms of WHV infection. .... 130

## List of Abbreviations

AFL	Acute liver failure
AH	Acute hepatitis
ALT	Alanine aminotransferase
Anti-HBc	Antibodies to hepatitis B virus core antigen
Anti-HBe	Antibodies to hepatitis B virus e antigen
Anti-HBs	Antibodies to hepatitis B virus surface antigen
Anti-WHc	Antibodies to woodchuck hepatitis virus core antigen
Anti-WHs	Antibodies to woodchuck hepatitis virus surface antigen
AP1	Activator protein 1
APC	Antigen presenting cell
ASGPR	Asialoglycoprotein receptor
ASHV	Artic squirrel hepatitis virus
AST	Aspartate aminotransferase
AT	Adenine-thymine nucleotides
BCR	B cell receptors
BHBV	Bat hepatitis B virus
BLAST	Basic local alignment search tool
bp	Base pair
cccDNA	Covalently closed circular deoxyribonucleic acid
CD	Cluster of differentiation
CD21	Cluster of differentiation molecule 21
cDNA	Complimentary deoxyribonucleic acid
CH	Chronic hepatitis
CHB	Chronic hepatitis B
CLR	C-type lectin receptor
CpG	Cytosine-phosphate-guanine motif
CREB	Cyclic AMP-responsive element binding protein
CTL	Cytotoxic T lymphocyte
DC	Dendritic cell
ddd	Double-distilled, deionized
DEPC	Diethyl pyrocarbonate
DHBV	Duck hepatitis B virus
DMSO	Dimethyl sulfoxide
dNTP	Deoxynucleotide triphosphate
dpi	Days post-infection
DTT	Dithiothreitol
EB	Ethidium bromide
ESCRT	Endosomal sorting complexes required for transport
ETV	Entecavir
FCS	Fetal calf serum
GC	Guanine-cytosine nucleotides
GSHV	Ground squirrel hepatitis virus
GTE	Glucose-Tris-ethylenediaminetetraacetic acid
HBcAg	Hepatitis B core antigen

HBeAg	Hepatitis B e antigen
HBsAg	Hepatitis B surface antigen
HBV	Hepatitis B virus
HBx	Hepatitis B X protein
HCC	Hepatocellular carcinoma
HHBV	Heron hepatitis B virus
HIV	Human immunodeficiency virus
HPRT	Hypoxanthine-guanine phosphoribosyltransferase
HSP	Heat shock protein
HSV	Herpes simplex virus
IC	Internal control
IFN	Interferon
IFN- $\alpha$	Interferon alpha
IFN- $\beta$	Interferon beta
IFN- $\gamma$	Interferon gamma
IFN- $\lambda$	Interferon lambda
IL-1R	Interleukin 1 receptor
IRAK	Interleukin 1 receptor-associated kinase
IRF	Interferon regulatory factor
ISS	Immunostimulatory sequence
JNK	JUN N-terminal kinase
Kb	Kilobase
LB	Luria-Bertani medium
LBP	Lipopolysaccharide binding protein
LMP	Low-melting point
LPS	Lipopolysaccharides
LRR	Leucine-rich repeat
LTA	Lipoteichoic acid
M-MLV	Moloney murine leukemia virus
MAL/TIRAP	MyD88-adaptor like/TIR-associated protein
MAPK	Mitogen-associated protein kinase
MCMV	Murine cytomegalovirus
MD-2	Lymphocyte antigen 96
MHC	Major histocompatibility complex
MPLA	Monophosphoryl lipid A
mRNA	Messenger RNA
MyD88	Myeloid differentiation primary response protein (88)
NaOH	Sodium hydroxide
NCBI	National Center for Biotechnology Information
NF- $\kappa$ B	Nuclear factor kappa-light-chain-enhancer activated B cells
NK	Natural killer cell
NKT	Natural killer T cell
NLR	NOD-like receptor
NTC	No template control
NTCP	Sodium taurocholate cotransporting polypeptide
OBI	Occult hepatitis B virus infection

ODN	Oligonucleotide
ORF	Open reading frame
PAMP	Pathogen-associated molecular patterns
PBMC	Peripheral blood mononuclear cells
PCR	Polymerase chain reaction
PD-1	Programmed cell death protein 1
PD-L1	Programmed cell death ligand 1
pDC	Plasmacytoid dendritic cell
pg	Pregenomic
POI	Primary occult infection
poly (I:C)	Polyinosinic-polycytidylic acid
PreAH	Pre-acute hepatitis
PRR	Pattern recognition receptor
PWH	Primary woodchuck hepatocyte
RC	Relaxed circular
RIN	RNA integrity number
RLR	RIG-I-like receptor
RNA	Ribonucleic acid
rpm	Revolutions per minute
rRNA	Ribosomal RNA
RT	Reverse transcription
RT-PCR	Reverse transcription polymerase chain reaction
RT-qPCR	Quantitative reverse transcription polymerase chain reaction
SDH	Sorbitol dehydrogenase
SDS	Sodium dodecyl sulfate
SLAH	Self-limited acute hepatitis
SOC	Super optimal broth with catabolite repression
SOI	Secondary occult infection
TAE	Tris-acetate-ethylenediaminetetraacetic acid
TE	Tris-ethylenediaminetetraacetic acid
T <sub>h</sub>	T helper cell
TIR	Toll-interleukin 1 receptor
TLR	Toll-like receptor
TNF	Tumor necrosis factor
TNF- $\alpha$	Tumor necrosis factor alpha
TRAF	Tumor necrosis factor receptor-associated factor
TRAM	Toll-receptor-associated molecule
TRIF	Toll-receptor-associated activator of interferon
VSV	Vesicular stomatitis virus
WHcAg	Woodchuck hepatitis virus core antigen
WHeAg	Woodchuck hepatitis virus e antigen
WHO	World Health Organization
WHsAg	Woodchuck hepatitis virus surface antigen
WHV	Woodchuck hepatitis virus
WMHBV	Woolly monkey hepatitis B virus
$\beta$ -Actin	Beta-actin

## List of Appendices

Figure A1. Expression levels of TLRs1-10 in sequential liver biopsy samples and PBMCs during the course of hepadnaviral infection in woodchuck #1 that progressed from acute hepatitis (AH) to chronic hepatitis (CH). .....	167
Figure A2. Expression levels of TLRs1-10 in sequential liver biopsy samples and PBMCs during the course of hepadnaviral infection in woodchuck #2 that progressed from acute hepatitis (AH) to chronic hepatitis (CH). .....	170
Table A1. GenBank Accession Numbers of Woodchuck TLR1-10 Partial Gene Sequences Identified in This Study .....	173
Table A2. Copy Number Values for the Housekeeping Gene HPRT and TLRs1-10 in Woodchuck Livers Investigated in This Study .....	174
Table A3. Copy Number Values for the Housekeeping Gene HPRT and TLRs1-10 in Woodchuck Hepatocytes Investigated in This Study .....	175
Table A4. Copy Number Values for the Housekeeping Gene HPRT and TLRs1-10 in Woodchuck PBMCs Investigated in This Study.....	176

## Chapter 1 – Introduction

### 1.1. Brief History of Studies on Hepatitis B Virus Identification

Virus-induced hepatitis is an inflammatory liver disease caused by DNA or RNA viruses that have a specific affinity for the liver, also known as hepatotropic viruses. The hepatitis B virus (HBV) is the largest causative agent of viral hepatitis in the world and is characterized by both its hepatotropic and lymphotropic nature. In the 1940's, the name "hepatitis B" was first introduced in order to categorize an infectious liver disease that was mainly transmitted by exposure to contaminated blood (MacCallum, 1946). It was not until 1965 when Dr. Baruch Blumberg discovered HBV envelope lipoprotein, then named the Australian antigen, in the blood of an Australian aboriginal (Blumberg *et al.*, 1965). Following further research, it was determined that the Australian antigen, now referred to as the hepatitis B surface antigen (HBsAg), was indicative of active HBV infection. In the 1970's, Dr. David Dane discovered viral particles with a diameter of 42-nm, known as Dane particles, that were eventually identified to be HBV virions (Dane *et al.*, 1970). Since the identification of HBsAg and the HBV virion, subsequent immunological and molecular analysis has led to the identification of HBV associated proteins and the sequencing of the entire HBV genome. Vaccine development began with Dr. Blumberg's early work, however, it was not until 1986 that a yeast-derived HBsAg vaccine became the standard vaccine against HBV (Gerlich, 2013). Currently, several recombinant HBV vaccines containing the major protein of HBsAg, named the S (small) protein, are available to generate protection against HBV (Lavanchy, 2012).

## 1.2. Epidemiology of HBV Infection

According to the World Health Organization (WHO), an estimated 240 million people worldwide are affected by chronic, serum HBsAg-positive, hepatitis B (CHB) and approximately one million persons die each year due to complications caused by HBV infection (World Health Organization, 2016). It is estimated that another 2 billion people may have occult HBV infection without showing any clinical symptoms. Furthermore, prophylactic vaccines that are available do not inhibit transmission of HBV from infected mothers to their babies, which is currently the main route of virus spread. In consequence, severe liver cirrhosis and liver cancer, called primary hepatocellular carcinoma (HCC), caused by the virus will remain a significant health problem for many decades to come. The rate of HBV infection varies depending on geographical region and is generally highest in developing countries. These countries are suffering from political and socio-economic problems that make it difficult to manage the prevention and treatment of the disease (Zampino *et al.*, 2015). HBV is highly endemic in regions such as South East Asia, China, sub-Saharan Africa, the Amazon Basin, and Northern Canada, where an estimated 8% of the population are chronic HBsAg-positive carriers (Hou *et al.*, 2005). In these areas, HBV is most commonly acquired during childhood, either through perinatal transmission (mother to child) or through horizontal transmission (individual to individual). Intermediate rates of endemicity are found in areas such as Eastern and Southern Europe, the Middle East, Japan and South America. It is estimated that 2-7% of individuals in these areas are chronically infected. In developed areas of the world, including North America, Northern and Western Europe and Australia, less than 1% of the population have CHB. The number of

countries that included HBV immunization in their national vaccination schedule has constantly increased since the WHO's recommendations in 1992 (Schweitzer *et al.*, 2015). However, immunization and proper disease management are still lacking in many countries, therefore, chronic HBV infection remains a very serious health problem in many regions of the world.

### **1.3. Hepatitis B Virus**

#### **1.3.1. Molecular Organization and Viral Proteins**

HBV is the prototypic member of the *Hepadnaviridae* family. Hepadnaviruses have small genomes formed by partially double-stranded and partially single-stranded DNA, referred to as relaxed circular (RC) DNA. HBV has a circular genome that is 3.2 kilobases (Kb) in length, consisting of a full length minus strand DNA and an incomplete plus strand DNA. The minus strand contains the entire coding information for the virus and its circularity is maintained by short cohesive overlapping regions at the 5'-ends of the plus and minus strands. The HBV genome is organized into four open reading frames (ORFs). These include the envelope or surface (S), core (C), polymerase (P), and X ORFs (Locarnini and Zoulim, 2010). In total, the HBV genome codes for 7 proteins, including pre-core, core, polymerase, X (HBx) and three surface or envelope proteins. The S ORF codes for the three envelope proteins, the large (preS1), the middle (preS2) and the small (S). They share a common C-terminus but differ at the N-terminus. All three proteins are glycosylated, type II transmembrane proteins that make up the components of the 22-nm-diameter noninfectious particles, also known as HBsAg (Seeger and Mason, 2000). The C ORF encodes the viral capsid protein, also

referred to as nucleocapsid or hepatitis B core antigen (HBcAg). In addition to HBcAg, the C ORF encodes the pre-core protein. The pre-core protein is essentially the core protein with an N-terminal signal peptide that gets proteolytically processed and secreted from infected cells. The secreted protein is known as hepatitis B e antigen (HBeAg) and its role has not yet been clearly elucidated (Seeger and Mason, 2015). The P ORF codes for virus polymerase and comprises nearly 80% of the hepadnaviral genome. The enzyme exhibits both DNA polymerase and RNA polymerase (reverse transcriptase) activity, and is critical to the replication of the HBV genome through a pregenomic (pg) RNA template. Lastly, the X ORF encodes the HBx protein and its role in the viral infection lifecycle is not well determined. It has been shown to regulate viral replication, as well as numerous host cellular processes, through transcriptional activation of both viral and host genes. It has also been implicated in the development of HCC (Tang *et al.*, 2006).

### **1.3.2. HBV Replication Cycle**

The first stage of HBV infection begins with attachment of the viral particle to its target cell. The specific receptor responsible for viral attachment and entry has recently been identified as sodium taurocholate cotransporting polypeptide (NTCP) (Yan *et al.*, 2012). Studies have shown that the preS1 domain of the HBV envelope is required for initiation of infection and it specifically binds to the NTCP receptor (Yan *et al.*, 2014; Slijepcevic *et al.*, 2015; Sankhyan *et al.*, 2016). After attachment, the viral envelope is shed and the core particle containing virus genome material is actively transported to the nucleus. In the nucleus, the genomic RC DNA is released from the nucleocapsid of

the virus and converted to covalently closed circular DNA (cccDNA) by the host's DNA cellular repair enzymes. The detection of cccDNA provides definitive proof of HBV replication. From the cccDNA, the cell's RNA polymerase II generates pgRNA from which core protein and DNA polymerase are translated (Gerlich, 2013). The pgRNA is then packaged within the core proteins of the virus, along with DNA polymerase, where it serves as the transcriptional template for the minus-strand DNA. The plus-strand DNA is then transcribed from the minus-strand, followed by simultaneous degradation of the pgRNA. Once the RC DNA is produced, the mature nucleocapsid particles can follow two pathways. They can re-enter the nucleus and contribute to another round of replication or be packaged into virions and released from the cell. Similar to other enveloped viruses, HBV uses the cellular endosomal sorting complexes required for transport (ESCRT) to release virions from the infected cell (Blondot *et al.*, 2016).

#### **1.4. Categories of HBV Infection**

HBV causes acute and chronic liver disease, liver cirrhosis, as well as HCC. More specifically, HBV is a non-cytopathic virus that causes tissue damage by inducing virus-specific immune responses. Due to infection, hepatocytes present viral epitopes complexed with major histocompatibility complex (MHC) class I molecules on their plasma membrane. This complex is recognized by cytotoxic T lymphocytes (CTLs) that target the cells for destruction. The clinical course of HBV infection varies between individuals and can lead to a wide spectrum of liver disease. Generally, infection with HBV can be divided in several categories, including acute hepatitis (AH), fulminant hepatitis, chronic hepatitis (CH), and occult HBV infection (OBI).

AH type B is usually diagnosed in patients anywhere from 1-6 months following exposure to the virus. AH is defined by the appearance of HBsAg in the serum. About 70% of patients with AH do not have clinical symptoms and the infection can go undetected (Liang, 2009). About 30% of adults with AH develop clinical symptoms that can range from mild fever, anorexia and nausea to more severe symptoms, including jaundice. Fulminant hepatitis, also known as acute liver failure (AFL), occurs in less than 1% of patients and is characterized by severe liver injury with necrosis, loss of liver function, and frequent death (Gotthardt *et al.*, 2007). Eventually, individuals with AH will clear HBsAg within 6 months from its appearance and develop antibodies to HBsAg (anti-HBs). AH diagnosis can be supported by the presence of other HBV serological markers, such as HBeAg, antibodies to HBcAg (anti-HBc) and HBeAg (anti-HBe), molecular markers (HBV DNA) and the increase in liver enzymes (*i.e.*, alanine aminotransferase [ALT] and aspartate aminotransferase [AST]). Persistence of HBsAg in circulation for longer than 6 months is recognized as a marker of the development of CHB.

Early CHB is characterized by the serological presence of serum HBsAg, HBeAg, anti-HBc antibodies and HBV DNA, along with the detection of HBV DNA, mRNA, and cccDNA in liver tissue that are indicative of active viral replication. Around 5-10% of adults who become infected with HBV will develop CHB, while the remaining individuals will resolve the infection and establish life-long, usually asymptomatic OBI that can be reactivated when the patient becomes immunocompromised. In contrast, about 90% of neonates who acquire HBV by perinatal transfer (transmission from mother to child) will develop CHB (Schillie *et al.*, 2015). In both situations, the immunological profile of CHB

can be categorized into three phases: immune tolerant, immune active and immune inactive.

Immune tolerant CHB occurs almost exclusively in neonates who acquire the infection at birth from their HBV-infected mothers. This phase of CHB is characterized by the presence of HBeAg, normal liver aminotransferases, high levels of serum HBV DNA (>100,000 copies/mL) and minimal to absent liver inflammation (McMahon, 2008). The immune tolerant phase can last for up to 30 years with little disease progression due to the absence of a CTL response (Hui *et al.*, 2007). However, following the immune tolerant phase, almost all individuals will enter the immune active phase during early adolescence or young adulthood. As previously indicated, about 5-10% of individuals who become infected as an adult will develop CHB and will experience the immune active phase in the early stages of CHB.

The immune active phase of CHB is characterized by the presence of HBeAg and HBV DNA (>10,000 copies/mL) in the serum, an increase in serum ALT levels, and histologically evident active liver inflammation (McMahon, 2008). Individuals will remain HBeAg-positive or can seroconvert to the HBeAg-negative stage with subsequent development of anti-HBe antibodies. In any case, these individuals are at highest risk of liver disease complications, such as cirrhosis and development of HCC. Following immune active CHB, some individuals can enter the immune inactive stage. This is defined by a reduction in HBV DNA (<10,000 copies/mL), normal serum ALT, and a decline of active liver disease (McMahon, 2008). However, reactivation can occur spontaneously and HBV infection in all phases should be monitored closely. Over time,

CHB can lead to liver fibrosis and cirrhosis, and the risk of HCC is 100-times greater than in healthy individuals (Busch and Thimme, 2015).

More recently, another category of HBV infection has been identified in which HBsAg is apparently cleared from the individual, however, the HBV genome and low level replication are still detectable. OBI is characterized by undetectable serum HBsAg by current clinical assays, while HBV DNA persists at the level of <100-200 copies/mL in the liver and/or lymphatic tissue (Michalak *et al.*, 1994; Michalak, 2000). Resolution of AH and the appearance of anti-HBs was thought to signify clearance of the virus, however, this is not the case (Raimondo *et al.*, 2008a; Raimondo *et al.*, 2008b). This was also clearly documented in the woodchuck model of hepatitis B (Michalak *et al.*, 1999). Furthermore, perinatal transmission of infectious hepadnavirus was demonstrated in offspring born to woodchuck mothers that had resolved AH (Coffin and Michalak, 1999). In humans, the mechanisms of OBI infection are not completely understood. More recently, HBV DNA and HBsAg detection techniques have become more sensitive, allowing for more reliable diagnosis of OBI. In the woodchuck model of HBV infection, it has been shown that OBI is accompanied by intermittent liver inflammation and may lead to the development of HCC. Two distinct forms of OBI have been documented to occur in woodchucks and humans (*i.e.*, secondary [SOI] and primary occult infection [POI]) (Michalak *et al.*, 2004; Zerbini *et al.*, 2008; Mulrooney-Cousins *et al.*, 2014).

## 1.5. Hepadnaviral Family

The hepadnaviral family is subdivided into two genera: *Orthohepadnaviridae* (mammalian viruses) and *Avihepadnaviridae* (avian viruses). All viruses from this family share unique structural, molecular and biological features. All hepadnaviruses have virions that are between 40-48-nm in diameter, and are spherical in shape. The genomes of these viruses are composed of partially double-stranded RC DNA that can range from 3.0-3.3 Kb in length. Replication strategies are similar, involving polymerase and reverse transcriptase activity, along with the excess production of subviral particles exclusively composed of envelope proteins and lipids (Dandri *et al.*, 2005).

Since the discovery of HBV, there have been several hepadnaviral infections identified in both avian and mammalian hosts. These include the woodchuck hepatitis virus (WHV), ground squirrel hepatitis virus (GSHV), arctic squirrel hepatitis virus (ASHV), duck hepatitis B virus (DHBV), heron hepatitis B virus (HHBV), woolly monkey hepatitis B virus (WMHBV) and more recently the bat hepatitis B virus (BHBV). WHV and DHBV have been the most extensively investigated in their respective hosts.

### 1.5.1. Duck Hepatitis B Virus

DHBV is a prototypic member of the avian hepadnaviral family. Although the DHBV has been proven to be a useful animal model for HBV infection, there are major differences between avian hepadnaviruses when compared to their mammalian counterpart. Firstly, avian viral genomes are smaller than mammalian viral genomes and share less nucleotide sequence homology with HBV. The DHBV genome lacks the

X ORF and only encodes two envelope proteins, instead of three (Dandri *et al.*, 2005). In the past, studies that have utilized the DHBV have helped to elucidate the mechanisms of hepadnaviral replication. However, DHBV is not a good model of liver inflammation and HCC, as infection usually results in a very mild liver pathology and HCC develops in the context of exposure to aflatoxins (Cova *et al.*, 1993).

### **1.5.2. Ground Squirrel Hepatitis Virus**

GSHV is a mammalian member of the hepadnaviral family. GSHV was the second HBV-related virus discovered in non-primate animals and was originally identified in the Beechy ground squirrel in 1979. Its virion is 47-nm in diameter, which is slightly larger than that of HBV (Marion *et al.*, 1980). GSHV was mainly used to elucidate the mechanism of hepadnaviral replication and was found to cause hepatitis and HCC (Minuk *et al.*, 1986; Enders *et al.*, 1987). Interestingly, GSHV is infectious to woodchucks and can eventually lead to HCC in some animals. Nevertheless, HCC development, when compared to WHV-infected woodchucks, is much slower in GSHV-infected woodchucks (Seeger *et al.*, 1991).

### **1.5.3. Woodchuck Model of HBV infection**

#### **1.5.3.1. Woodchuck Hepatitis Virus**

WHV was first discovered in a colony of woodchucks (*Marmota monax*) that exhibited hepatitis and HCC at the Philadelphia Zoological Garden (Summers *et al.*, 1978). Since its discovery, studies have shown that WHV has significant molecular and pathogenic similarities to HBV. With time it became apparent that woodchucks infected

with WHV represent the closest natural model of human HBV infection. Both HBV and WHV genome size is almost identical (~3.2 Kb and ~3.3 Kb in length, respectively), while their nucleotide sequence homology is anywhere from 62% to 72% (Mulrooney-Cousins and Michalak, 2015). This high homology translates to a high degree of antigenic cross-reactivity between HBV and WHV envelope and core proteins. Like HBV, the WHV virion, at 45-nm in diameter, consists of an exterior envelope protein (WHV surface antigen [WHsAg]) and an inner nucleocapsid (WHV core antigen [WHcAg]) containing the WHV genome. Furthermore, replication strategy, viral proteins and tropism towards hepatocytes and immune cells are almost identical to HBV (Menne and Cote, 2007; Mulrooney-Cousins and Michalak, 2015).

#### **1.5.3.2. Categories of WHV Infection**

Progression and outcomes of WHV infection in woodchucks are very similar to HBV infection in humans. In both infections, liver involvement begins with AH and can advance to CH and eventually HCC. Excluding the apparent lack of liver cirrhosis in woodchucks, histological features of liver inflammation are comparable to HBV infection (Hodgson and Michalak, 2001). Following exposure to WHV, the AH stage of infection normally becomes evident with the detection of WHsAg in the serum and liver injury through detection of biochemical indicators (*i.e.*, sorbitol dehydrogenase [SDH] and ALT). Undetectable WHsAg prior to 6 months post-infection denotes spontaneously resolution of AH and the animal is designated to have self-limited acute hepatitis (SLAH). Approximately 90% of adult woodchucks will resolve AH, however, residual amounts of replicating WHV remains detectable in the liver and the lymphatic system to

the end of life (Michalak *et al.*, 1999; Menne and Cote, 2007). Even with resolution of hepatitis, these woodchucks still have a lifetime risk of about 20% for the development of HCC. If WHsAg persists in circulation for longer than 6 months, CH is diagnosed. Comparable to humans, CH infection occurs in about 5-10% of woodchucks who acquire the infection as an adult, while roughly 60-75% of woodchucks with perinatally acquired WHV infection progress to chronicity (Cote *et al.*, 2000). A major difference between HBV and WHV CH is that the development of HCC in woodchucks occurs at much higher rate (80%-90%) than in humans with CH type B (~5%)(Popper *et al.*, 1981; Korba *et al.*, 1989; Mulrooney-Cousins and Michalak, 2015). Due to the development of highly sensitive nucleic acid detection assays, occult WHV infection is being recognized for its involvement in the development of cryptogenic HCC (Mulrooney-Cousins *et al.*, 2014; Mulrooney-Cousins and Michalak, 2015).

The presence of HBV DNA or WHV DNA with the absence of identifiable HBsAg or WHsAg, is defined as an occult infection. Two forms of occult infection have been identified in WHV-infected woodchucks, SOI and POI. First to be identified, SOI is characterized by low levels of WHV DNA, the presence of antibodies against WHV core antigen (anti-WHc), and residual liver inflammation after resolution of AH (Michalak *et al.*, 1999). Furthermore, animals with SOI have detectable WHV DNA in their lymphatic system which may contribute to the lifelong maintenance of the virus. It has been demonstrated that WHV is transmissible from SOI mothers to their offspring without evident serological markers of infection but detectable WHV DNA in both serum and lymphatic system (Coffin and Michalak, 1999). This observation provoked further studies investigating the transmission of low level WHV-infection. It was found that

WHV from these offspring could be serially transmitted between adult immunocompetent hosts and induce serologically silent but molecularly evident, asymptomatic infection, referred to as POI (Michalak *et al.*, 2004). Additionally, animals experimentally infected with WHV doses of less than 1000 virions develop POI. POI is characterized by the absence of classical serological markers of WHV infection, such as serum WHsAg, anti-WHc and anti-WHs antibodies, however, viral DNA is detectable in the plasma and the immune system. Over time, POI can spread to the liver without induction of hepatitis, but HCC develops in about 20% of the animals (Mulrooney-Cousins and Michalak, 2007; Mulrooney-Cousins and Michalak, 2015). The woodchuck model of OBI can be used to advance our understanding of occult infection in humans, including mechanisms of reactivation of asymptomatic infection, clinically unapparent viral transmission, and its potential role in the development of cryptogenic HCC.

## **1.6. Immune System Organization**

The mammalian immune system is made up of a network of cells, tissues and organs that work in concert to protect against invading pathogens through recognition of self and non-self. To elicit a response to a foreign agent, the body has evolved several mechanisms to evade or destroy the potentially harmful pathogen. The first line of defense in mammals is a non-specific immune response, referred to as innate immunity. The innate immune system includes all anatomical barriers, as well as certain cells and soluble factors that are strategically located in the body. Infection of host cells leads to the initiation of the innate immune responses, resulting in the induction and expression of type I interferons (IFNs) (*i.e.*, IFN- $\alpha$  and IFN- $\beta$ ), type III IFNs (*i.e.*, IFN- $\lambda$ ) and pro-

inflammatory cytokines (Ank *et al.*, 2008; Bowie and Unterholzner, 2008; Egli *et al.*, 2014). Upon recognition of a pathogen, the innate immune response is nonspecific and generalized. In the event that the infectious agent persists, the body has evolved a more specific immune response that is tailored towards a particular antigen, known as adaptive immunity.

The adaptive side of the immune response relies on antigen-specific receptors expressed by lymphocytes, T and B cells, that are capable of recognizing and selectively eliminating pathogens. Generally speaking, T lymphocytes are involved in pathogen elimination through direct binding and cytokine secretion, while B lymphocytes rely on the production of antigen-specific neutralizing antibodies. These cells possess membrane bound and soluble proteins that have high specificity towards antigenic sites on foreign microorganisms and molecules. The adaptive immune system is able to recognize millions of antigens and is highly specific due to the rearrangement of immunoglobulin and T cell receptor genes that produce an immense number of antigen-specific receptor combinations. Unlike the innate immune system, which relies primarily on phagocytic cells and antigen presenting cells (APCs), the adaptive immune response relies on clonal gene rearrangement to form a large repertoire of antigen-specific T and B cells (Mogensen, 2009). Historically, management of the adaptive immune response was the focus of treatments for infectious diseases and cancers. However, the therapeutic importance of innate immunity has been recently recognized in the context of several infection models.

## **1.6.1. Innate Immunity**

### **1.6.1.1. Cells of the Innate Immune System**

Innate immune cell subsets include dendritic cells (DCs), monocytes/macrophages, granulocytes (neutrophils, eosinophils, basophils), mast cells, natural killer (NK) and natural killer T (NKT) cells. Each cell type possesses unique receptors that are able to detect and initiate downstream signaling which may mediate further innate immune responses or help activate the adaptive immune system. Furthermore, innate immune cells release soluble molecules, such as complement, antimicrobial peptides and cytokines that detect and initiate immune clearance through phagocytosis, apoptosis or necrosis (Kumar *et al.*, 2013).

### **1.6.1.2. Pattern Recognition Receptors (PRRs)**

The first step in the initiation of the innate immune response against microbial pathogens involves sensing of pathogen-associated molecular patterns (PAMPs) through use of PRRs that are expressed on the plasma membrane and in the cytoplasm of innate immune cells. Recognition of a pathogen initiates a series of signaling events that results in the production of pro-inflammatory cytokines, including type I IFNs, chemokines and antimicrobial peptides. In addition to eliminating early infection, activation of PRRs and the release of IFNs help initiate the adaptive immune response by priming T helper ( $T_h$ ) cells and CTLs (Bowie and Unterholzner, 2008). PRRs have evolved to recognize a wide range of microbial PAMPs and are expressed by a variety of innate immune cells, such as granulocytes, monocytes/macrophages and DCs.

PRRs include Toll-like receptors (TLRs), NOD-like receptors (NLRs), RIG-I-like receptors (RLRs), and C-type lectin receptors (CLRs) (Owen *et al.*, 2013). PRRs can be classified based on their cellular localization as membrane-bound or intracellular. Membrane-bound PRRs include TLRs and CLRs, while NLRs and RLRs are found intracellularly. PRRs cooperate to detect a wide variety of molecules from microbial pathogens, including bacterial carbohydrates (*e.g.*, lipopolysaccharides [LPS]), bacterial peptides (*e.g.*, flagellin), viral nucleic acids and proteins, and fungal glucans. PRRs play an important role in viral recognition and have been implicated in the pathogenesis of hepadnaviral infection. The main subject of this study is the identification of woodchuck TLRs and the delineation of their expression during the course of hepadnaviral infection in woodchucks. TLRs will be covered in detail in Section 1.7.

## **1.6.2. Adaptive Immunity**

### **1.6.2.1. Humoral Immune Response**

The adaptive immune response relies on antibody production by B cells to neutralize and clear invading pathogens. The diversity of antigen recognition is due to the combinatorial joining of variable (V), diversity (D) and joining (J) gene fragments which encode the antigen-binding regions of B cell receptors (BCRs) (Notarangelo *et al.*, 2016). The large diversity of antigen recognition allows for the generation of a response that is specific for a particular pathogen or pathogen-infected cell. The most important aspect of humoral immunity is the generation of antibodies by memory B cells and plasma cells that have long lasting, high-affinity for a foreign agent. Clonal selection of B lymphocytes generally occurs through one of three mechanisms: T cell-

dependent activation, and type 1 or type 2 T cell-independent activation (Owen *et al.*, 2013). T cell-dependent activation occurs when an antigen binds to the immunoglobulin receptor on a B cell and is internalized and presented to a T<sub>h</sub> cell. Subsequently, the T<sub>h</sub> cell binds to the MHC class II-peptide antigen complex presented by the B cell and delivers activation signals through co-receptor interactions and cytokine production. Conversely, type 1 T cell-independent activation occurs when an antigen binds to both an immunoglobulin receptor and an innate immune receptor (*i.e.*, TLR) located on the B cell. While type 2 T cell-independent activation is taking place when the B cell recognizes an antigen that has already been identified and bound by complement proteins. In this case, crosslinking occurs when the B cell binds the antigen and complement proteins through immunoglobulin and cluster of differentiation (CD) molecule 21 (CD21) receptors (Vos *et al.*, 2000). The resulting crosslink is sufficient to initiate an activation signal for B cell clonal expansion. Ultimately, activation and clonal expansion of plasma and memory B cells that express antigen-specific antibodies is vital to the development of a long-term humoral immune response.

#### **1.6.2.2. T Cell-Mediated Immune Response**

T lymphocytes play a critical role in the adaptive immune response and are largely divided in two groups: CD4<sup>+</sup> T cells and CD8<sup>+</sup> T cells. T cells are activated by professional APCs, typically DCs, that have engulfed a foreign pathogen and presented its associated peptides on MHC class I or MHC class II molecules on the cell surface. Additionally, T cells can become activated when foreign peptides are recognized by circulating naive CD4<sup>+</sup> or CD8<sup>+</sup> T cells. Activation results in differentiation and clonal

expansion into effector CD4+ and CD8+ T lymphocytes. Classically, CD4+ T cells, also referred to as T<sub>h</sub> cells, differentiate into either a type 1 (T<sub>h</sub>1) or type 2 (T<sub>h</sub>2) cell that are classified by the cytokines they secrete. More recently, additional T<sub>h</sub> cell subsets have been identified, including T<sub>h</sub>9, T<sub>h</sub>17, T<sub>h</sub>22, T follicular-helper (T<sub>fh</sub>) and T-regulatory (Tregs) (Hirahara and Nakayama, 2016). In any case, T<sub>h</sub> cells can influence a variety of immune cells indirectly through the production of cytokines, resulting in an immune response that is catered to the type of infection. In contrast, CD8+ T cells, also referred to as CTLs, induce death of infected cells directly. When activated, CD8+ CTLs can recognize and destroy target cells through activation of the cell's internal apoptotic cycle. Cells are targeted based on their expression of pathogenic peptides on MHC class I molecules. In addition to cell cytotoxicity, CTLs produce proinflammatory and antiviral cytokines (*i.e.*, TNF- $\alpha$  and IFN- $\gamma$ ) to aid in immune clearance. Both CD4+ and CD8+ T cells can differentiate into memory T cells for long-lasting immune protection. However, the exact mechanism and sequence of immunological events leading to the development of memory T cells is not completely understood (Gerritsen and Pandit, 2016).

## **1.7. Toll-like Receptors**

### **1.7.1. Background**

The name Toll-like receptor is derived from the Toll receptor originally identified in *Drosophila* that is required for dorsal-ventral patterning during development (Hashimoto *et al.*, 1988). Investigation into *Drosophila*'s immune response to fungal agents implicated the Toll protein in the control of expression of the antifungal peptide

gene drosomycin (Lemaitre *et al.*, 1996). Due to the similarities between the cytoplasmic domains of *Drosophila* Toll and human interleukin-1 (IL-1) receptors, it was thought that both may be related to ancient evolutionary immune responses. This discovery ultimately led to the identification of a family of human TLR genes residing on chromosome 4 (TLRs 1, 2 and 3), chromosome 9 (TLR4), and chromosome 1 (TLR5) (Rock *et al.*, 1998). Since their discovery, 13 TLRs have been identified. Genes encoding TLR1-11 are expressed by both human and mouse; however, mouse TLR10 is a pseudogene and human TLR11 contains a stop codon, resulting in no protein expression for these two TLR genes. While TLR12 and TLR13 are expressed in mouse, they are not expressed in humans (Broz and Monack, 2013; Yarovinsky, 2014).

### **1.7.2. Structure and Cellular Localization**

TLRs are a family of type I transmembrane proteins characterized by an extracellular, horseshoe shaped, leucine-rich repeat (LRR) domain and a cytoplasmic domain referred to as the Toll/IL-1 receptor (TIR) domain (Owen *et al.*, 2013). The cytoplasmic domain was given its name due to its similarities to the cytoplasmic domain of the mammalian IL-1 receptor (IL-1R). When the extracellular domain binds specific PAMPs, the intracellular domain alters its configuration causing the initiation of signaling events. These events include translocation of transcription factors into the nucleus, interferon-stimulated gene regulation, and cytokine modulation.

Diverse cell types have been found to express TLRs, such as airway and gut epithelial cells, endothelial cells, B cells, T cells, NK cells, macrophages, monocytes, DCs, neutrophils, basophils and mast cells (Pandey and Agrawal, 2006). In innate

immune cells (*i.e.*, macrophages and DCs), ligand recognition and binding is followed by a series of signaling events that result in an inflammatory response and release of antimicrobial agents. Activation of TLRs is a critical step in the development of antigen-specific adaptive immunity (Takeda and Akira, 2005). In B cells, TLRs have been implicated as important regulators of innate signals regulating adaptive immune responses (Hua and Hou, 2013). TLRs recognize a wide range of pathogens and, for the most part, can be categorized by their subcellular localization. Thus, TLR1, 2, 4-6 and 10 are located on the cell surface, while TLR3, 7-9 and 11-13 are located intracellularly. In general, extracellular TLRs are involved in the recognition of PAMPs composed of lipids and proteins, while intracellular TLRs recognize nucleic acid sequence motifs.

### **1.7.3. Ligand Recognition**

#### **1.7.3.1. Extracellular TLRs**

##### **1.7.3.1.1. TLR1, 2 and 6**

TLR2 recognizes a wide range of PAMPs and is known as the most promiscuous TLR of the family. Ligands for TLR2 include lipoproteins from Gram-negative bacteria, mycoplasma and spirochetes, peptidoglycan and lipoteichoic acid (LTA) from Gram-positive bacteria, lipoarabinomannan from mycobacteria, phenol-soluble modulins from *Staphylococcus epidermidis*, glycoinositolphospholipids from *Trypanosoma cruzi*, as well as various lipopolysaccharides from non-enterobacteria (Takeda *et al.*, 2003). TLR2's capability to recognize such a wide range of microbial PAMPs may be attributed

to its ability to form heterodimers with TLR1 or TLR6. Studies in mice have shown that diacylated lipoproteins require TLR2/6 association for recognition, whereas triacylated lipoprotein recognition requires TLR2/1 association (Takeuchi *et al.*, 2001; Takeda *et al.*, 2002). The crystal structure of this heterodimer formation was eventually solved (Jin *et al.*, 2007). Thus, heterodimer formation of TLR2 with either TLR1 or TLR6 allows for the recognition of a wide range of microbial PAMPs. It has been suggested that TLR2 may also form heterodimers with TLR10 and play a role in the recognition of triacylated lipopeptides (Guan *et al.*, 2010).

#### **1.7.3.1.2. TLR4**

TLR4 is involved in the recognition of LPS on Gram-negative bacteria; however, like TLR2, it is able to recognize a variety of PAMPs from various microorganisms. LPS recognition by TLR4 requires the cooperation of several accessory molecules. Initially, LPS binds to LPS-binding protein (LBP) and this complex is then recognized by a CD14 receptor commonly expressed on monocytes, macrophages and neutrophils (Takeda and Akira, 2015). Once bound, the complex can associate in close proximity with TLR4. Furthermore, for effective recognition and induction of an innate response, the presence of an additional protein, lymphocyte antigen 96 (MD-2), is needed (Nagai *et al.*, 2002). In addition to LPS, TLR4 has been shown to be involved in the recognition of taxol, a diterpene anti-tumor agent developed from the Pacific yew, *Taxus brevifolia* (Kawasaki *et al.*, 2000). It has also been demonstrated that TLR4 can recognize endogenous ligands released during inflammatory responses and tissue damage, referred to as danger signals. These endogenous danger signals include heat shock proteins (HSP),

HSP-60 and HSP-70, and extracellular matrix degradation products, biglycan, hyaluronan, and fibronectin (Ohashi *et al.*, 2000; Okamura *et al.*, 2001; Termeer *et al.*, 2002; Vabulas *et al.*, 2002; Schaefer *et al.*, 2005). TLR4 is primarily expressed on the cell surface, however, studies have also shown that the TLR4/MD-2 complex can be localized intracellularly and play a role in sensing Gram-negative bacteria and LPS within the cell (Shibata *et al.*, 2011).

#### **1.7.3.1.3. TLR5**

Mainly expressed by epithelial cells, TLR5 is responsible for the detection of the bacterial protein flagellin. Flagellin is the main component of bacterial flagellum, an organelle that is involved in propulsion. TLR5 is functionally expressed in intestinal, respiratory, and kidney/urogenital tract epithelial cells, as well as human macrophages and DCs (Vijay-Kumar and Gewirtz, 2009). Polymorphisms in the ligand-binding domain of TLR5 has been correlated with a susceptibility to pneumonia caused by the bacterium *Legionella pneumophila* (Hawn *et al.*, 2003). Thus, TLR5 plays a critical role in the recognition and elimination of bacterium at the mucosal level.

#### **1.7.3.1.4. TLR10**

For the most part, subcellular localization and ligand recognition by TLR10 has only recently been elucidated. TLR10 was first cloned in 2001, however, since then little has been discovered about the receptor. Recent studies suggest that TLR10 works in cooperation with TLR2 in sensing triacylated lipopeptides (Guan *et al.*, 2010). Furthermore, TLR10 has been implicated as an important receptor involved in the

induction of innate immune responses to influenza virus infection (Lee *et al.*, 2014). One reason why TLR10 continues to elude researchers is the absence of a suitable mouse model, as TLR10 is a pseudogene in mice due to the presence of gaps and retroviral insertions into its sequence.

### **1.7.3.2. Intracellular TLRs**

#### **1.7.3.2.1. TLR3**

TLR3 is expressed intracellularly and recognizes double stranded RNA (dsRNA). In resting cells, TLR3 is located in the endoplasmic reticulum and upon activation becomes localized in endosomal compartments where it initiates innate immune signaling (Zhang *et al.*, 2013). It has been shown that polyinosinic-polycytidylic acid [poly (I:C)], a synthetic dsRNA analog, is a potent activator of TLR3-induced production of type I IFNs (Alexopoulou *et al.*, 2001). Additionally, cell-endogenous mRNA double stranded regions have been shown to activate TLR3 signaling (Kariko *et al.*, 2004). TLR3 has been postulated to play a role in antiviral immunity, since dsRNA is a universal viral PAMP (Akira *et al.*, 2006). Many viruses produce dsRNA during their replicative cycle as an intermediate in RNA synthesis or as a byproduct of symmetrical transcription of DNA virus genomes (Takeda *et al.*, 2003). Although it has been demonstrated that TLR3 plays an indirect role in antiviral response (Zhang *et al.*, 2013), it remains unclear the exact mechanisms of viral recognition. Interestingly, it has been shown that TLR3 knockout mice fail to show increased susceptibility to viral infections (Edelmann *et al.*, 2004), which further discredits TLR3's role in the recognition of viruses.

#### **1.7.3.2.2. TLR7 and 8**

Located in endosomes, TLR7 acts as an intracellular sensor of single-stranded RNA (ssRNA). TLR7 has been shown to recognize viral origin guanosine-rich and adenosine-rich ssRNA sequences from the human immunodeficiency virus (HIV), vesicular stomatitis virus (VSV), and influenza virus (Diebold *et al.*, 2004; Heil *et al.*, 2004; Lund *et al.*, 2004). TLR7 mediated recognition of bacterial RNA in lysosomes has also been demonstrated in conventional DCs (Mancuso *et al.*, 2009). In addition to ssRNA, synthetic compounds have been identified to be potent activators of TLR7 induced antiviral immunity. For instance, imidazoquinolone derivatives, such as imiquimod and resiquimod, are potent activators of proinflammatory cytokines through TLR7-mediated signaling.

Phylogenetically similar to TLR7, TLR8 also recognizes ssRNA in endosomes. Both are structurally similar and recognize many of the same ligands. For example, TLR8 responds to imidazoquinolone derivatives and recognizes viral origin guanosine-rich and adenosine-rich ssRNA sequences from many viruses. Although TLR7 and TLR8 are expressed in human and mice, mouse TLR8 lacks the presence of 5 conserved amino acids rendering it nonfunctional (Kugelberg, 2014).

#### **1.7.3.2.3. TLR9**

Based on sequence homology, TLR9 is phylogenetically related to both TLR7 and TLR8. Also expressed intracellularly, TLR9 is involved in the recognition of unmethylated cytosine-phosphate-guanine (CpG) motifs exhibited by some bacterial

and viral DNA. Studies have revealed that TLR9 can detect CpG DNA motifs of murine cytomegalovirus (MCMV), herpes simplex virus (HSV) type 1, and HSV type 2 (Hochrein *et al.*, 2004; Krug *et al.*, 2004; Tabeta *et al.*, 2004). TLR9 is also involved in the recognition of self CpG DNA that can lead to the development of autoimmune disorders, including rheumatoid arthritis and systemic lupus erythematosus (Leadbetter *et al.*, 2002; Boule *et al.*, 2004).

#### **1.7.3.2.4. TLR11 and 12**

TLR11 is localized in endolysosomal compartments and functions to recognize proteins of uropathogenic and enteropathogenic bacteria (Broz and Monack, 2013). In mice, TLR11 has been shown to recognize uropathogenic bacteria in the bladder, as mice lacking TLR11 are highly susceptible to this infection (Zhang *et al.*, 2004). Additionally, TLR11 has been linked to the resistance to *Toxoplasma gondii* through recognition of the protein profilin (Yarovinsky *et al.*, 2005). Like TLR5, TLR11 recognizes flagellin, however, both receptors function in different subcellular compartments. TLR12 is also located in endosomal compartments and can function alone or as a heterodimer with TLR11. TLR12 also plays a crucial role in resistance to *Toxoplasma gondii* through profilin recognition (Koblansky *et al.*, 2013). As mentioned, TLR11 is not functional in humans as there is a stop codon inserted in the TLR11 gene sequence, while a TLR12 compatible sequence is not found in the human genome.

#### **1.7.3.2.5. TLR13**

The most recently identified, TLR13 functions inside the cell to recognize large bacterial ribosomal RNAs (rRNAs). More specifically, it recognizes conserved CGGAAAGACC motifs of 23S rRNA (Broz and Monack, 2013). A recent study has shown that the 23S rRNA of *E. coli* was able to induce the production of pro-IL1- $\beta$  through a TLR13-dependant pathway. Like TLR11 and TLR12, TLR13 is not expressed in humans.

#### **1.7.4. TLR Signaling**

Binding of a TLR-specific ligand on the plasma membrane or in endosomal compartments leads to ligand-induced receptor dimerization and recruitment of cytosolic TIR domain-containing adaptor molecules. The TIR domain of the activated TLR will signal through either the myeloid differentiation primary response protein 88 (MyD88) and MyD88-adaptor like/TIR-associated protein (MAL/TIRAP) or Toll-receptor-associated molecule (TRAM) and Toll-receptor-associated activator of interferon (TRIF) (O'Neill *et al.*, 2013). With the exception of TLR3, all TLRs require MyD88 for downstream signaling as studies have shown that cells lacking MyD88 are only responsive to TLR3 ligands (Kawai *et al.*, 1999; Akira *et al.*, 2003). Following adaptor molecule recruitment, intracellular signaling results in the interaction of IL-1R-associated kinases (IRAKs) and the adaptor molecules TNF receptor-associated factors (TRAFs). This leads to the activation of mitogen-activated protein kinases (MAPKs), JUN N-terminal kinase (JNK) and p38, and IRAKs (O'Neill *et al.*, 2013). This results in the activation of transcription factor nuclear factor- $\kappa$ B (NF- $\kappa$ B), interferon regulatory factors

(IRFs), cyclic AMP-responsive element-binding protein (CREB), and activator protein 1 (AP1). Ultimately, TLR signaling leads to the induction of an innate immune response with the production of pro-inflammatory cytokines, including IL-1 and TNF- $\alpha$ , and type I IFNs.

### **1.8. TLRs and Antiviral Immunity**

TLRs have been implicated in the detection of several viruses resulting in the subsequent induction of antiviral immunity. The antiviral innate immune response against viruses is characterized by the production IFNs, inflammatory cytokines and chemokines that aid in prevention of viral entry, replication and persistence. IFN production plays a critical role in the upregulation of hundreds of IFN-stimulated genes that have a wide spectrum of antiviral properties (Lester and Li, 2014). In addition, IFNs act in a paracrine manner to initiate an antiviral state in neighboring cells, as well as activation of various innate immune cells to mediate viral clearance. Furthermore, the production of inflammatory cytokines and chemokines aids in the facilitation of the innate immune responses and induction of adaptive immunity. Recognition of viral components by TLRs can occur on the surface of the cell (*e.g.*, interaction with viral envelope proteins) or intracellularly (*e.g.*, interaction with viral nucleic acids). In both situations, the resulting innate immune response is catered toward elimination of the virus.

### 1.8.1. TLRs and Hepadnaviruses

Historically, HBV was considered to be a 'stealthy virus' in the early phase of infection due to its inability to activate the innate immune response and induce the production of IFNs and IFN-stimulated genes (Wieland and Chisari, 2005). However, these observations were obtained in chimpanzees one week after infection with HBV, which was too late to correctly evaluate early innate responsiveness that usually is activated in minutes or hours post infection. In woodchucks experimentally infected with WHV, markers of the innate immune response were detected in the first few hours post-injection (Guy *et al.*, 2008). In this study, WHV replication was detected in the liver as early as one hour after infection. Between 3-6 hours post infection, there was a significant increase in intrahepatic transcription of IFN- $\gamma$  and IL-12 indicating activation of the innate immune response. By day 3, NK and NKT cells had become activated, which coincided with reduction of virus replication. Thus, in contrast to earlier reports, the innate immune system was found to play a role in early recognition of WHV. Although direct binding of hepadnaviral antigens to TLRs has not yet been demonstrated, there is increasing evidence that TLRs play an important role in the immune response to HBV infection.

Viral lipoproteins and glycoproteins have been shown to be recognized by TLR2, thus, HBV glycoproteins seem like viable candidates for TLR ligands. Studies have implicated TLR2 in the induction of cytokines in macrophages due to HBV infection (Cooper *et al.*, 2005). Additionally, TLR2 expression is downregulated in HBeAg-positive CHB patients when compared to HBeAg-negative CHB patients and healthy

controls (Visvanathan *et al.*, 2007). This suggests that HBeAg may play a role in suppression of the immune response through inhibition of TLR2. This is supported by a recent study showing inhibition of expression and function of TLR2 in patients with CHB (Huang *et al.*, 2015b).

TLR3, a nucleic acid sensor that recognizes dsRNA, has been implicated in the pathogenesis of HBV infection. Previous investigations in the transgenic mouse model of HBV have demonstrated that TLR3 ligand signaling induces antiviral cytokines to inhibit HBV replication (Isogawa *et al.*, 2005). Furthermore, TLR3-knockout mice have an inability to induce innate immune response against HBV infection (Maire *et al.*, 2008). It has been shown that TLR3 expression and function is significantly impaired in patients with CHB, when compared to healthy controls (An *et al.*, 2007; Li *et al.*, 2009). This is suggested to contribute to the prolonged viral persistence in these patients. Moreover, genetic variants of TLR3 have been correlated with a higher risk of HBV-related liver disease (Huang *et al.*, 2015a). Modulation of TLR3 remains a plausible approach to the development of immunotherapies against HBV.

Although TLR4 is primarily involved in the recognition of LPS from Gram-negative bacteria, it has been implicated in the progression of CHB related HCC. Studies have shown a correlation between upregulated TLR4 on T cells of CHB patients is correlated with an increase in liver damage (Xu *et al.*, 2015). In support of these findings, it was also discovered that polymorphisms in the TLR4 gene is associated with delayed progression of liver fibrosis and a reduced risk of HCC (Guo *et al.*, 2009). More recently, both soluble CD14 and TLR4 have been implicated in binding HBsAg, as

blocking of these receptors resulted in abrogation of HBsAg-induced DC maturation (van Montfoort *et al.*, 2016).

TLR7 has not yet been implicated in direct binding to HBV antigens, however, activation of TLR7 results in endogenous production of type I IFNs that inhibit viral replication. Additionally, TLR7 is highly expressed on plasmacytoid DCs (pDCs) and B cells, thus engagement of TLR7 on these cells should result in the priming of the adaptive immune response. Recent studies in chimpanzees has shown that activation of TLR7 signaling using a synthetic TLR7 agonist resulted in prolonged suppression of HBV in chronically infected animals (Lanford *et al.*, 2013). Currently, clinical trials are underway to evaluate the orally administered TLR7 agonist GS-9620 for its safety, tolerability, and efficacy in CHB patients (for more detail see Section 1.8.2).

Studies involving TLR8 have been focused on the induction of a potent antiviral response. TLR8 activation using the agonist ssRNA40 was found to selectively activate liver-resident innate immune cells to produce robust quantities of IFN- $\gamma$  (Jo *et al.*, 2014). Furthermore, immunization with HBV antigens and a TLR7/8 agonist adjuvant was able to induce antigen-specific immune response in HBV-transgenic mice (Wang *et al.*, 2014). More recently, TLR8 expression on trophoblastic cells was found to play a role in the prevention of intrauterine HBV transmission by inhibiting viral translocation across the trophoblast (Tian *et al.*, 2015).

Human TLR9 is highly expressed on pDCs and B cells in comparison to other mononuclear cells (Medzhitov and Janeway, 2000). Although the direct mechanism is unknown, functional impairment of pDCs has been observed in several viral infections,

including HBV (Barchet *et al.*, 2005; Xu *et al.*, 2012). HBV has developed escape mechanisms to avoid TLR9 activation in both pDCs and B cells that, in turn, diminishes immune control of the virus and may contribute to the establishment of CHB infection (Vincent *et al.*, 2011; Martinet *et al.*, 2012). Studies have shown that nanoparticle encapsulated HBV-CpG can reverse suppression of IFN production through TLR9 signaling (Lv *et al.*, 2014). Treatments designed to target TLR9 and restore its signaling pathways may be beneficial in the treatment of long-term HBV infection (Shahrakyvahed *et al.*, 2014). A recent study in the woodchuck model of HBV infection has revealed that combination immunotherapy of CpG oligonucleotides (ODNs) and entecavir (ETV) results in suppression of WHV replication and lowering of serum WHsAg levels (Meng *et al.*, 2016). Unfortunately, there was a lack of WHsAg seroconversion to anti-WHs antibodies during treatment and viral replication rebounded after treatment had been stopped.

### **1.8.2. Targeting TLRs in HBV Antiviral Therapy**

Current treatments for chronic HBV infection (*i.e.*, pegylated IFN- $\alpha$  and nucleoside/nucleotide analogs) are only partially effective at controlling the virus in chronically infected patients and none of them are able to eliminate virus completely. There is a need for the development of an antiviral treatment, likely in combination with an immune modulator, that will stop viral replication and induce a HBV-specific cell-mediated immune response to fully resolve hepatitis and prevent development of HCC.

Activation of the innate immune system through TLR stimulation has been the recent focus in the development of effective treatments for patients with CHB. More

specifically, CpG ODNs targeting TLR9 have showed promising results in their effectiveness to control the virus *in vitro*. However, trials using a combination therapy of CpG ODNs and ETV in WHV-infected woodchucks did not succeed in long-term control of viral replication (Martinet *et al.*, 2012). As mentioned previously (Section 1.8.1), the TLR7 ligand GS-9620 is currently being tested in phase 2 clinical trials in individuals with CHB. Preclinical studies using the orally administered drug has demonstrated an ability to control viral replication in WHV-infected woodchucks and HBV-infected chimpanzees (Lanford *et al.*, 2013; Menne *et al.*, 2015). At low doses, GS-9620 has also been shown to be induce antiviral innate immune responses without inducing systemic IFN- $\alpha$  production (Fosdick *et al.*, 2014). In two double-blind phase 1b clinical trials, GS-9620 was proven to be safe and was associated with the induction of antiviral immunity without adverse effects in patients with CHB (Gane *et al.*, 2015). Although more investigation is needed to enhance our understanding of the mechanisms of action of GS-9620, it has great potential to be an effective CHB treatment alternative. Future potential targets for CHB treatment may include TLR2, TLR3, TLR4, TLR6 and TLR8; however, supporting evidence is not yet strong enough to warrant preclinical or clinical testing.

### **1.8.3. TLRs as Vaccine Adjuvants**

The innate immune system plays a major role in the development of an adaptive immune response. Therefore, developing vaccines that target the innate immune system (*i.e.*, TLRs) should enhance virus-specific adaptive immune responses. To date, several TLR ligands have been tested as adjuvants in HBV vaccines. For

example, a vaccine that incorporates a TLR2 agonists, called Theradigm-HBV, was tested for its ability to induce a HBV-specific CTL response in healthy individuals and those with CHB (Livingston *et al.*, 1997; Livingston *et al.*, 1999). In phase I and phase II clinical trials, the vaccine was able to induce a HBV-specific CTL response in healthy volunteers; however, a CTL response was not induced in patients with CHB. Thus, the vaccine did not make it past phase II clinical trials. Currently, there are two HBV vaccines for adults, Fendrix and Supravax, that utilize TLR4 agonists as an adjuvant. The TLR4 agonist, monophosphoryl lipid A (MPLA), has been incorporated into HBV vaccines and has been proven to induce protective titers of anti-HBs antibodies in multiple studies and phase III clinical trails (Thoelen *et al.*, 1998; Levie *et al.*, 2002; Lu *et al.*, 2003; Boland *et al.*, 2004). In a similar manner, TLR9 CpG ODNs have also been used in HBV vaccines as an adjuvant. Of the CpG ODNs tested, a CpG ODN called 1018 immunostimulatory sequence (ISS) is the most extensively studied. A 1018 ISS conjugated HBV vaccine has demonstrated to be immunogenic and well tolerated in healthy adults in a phase I study and in young adults in a phase 2 study (Halperin *et al.*, 2003; Halperin *et al.*, 2006). More recently, it was discovered that HBV 1018 ISS, in comparison with the currently licensed aluminum-adjuvanted vaccine, is more effective and provides earlier onset of protection against HBV infection (Halperin *et al.*, 2012). More investigations into the immunogenic response of adolescents, children, and immunocompromised hosts are needed before this vaccine becomes commercially available.

## 1.9. TLRs and the Woodchuck Model of HBV Infection

In the past, studies involving TLRs in the context of viral infection have been limited to *in vitro* conditions and HBV-transgenic mice. In recent years, investigations using WHV-infected woodchucks have implicated TLRs in the pathogenesis of hepadnaviral infection. One study investigating TLR signaling pathways in primary woodchuck hepatocytes (PWHs) attempted to elucidate an antiviral effect through TLR stimulation with its respective ligand (Zhang *et al.*, 2009). Ligands for TLR3 [poly (I:C)], TLR4 (LPS), TLR7 and TLR8 (R848), and TLR9 (CpG) were investigated for their ability to induce innate immune responses and reduce WHV replication in woodchucks. The results showed that stimulation of TLR3 and TLR4 was able to induce production of IFN and IFN-stimulated genes; however, signaling through TLR7, TLR8, and TLR9 failed to do so. Interestingly, only LPS treatment was able to reduce WHV replication in cultured PWHs, despite the strong innate immune response induced by treatment with poly (I:C). Another study has proposed that PWHs play an active role in TLR2-mediated antiviral response during WHV infection (Zhang *et al.*, 2012). Using the synthetic ligands Pam2CSK4 and Pam2CSK4 to activate TLR2/TLR6 and TLR2/TLR1, respectively, there was observed induction of anti-inflammatory cytokines that downregulated WHV replication in PWHs. Additionally, they showed that TLR2 was significantly downregulated in PBMCs of WHV-infected woodchucks compared to WHV-naïve woodchucks. Interestingly, TLR2 expression in cultured PBMCs from chronically infected woodchucks was restored after overnight culture, suggesting that circulating virus and its products may have an inhibitory effect on TLR2 expression. As mentioned in Section 1.8.1, a combination therapy of CpG ODNs and ETV have been shown to

enhance innate immune antiviral response and reduce WHV replication in infected woodchucks (Meng *et al.*, 2016). However, more investigation is needed as there was no seroconversion and long-term protection in these animals. Also mentioned in Section 1.8.1 and Section 1.8.2, the TLR agonist GS-9620 has been extensively studied in the woodchuck model and is currently undergoing clinical trials. The TLR7 ligand appears to be highly effective at inducing a sustained antiviral response and anti-WHs antibody seroconversion in chronically infected woodchucks (Menne *et al.*, 2015). The most recent study has implicated TLRs in the induction of the programmed cell death 1 (PD-1)/programmed cell death ligand 1 (PD-L1) system and a role of this system in negative regulation of T cell function (Zhang *et al.*, 2011). Using commercially available TLR1-9 ligands, it was found that woodchuck PD-L1 mRNA was upregulated in PWHs after stimulation with TLR3 and TLR4 ligands, while PD-L1 mRNA in PBMCs was upregulated by TLR4 and TLR7 ligands. This study has implicated TLRs in the upregulation of PD-1/PD-L1 system, thus, suggesting their contribution to reduced T cell responses in chronic hepadnaviral infection. In any case, there is strong evidence implying that TLRs play major roles in the control of WHV replication as well as in the pathogenesis of hepadnaviral infection. Understanding the role of TLRs in WHV infection in the woodchuck model of hepatitis B and HBV-associated HCC may be crucial to the development of novel therapeutics to eradicate hepadnaviral persistence.

### **1.10. Objectives**

The woodchuck (*Marmota monax*) infected with WHV represents the closest natural model of human HBV infection, chronic hepatitis B, and HBV-associated HCC.

The mechanisms by which hepadnaviruses are recognized by the immune system are not fully understood. It is expected that TLRs play important roles in the pathogenesis of hepadnaviral hepatitis and persistence. However, little is known about expression of individual TLRs in primary hepatocytes and in the liver during the course of WHV infection and in different forms of hepatitis. Thus, the purpose of this study was to identify partial sequences of woodchuck TLRs, and design specific primers and quantitative reverse transcription polymerase chain reaction (RT-qPCR) assays to quantify TLR expression. Previous studies on TLR expression profiles during the course of HBV infection were largely limited to investigation of PBMCs, as taking liver biopsies from a human during the course of HBV infection is rarely feasible. In contrast, the woodchuck infected with WHV represents a very convenient model to collect both liver biopsies and PBMC samples throughout the course of infection and in different forms of hepatitis. Thus, the objectives of this study included:

1. To identify partial gene sequences of woodchuck TLRs 1-10.
2. To delineate the profiles of transcription of individual TLRs in primary hepatocytes and corresponding liver tissue samples obtained from healthy woodchucks and animals with different stages of experimental WHV infection.
3. To assess TLRs1-10 expression in sequential liver biopsies acquired prior to and during WHV infection progressing from AH to SLAH or from AH to CH, and in the course of POI.
4. To recognize profiles of TLRs1-10 expression in PBMCs of healthy animals and those with different stages of experimental WHV infection and forms of WHV hepatitis.

## **Chapter 2 - Methods and Materials**

### **2.1. Collection of Woodchuck Tissue Samples**

All woodchucks were maintained in a facility operated by Animal Care Services of Memorial University of Newfoundland in accordance with the guidelines of the Canadian Council on Animal Care. All animal procedures were approved by the Institutional Animal Care Committee of Memorial University of Newfoundland.

#### **2.1.1. Liver Biopsies**

Liver biopsies were obtained through surgical laparotomy as previously reported (Michalak *et al.*, 1999). Briefly, animals were sedated with an intramuscular injection of ketamine (23 mg/kg; Ketaset; CDMV Inc., St. Hyacinthe, Quebec) and xylazine (10 mg/kg; Lloyd Laboratories, Shenandoah, Iowa), and then anaesthetized with 2% to 4% isofluorane (CDMV Inc., St. Hyacinthe, Quebec). Liver biopsies were removed aseptically and divided into 1-2 mm<sup>3</sup> fragments and immediately snap frozen in liquid nitrogen and stored at -80 °C for further isolation of nucleic acids. Other liver tissue fragments were collected and processed for downstream histological and immunohistochemical examinations as previously reported using standard procedures (Michalak, 1978).

#### **2.1.2. Autopsy Liver and Spleen Tissues**

Animals were injected with an overdose mixture of ketamine and xylazine. Blood was collected by cardiac puncture and used for serum and PBMC isolation (see Section

2.1.3). Liver and spleen samples, as well as other organs, were aseptically removed and snap frozen upon collection. Tissue samples were stored at -80 °C. Other liver tissue fragments were processed for histological and immunohistochemical investigations.

### **2.1.3. Preparation of Primary Hepatocytes and PBMCs**

Hepatocytes were isolated from the livers of autopsied woodchucks by two-step collagenase microperfusion, method described before in detail (Churchill and Michalak, 2004). Using phase-contrast microscopy, hepatocyte preparations were confirmed to be at least 98% pure. Display of albumin and asialoglycoprotein receptor (ASGPR) by immunohistochemical staining was used as an indicator of differentiated hepatocyte phenotype (Churchill and Michalak, 2004). PBMCs were isolated by Ficoll-Hypaque density gradient centrifugation as previously reported (Michalak *et al.*, 1995). Cell preparations were cryopreserved at  $1.0 \times 10^6$  –  $5.0 \times 10^6$  cells/mL in heat-inactivated fetal calf serum (FCS) with 10% dimethyl sulfoxide (DMSO) and kept in liquid nitrogen until used in the current study.

## **2.2. RNA Extraction**

Total RNA was isolated from woodchuck liver and spleen tissue samples, liver biopsies, and PBMCs using TRIzol® Reagent (Invitrogen Life Technologies, Burlington, Canada). A 100 mg tissue sample or  $5.0 \times 10^6$  PBMCs was supplemented with 0.5 mL of TRIzol® and homogenized using a sterile plastic pestle. Another 0.5 mL of TRIzol® was added and the mixture was placed on a rotator at room temperature for 30 minutes. 0.2 mL of

chloroform (Fisher Scientific, Ottawa, Ontario) was added and the sample was vigorously shaken for 15 seconds and incubated at room temperature for 3 minutes. The suspension was then centrifuged at 12,000 x *g* at 4 °C for 15 minutes. The top aqueous layer was transferred to a new Eppendorf tube and 0.5 mL of isopropanol (Fisher Scientific, Ottawa, Ontario) was added. The sample was then precipitated overnight at -20 °C. Then, the aliquot was centrifuged at 12,000 x *g* at 4 °C for 10 minutes. The supernatant was discarded and the RNA pellet washed once with 75% ethanol. The RNA was centrifuged at 7,500 x *g* at 4 °C for 5 minutes, the supernatant was removed, and the pellet resuspended in 40 µL of 0.1% diethyl pyrocarbonate (DEPC)-treated water and stored at -80 °C.

### **2.2.1. DNase Treatment of RNA**

In order to remove DNA possibly contaminating the RNA sample, 8 µL of RNA aliquot was supplemented with one µL of 10x reaction buffer and one µL of amplification grade DNase I (Invitrogen Life Technologies, Burlington, Canada). The sample was mixed gently and incubated at room temperature for 15 minutes. Following incubation, one µL of stop solution was added and the mixture incubated in a water bath at 70 °C for 10 minutes and chilled on ice.

### **2.2.2. RNA Concentration, Purity, and Integrity Assessment**

Nucleic acid concentration and purity were determined using a DU 530 spectrophotometer (Beckman Instruments Inc., Fullerton, California) and the NanoDrop 2000 (Thermo Scientific, Waltham, Massachusetts). For spectrophotometric analysis, 2

$\mu\text{L}$  of the RNA sample was supplemented with 98  $\mu\text{L}$  of DEPC-treated water (1:50 dilution) and placed into a glass cuvette. Absorbance was measured at 260 nm and 280 nm. The final concentration of RNA was calculated using the following equation:

$$\text{RNA concentration} = (\text{net absorbance at 260 nm}) \times (\text{dilution factor}) \times (0.04 \mu\text{g}/\mu\text{l})$$

Purity of RNA was determined by calculating the 260 nm/280 nm absorbance ratio. For RNA, a pure sample will yield a ratio of approximately 2.0. Analysis of samples in the NanoDrop 2000 was used as an additional method for quantifying RNA concentration and determining purity. The NanoDrop applies the same principle as the spectrophotometer and measures the absorbance at both 260 nm and 280 nm. However, the NanoDrop requires less RNA and gives more accurate readings. Prior to reading, one  $\mu\text{L}$  of sterile deionized water was used as a blank. RNA measurements were performed by loading one  $\mu\text{L}$  of the RNA sample. Readouts of RNA concentration and purity were automatically generated using the NanoDrop 2000 software.

RNA integrity was determined using an Agilent 2100 Bioanalyzer (Agilent Technologies, Santa Clara, California) and Agilent 2100 Expert Software. All microfluidic nanochips used in the analysis were prepared according to the manufacturer's protocol. Briefly, the gel-dye mix was prepared by adding 400  $\mu\text{L}$  of gel matrix to 4  $\mu\text{L}$  of dye concentrate and then filtered through a spin filter. The nanochip was filled with the prepared gel-dye mixture and 5  $\mu\text{L}$  of sample buffer was added to each of the sample wells. One  $\mu\text{L}$  of RNA was then loaded into each well of the chip. Finally, one  $\mu\text{L}$  of the RNA ladder was loaded into the designated ladder well. The chip was vortexed and inserted into the Agilent 2100 Bioanalyzer. Following the analysis, an RNA Integrity Number (RIN) was

generated for each RNA sample and scored on a scale from 1-10 (1 = lowest quality, 10 = highest). The RIN is calculated based on characteristics of an RNA electropherogram tracing RNA degradation. Generally, samples with a RIN of 8 or above are acceptable.

### **2.3. Reverse Transcription (RT) of RNA**

A volume of 2  $\mu$ L of RNA sample (corresponding to 2  $\mu$ g of RNA) was resuspended in a total volume of 8  $\mu$ L and supplemented with 2  $\mu$ L of 0.1 M dithiothreitol (DTT), 4  $\mu$ L of 5x RT reaction buffer, 2  $\mu$ L of deoxynucleotides triphosphate (dNTPs), 2  $\mu$ L of 100 ng/ $\mu$ L oligonucleotide random primers, 2  $\mu$ L of Moloney murine leukemia virus (M-MLV) reverse transcriptase, and 0.25  $\mu$ L of RNase Out (all from Invitrogen, Carlsbad, California). Controls consisted of a mock solution that contained all reagents for the RT reaction except RNA that was replaced by double-distilled, deionized (ddd) water. The reaction mix was incubated at 37 °C for one hour and then heated to 95 °C for 5 minutes.

### **2.4. Sense and Anti-Sense Primer Design for Detection of Woodchuck TLRs**

TLR forward (sense) and reverse (anti-sense) oligonucleotide primers were designed during this study for woodchuck TLR1, TLR2, TLR4, TLR5, TLR6, TLR7, TLR8, TLR9 and TLR10. Primers for woodchuck TLR3 (GenBank accession number EU586552) were previously published (Zhang *et al.*, 2009). Our primers were designed using aligned TLR nucleotide sequences from a variety of mammalian species deposited in the Entrez Nucleotide Database (website: <http://www.ncbi.nlm.nih.gov/nuccore>). Complete protein coding sequences were quarried and aligned using Sequencher v4

software (Gene Codes Corporation, Ann Arbor, Michigan). The consensus sequences were constructed and primers were designed to amplify TLR fragments in regions of the highest homology between species. Standard rules of primer design were followed. Thus, primer length was kept between 20 - 25 nucleotides, primer melting temperatures within 5 °C of one another and in the range between 47 and 55 °C (Table 2.1). The guanine-cytosine (GC) content of primers was kept between 40% and 60%. Additionally, primers were designed to contain a G or C base within the last five nucleotides from the 3'-end of the primer, known as a GC clamp. This helps to promote binding specificity due to the stronger bonding of G and C bases. Nucleotide repeats (*i.e.*, ATATAT) and runs (*i.e.*, AAAAA) were avoided due to their tendency to misprime. Primers used for the initial identification of woodchuck TLR1 to TLR10 are presented in Table 2.1.

## **2.5. End-Point PCR Conditions for Initial Amplification of Woodchuck TLRs**

Five µL of the resulting cDNA (500 ng RNA equivalent) from the RT step was supplemented with 72 µL of ddd water, 10 µL of 10x reaction buffer, 8 µL of 2.5 mM of dNTP, 3 µL of 50 mM MgCl<sub>2</sub>, one µL of each TLR-specific forward (+) and reverse (-) primer, and 0.4 µL of Taq DNA polymerase (2 U) (all from Invitrogen). Thermal cycling conditions consisted of: 35 cycles at 95 °C for one minute (denaturation), 50 °C for one minute (annealing) and 72 °C for one minute (extension). A final extension at 72 °C for 10 minutes was also done to fully elongate synthesized products. In this initial part of the study, beta-actin (β-actin) was routinely used in order to confirm RNA integrity and as a house-keeping gene.

**Table 2.1. Oligonucleotide Primer Sequences and PCR Conditions Used for Initial Amplification of Woodchuck TLRs1-10**

Gene	Primer Sequences (5' - 3')	Length (bp)	Melting Temperature (°C)	Amplicon Size (bp)	Uniqueness* (bp)
TLR1	+ CAT TTG ATG CCC TGC CTA TAT G - TAT GCC AAA CCA GCT GGA GGA T	22 22	53 55	435	435/435
TLR2	+ TGC TCC TGT GAA TTC CTC TCC TT - CTG GAC CAT AAG GTT CTC CAC CCA	23 24	55 59	375	75/375
TLR3	+ AGG GAC TTT GAG GCA GGT GT - CGC AAA CAG AGT GCA TGG T	20 19	54 51	230	0/230
TLR4	+ CTC TGC CTT CAC TAA GAG ACT T - CTC CAG AAG ATG TGC CGC CCC AG	22 23	55 62	313	116/313
TLR5	+ GCC TTG AAG CCT TCA GTT ATG C - CCA ACC ACC ACC ATG ATG AG	22 20	55 54	76	76/76
TLR6	+ GCC CAA ACC TGT GGA ATA TCT CA - CAA AGA ATT CCA GCT AAC ATC CA	23 23	55 52	424	424/424
TLR7	+ GCT GTA TGG TTT GTC TGG TGG GT - CAC TGC CAG AAG TAT GGG TGA GC	23 23	57 59	713	0/713
TLR8	+ CAC ATC CCA AAC TTT CTA TGA TG - CTC TTC AAG GTG GTA GCG C	23 19	52 53	100	100/100
TLR9	+ CTC TGC GGC TGG GAC GTC TGG TA - CAG AAG TTC CGG TTA TAG AAG TGG	23 24	62 56	551	551/551
TLR10	+ ATC CAT TCC GGG TGT ACT TGT GAA T - CAA AGA TGG ACT TAT AGC TTT TCT C	25 25	56 53	520	520/520

\*Uniqueness refers to the number of nucleotides in a given sequence that have not been reported in the literature. For example, TLR2 has 75 nucleotides newly identified in this study and 300 previously reported.

### **2.5.1. Agarose Gel Electrophoresis**

A volume of 20  $\mu$ L of PCR product was mixed with tracking dye and then loaded on a 1% agarose gel containing ethidium bromide (EB). A 100-base pair (bp) ladder was run in parallel as a molecular weight marker. Agarose gels were electrophoresed in 1x Tris-acetate-ethylenediaminetetraacetic acid (EDTA) (TAE) buffer at 120 V for 25 to 30 minutes. Images of agarose gels were captured using a Chemi Genius 2 Bio-Imaging System (Syngene, Frederick, Maryland).

## **2.6. Plasmid Construction**

### **2.6.1. DNA Purification from Agarose Gel**

PCR products were selected for downstream purification based on expected molecular size of the amplicon band on the EB-gel. After selection of PCR products of interest, amplified products were purified from low-melting point (LMP) agarose gel. Briefly, 0.5 g LMP agarose was added to 50 mL of TAE containing EB, melted and allowed to set. 50  $\mu$ L of the chosen PCR product was separated by electrophoresis in 1x TAE at 80 V for 25 to 30 minutes. Bands of expected bp length were visualized under ultraviolet light, excised using a sterile scalpel blade, placed in a sterile Eppendorf tube, and agarose melted at 70 °C in a water bath. Once the gel had melted, one mL of purification resin (Wizard DNA Purification kit, Promega, Madison, Wisconsin) was added to the tube and shaken for 20 seconds. The mixture was then loaded onto a syringe barrel with a filter attached and the aliquot collected by vacuum filtration. Two mL of 80% isopropanol was added to wash the DNA on the filter. After centrifugation at

10,000 x *g* for 2 minutes to remove residual isopropanol, the mini-column was transferred to a clean Eppendorf tube and 50  $\mu$ L of ddd water was added. The tube was centrifuged at 10,000 x *g* for 30 seconds and the eluted DNA was stored at -20 °C until needed.

### **2.6.2. Cloning of Purified TLR DNA Fragments**

A TOPO® TA cloning kit (Invitrogen) was used to clone each purified TLR DNA fragment. 4.5  $\mu$ L of purified PCR product, one  $\mu$ L of salt solution, and 0.5  $\mu$ L of TOPO® vector were mixed and incubated at room temperature for 30 minutes. One Shot chemically competent *Escherichia coli* cells (Invitrogen) were thawed on ice, the ligation mixture was added, and then incubated on ice for 30 minutes. Cells were subsequently heat shocked at 42 °C for 30 seconds. 250  $\mu$ L of pre-warmed super optimal broth with catabolite repression (SOC) medium was added to the cells. The transformation was performed by incubation at 37 °C for 60 minutes and shaking at 200 revolutions per minute (rpm). 100  $\mu$ L of the resulting bacterial suspension was spread on a prewarmed Luria-Bertani (LB) plate containing kanamycin (50  $\mu$ g/mL) and incubated overnight at 37 °C.

### **2.6.3. Mini-scale Preparations of Plasmid DNA**

After 16 hours of growth, individual colonies were picked from LB plates and each colony added to 3 mL of LB medium containing kanamycin. Individual colonies were allowed to grow for 18 hours at 37 °C while shaking at 200 rpm. The next day, 1.5 mL of the bacterial growth was centrifuged at 14,000 x *g* for 20 seconds and the

supernatant was discarded. The pellet was resuspended in 100  $\mu\text{L}$  of glucose-Tris-ethylenediaminetetraacetic acid (GTE) buffer and incubated at room temperature for 5 minutes. Then, 200  $\mu\text{L}$  of sodium hydroxide (NaOH)-sodium dodecyl sulfate (SDS) lysis buffer was added and the mixture was placed on ice for 5 minutes. 150  $\mu\text{L}$  of 3 M potassium acetate was added and the mixture vortexed for 2 seconds and placed on ice for 5 minutes before centrifugation at 14,000  $\times g$  for 3 minutes. The supernatant was then transferred to a fresh tube and one mL of 95% ethanol added to precipitate the plasmid DNA. The DNA was collected by centrifugation at 14,000  $\times g$  for 3 minutes. Finally, one mL of 70% ethanol was used to wash the DNA pellet, which after air drying was resuspended in 30  $\mu\text{L}$  of ddd water.

#### **2.6.4. Restriction Enzyme Digestion of Miniprep**

To determine if specific clones contained a DNA insert, a restriction enzyme digestion was performed. For this purpose, 10X reaction buffer, 10 U of *EcoRI*, 0.1  $\mu\text{g}$  of RNase and 10  $\mu\text{L}$  of plasmid DNA were combined in a 20  $\mu\text{L}$  volume and incubated at 37  $^{\circ}\text{C}$  for 4 hours. Samples were separated on a 1% agarose gel (see Section 2.5.1) to determine if the inserts of interest were present.

#### **2.6.5. Automated DNA Sequencing**

After determining plasmid DNA concentration, approximately 500 ng of each positive miniprep carrying DNA for each of the woodchuck TLR genes examined was sent for sequence analysis to either the Genomics and Proteomics Facility at Memorial University or The Centre for Applied Genomics at the Hospital for Sick Children,

Toronto, Ontario. In each facility, bidirectional sequencing was performed using universal forward and reverse M13 plasmid primers.

#### **2.6.6. Maxi-scale Preparation of Plasmid DNA**

To ensure that a large scale stock of each confirmed TLR sequence was available, a maxi-scale preparation was performed. Recombinant plasmid DNA was isolated using the PureLink HiPure Maxi Prep kit (Invitrogen). To begin, 100 mL of a bacterial culture grown over night at 37 °C was centrifuged at 6,000 x *g* at 4 °C for 15 min in a Sorvall Evolution RC centrifuge with a SS-34 rotator. The supernatant was discarded and 10 mL of resuspension buffer containing RNase was added to the pellet. The tube was then inverted until the contents became homogeneous. Ten mL of lysis buffer was added and the solution was mixed by inversion. The lysate was incubated at room temperature for 5 minutes. A volume of 10 mL of precipitation buffer was added and the solution was mixed by inversion until homogenous. The mixture was centrifuged again at 15,000 x *g* for 10 minutes at room temperature. The supernatant was transferred to an elution column that was equilibrated with 30 mL of equilibration buffer. The supernatant was allowed to drain by gravity flow and the flow-through was discarded. The column was then washed with 60 mL of wash buffer by gravity flow. A volume of 15 mL of elution buffer was passed through the column and the flow-through containing plasmid DNA was collected in a sterile 30 mL tube. 10.5 mL of isopropanol was added to the DNA and mixed. The tube was then centrifuged at 15,000 x *g* for 30 min at 4 °C. Five mL of 70% ethanol was used to wash the pellet. The DNA was pelleted by

centrifuging at 15,000 x *g* for 5 min at 4 °C, air-dried for 10 minutes and resuspended in 200 µL of Tris-EDTA (TE) buffer.

## **2.7. Real-Time RT-qPCR for Quantification of Woodchuck TLRs**

### **2.7.1. Primer Optimization**

Prior to assessing TLR expression levels in woodchuck test samples it was necessary to optimize amplification conditions for detection of TLRs by real-time RT-qPCR using woodchuck TLR-specific primers. TLR primers used in the initial identification of woodchuck TLR fragments (see Section 2.4. and Table 2.1) were redesigned to be 100% woodchuck specific. Each TLR primer pair then underwent a series of experiments testing different primer concentrations, template concentrations and annealing temperatures for optimal detection of amplicons by RT-qPCR. Primers were tested at a concentration of 2.5 pmol and 5 pmol with the equivalent of 50 ng of RNA from healthy woodchuck liver and spleen. As a positive control, plasmid standards carrying TLRs1-10 gene fragments were included in the reaction. The annealing temperature of each amplification reaction was tested at temperatures ranging from 47 °C to 55 °C, depending on the average annealing temperature of a given primer pair. It was found that TLR1, TLR3, TLR5, TLR6, and TLR8 primer pairs specifically amplified woodchuck gene fragments in both liver and spleen tissue samples, in addition to their respective TLR plasmids that were used as positive controls. Therefore, no modification of the primer sequences for these TLR gene fragments was needed (Table 2.1). In contrast, TLR2, TLR4, TLR7, TLR9, and TLR10 primer sets were redesigned to

specifically amplify their respective woodchuck gene fragments. The final woodchuck specific primers used for TLR1-10 expression analysis are presented in Table 2.2.

### **2.7.2. Determination of Sensitivity of Detection**

To determine the sensitivity of detection for each TLR primer pair, serial 10-fold dilutions of plasmid containing TLR1-10 inserts were amplified by real-time RT-qPCR. It was determined that all TLR primer pairs were able to detect at least 100 copies of a given TLR. TLR1, TLR2, TLR6, TLR9 and TLR10 detected at a level as low as 10 copies per reaction (Table 2.2). Amplification of serial plasmid dilutions of known concentrations allowed for the generation of a standard curve for absolute quantification of a given TLR in test woodchuck tissue and PBMC samples. Samples with Ct values that fell within the standard curve range were assigned a copy number for the TLR tested.

### **2.7.3. Absolute Quantification**

Briefly, woodchuck liver, hepatocytes and PBMC samples were evaluated for expression of TLR1-10 by RT-qPCR using SsoFast™ EvaGreen® Supermix (Bio-Rad, Mississauga, Ontario), the LightCycler® 480 System, and LightCycler® 480 software (Roche Diagnostics, Mannheim, Germany). Each individual reaction included the cDNA equivalent of 50 ng of total RNA and primers specific for a given woodchuck TLR gene at a concentration of 5 pmol each. Serial 10-fold plasmid dilutions containing known copy numbers of the respected TLR were included as quantitative standards in each qPCR run. All samples were tested in triplicate. Absolute quantification of test samples was calculated using the LightCycler® 480 software based on copy numbers of

**Table 2.2. Woodchuck TLR-Specific and Housekeeping Primer Sequences Used for Expression Analysis of Woodchuck TLRs1-10 by Real-Time RT-qPCR**

Gene	Primer Sequences (5' - 3')	Length (bp)	Melting Temperature	Amplicon Size (bp)	Sensitivity of Detection (Copy Number/Reaction)
TLR1	+ CAT TTG ATG CCC TGC CTA TAT G	22	53	435	1.0x10 <sup>1</sup>
	- TAT GCC AAA CCA GCT GGA GGA T	22	55		
TLR2	+ TGA CTC TCC CTC CCA C	16	49	235	1.0x10 <sup>1</sup>
	- GTC GTA GCA GAT GTC CC	17	49		
TLR3	+ AGG GAC TTT GAG GCA GGT GT	20	54	230	1.0x10 <sup>2</sup>
	- CGC AAA CAG AGT GCA TGG T	19	51		
TLR4	+ AAG GTT TCC ATA AAA GCC G	19	47	193	1.0x10 <sup>2</sup>
	- AGT AGG CGG TAC AAC TC	17	47		
TLR5	+ GCC TTG AAG CCT TCA GTT ATG C	22	55	76	1.0x10 <sup>2</sup>
	- CCA ACC ACC ACC ATG ATG AG	20	54		
TLR6	+ GCC CAA ACC TGT GGA ATA TCT CA	23	55	424	1.0x10 <sup>1</sup>
	- CAA AGA ATT CCA GCT AAC ATC CA	23	52		
TLR7	+ GCC TGT TCT GTA AAG G	16	43	471	1.0x10 <sup>2</sup>
	- ACT CCC GGA ATG ATT G	16	43		
TLR8	+ CAC ATC CCA AAC TTT CTA TGA TG	23	52	100	1.0x10 <sup>2</sup>
	- CTC TTC AAG GTG GTA GCG C	19	53		
TLR9	+ TGG TAC TGC TTC CAC CT	17	47	358	1.0x10 <sup>1</sup>
	- ACA CCA CGA CAT CCT T	16	43		
TLR10	+ GAT GGT CAG ATT CAT ACA TCT G	22	51	124	1.0x10 <sup>1</sup>
	- ATG ATG GCC ACA ATG GTG AC	20	52		
HPRT	+ TGA CAC TGG CAA AAC AAT GCA	21	51	96	1.0x10 <sup>2</sup>
	- GGT CCT TTT CAC CAG CAA GCT	21	54		

the plasmid standards. Expression of  $\beta$ -actin was evaluated for gene housekeeping purposes and was found to be unreliable in liver and hepatocytes (see Section 3.4). Therefore, TLR expression in subsequent experiments was normalized to the expression of hypoxanthine-guanine phosphoribosyltransferase (HPRT). HPRT was chosen based on previously published works (Dheda *et al.*, 2004; de Kok *et al.*, 2005; Chen *et al.*, 2006; Nishimura *et al.*, 2006; Tsaur *et al.*, 2013). Studies comparing the expression of multiple housekeeping genes have concluded that HPRT is one of the most stably transcribed genes in human and rat livers and hepatocytes (Chen *et al.*, 2006; Nishimura *et al.*, 2006).

## **2.8. Real Time RT-qPCR for Quantification of Expression of Individual Woodchuck TLRs**

### **2.8.1. Plate Layout and Controls**

The layout for real-time RT-qPCR 96-well plates used in this study was designed to contain multiple controls for each set of TLR amplification reactions (Figure 2.1). On each plate, controls included: (1) all components of the amplification reaction except the cDNA template (no template control, NTC), (2) water was used instead of RNA template when reverse transcribing RNA to cDNA (negative RT, mock), (3) internal controls (ICs) from two healthy woodchuck livers (IC1 Liv and IC2 Liv) and spleens (IC1 Spl and IC2 Spl), (4) 10-fold serial dilutions from  $10^1$  to  $10^6$  copies of the appropriate plasmid containing a given TLR fragment as quantitative standards ( $10^1$  and  $10^6$  plasmid standards). The NTC was essential for detecting potential contamination in the PCR reagents, while the mock controlled for any contamination carryover from RT reagents.

**Figure 2.1. Plate layout for RT-qPCR quantification of individual TLRs in woodchuck samples.**

96-well plate layout used in this study for RT-qPCR quantification of individual TLRs in woodchuck liver, spleen, and PBMC samples. This layout represents a single plate that was used to quantify expression of individual TLRs in woodchucks. Each plate tested included a no template (water) control (NTC), negative RT reaction control (mock), internal natural controls (IC), woodchuck test samples, and quantitative plasmid standards ( $10^1 - 10^6$  copies). All samples were loaded in triplicate.

	1	2	3	4	5	6	7	8	9	10	11	12
A	NTC			Test Samples			Test Samples			$10^1$  $10^6$ Plasmid Standards		
B	Mock											
C	IC1 Liv											
D	IC1 Spl											
E	Test Samples											
F				Test Samples								
G							IC2 Liv					
H	Test Samples			IC2 Spl								

The expression levels of each TLR gene were previously determined for IC1 and IC2 liver and spleen cDNA. The ICs were used to assess consistency of TLR quantification throughout all runs of the assay. Expression levels of the target gene should be consistent from plate to plate, controlling for the efficiency of each PCR reaction. Finally, serial 10-fold dilutions of plasmid standards of an individual TLR were included for absolute quantification of test samples. All samples were loaded in triplicate, with NTC and mock controls loaded first to avoid potential contamination. All cDNA samples (*i.e.*, ICs and woodchuck test samples) were loaded next. Finally, all wells of the plate were carefully covered with plastic wrap before loading of the plasmid standards, which were loaded on the far right side of plate (Figure 2.1).

## **2.9. Multiplex Real-Time RT-qPCR for Simultaneous Quantification of Woodchuck TLRs1-10**

### **2.9.1. Plate Layout and Controls**

In this study, RT-qPCR quantification of TLRs1-10 was designed in a multiplex format. All TLRs are amplified under the same conditions, thus, it was possible to assess the expression of all ten TLRs in woodchuck test samples on the same PCR plate (Figure 2.2). Each plate included a NTC, mock, and a single plasmid standard ( $10^3$  copies) for each TLR. Samples were loaded in triplicate, with negative controls loaded first, then the cDNA samples (*i.e.*, ICs and test samples), followed by the plasmid standards. Again, wells of the plate were covered before loading of the plasmid standards. A representative multiplex real-time RT-qPCR plate layout is shown in Figure 2.2.

**Figure 2.2. Plate layout for multiplex RT-qPCR quantification of woodchuck TLRs1-10.**

96-well plate layout used for multiplex RT-qPCR quantification of TLRs1-10 in woodchuck tissues and cells. This layout represents a single plate to quantify woodchuck TLRs1-10 in two test samples in a single run. Each plate included a no template (water) control (NTC), negative RT reaction control (mock), two test samples (1 and 2) and a plasmid (P) standard for each TLR tested at  $10^3$  copies/reaction. All samples were loaded in triplicate.

	1	2	3	4	5	6	7	8	9	10	11	12
A	NTC			TLR4-1			TLR8-1			P3		
B	Mock			TLR4-2			TLR8-2			P4		
C	TLR1-1			TLR5-1			TLR9-1			P5		
D	TLR1-2			TLR5-2			TLR9-2			P6		
E	TLR2-1			TLR6-1			TLR10-1			P7		
F	TLR2-2			TLR6-2			TLR10-2			P8		
G	TLR3-1			TLR7-1			P1			P9		
H	TLR3-2			TLR7-2			P2			P10		

## **2.10. Animals and Categories of WHV Infection**

### **2.10.1. Categories of WHV Infection**

Woodchucks (*Marmota monax*) examined in this study were maintained in the Woodchuck Viral Hepatitis Research Facility at Memorial University of Newfoundland, St. John's, Newfoundland. Healthy animals were not exposed to WHV, as confirmed by testing of serum samples for WHV DNA by highly sensitive PCR-based assays (Michalak *et al.*, 1999). They were also negative for anti-WHc and anti-WHs, and nonreactive for WHsAg (Michalak *et al.*, 1989; Michalak *et al.*, 1999). Animals infected with WHV at doses of less than 1000 virions develop POI (Michalak *et al.*, 2004). Animals with POI are characterized by the lack of classical serological markers of WHV infection, such as WHsAg, anti-WHs and anti-WHc. However, WHV DNA is detectable in plasma and the lymphatic system. Over time, this infection can spread to the liver without induction of hepatitis (Mulrooney-Cousins and Michalak, 2015). When WHV-naïve woodchucks are infected with WHV doses greater than 1000 virions, animals develop AH where high WHV DNA levels and WHsAg are detectable in serum, as well as biochemical indicators of liver injury are evident. The initiation of AH is considered when serum WHsAg becomes detectable and serum biochemical markers of liver injury, SDH and ALT, increase. If WHsAg clears prior to 6 months post-infection, the woodchuck has spontaneously resolved AH and SLAH is diagnosed. This is accompanied by the persistence of WHV DNA at low levels and anti-WHc reactivity for life. If WHsAg persists in circulation for longer than 6 months, CH is diagnosed. In addition to serological indicators, histological examination of liver biopsies obtained in 6

– 12 month intervals are used to identify liver disease status (Michalak and Lin, 1994; Michalak *et al.*, 2000). For the purpose of this study, pre-acute hepatitis (PreAH) refers to samples collected three days post infection (dpi), prior to the establishment of serologically and biochemically confirmed AH.

### **2.10.2. Animals and Samples Examined**

This study included autopsy liver and hepatocytes isolated from these livers, liver biopsies, and PBMCs isolated from a total of 32 woodchucks. Autopsy livers and paired hepatocytes were investigated for expression of TLR1-10 from 26 woodchucks, including five healthy, four with PreAH, eight with SLAH, six with CH, and three with POI. Sequential liver biopsies acquired from 28 woodchucks were also analyzed for their TLR expression profiles, including two healthy, four with PreAH, eight with SLAH, nine with CH, and five with POI. Sixty-one liver biopsies were investigated in total. Finally, 51 sequential PBMC samples were collected from four woodchucks prior to and throughout the course of WHV infection and examined for their expression of TLR1-10. Two of the woodchucks developed AH and resolved hepatitis while acquiring SOI, and two others progressed from AH to CH. Numbers of autopsy liver samples and hepatocytes, liver biopsies and PBMCs from healthy woodchucks and different stages of WHV hepatitis are summarized in Table 2.3.

**Table 2.3. Woodchuck Samples from Different Categories of WHV Infection Used in This Study**

Sample Type	Number of Woodchucks	Sample Number and Stages of WHV Hepatitis						Total Sample Number Tested
		Healthy	PreAH	AH	SLAH	CH	POI	
Autopsy Livers	26	5	4	0	8	6	3	26
Hepatocytes	26	5	4	0	8	6	3	26
Liver Biopsies	28	20	4	8	3	12	14	61
PBMCs	4	11	8	18	6	8	0	51

PreAH, pre-acute hepatitis; AH, acute hepatitis; SLAH, self-limited acute hepatitis; CH, chronic hepatitis; POI, primary occult infection.

## **2.11. Calculation of Relative Expression**

Relative expression of TLRs1-10 in liver, hepatocyte and PBMC samples was calculated using HPRT gene expression for normalization. For each sample, the absolute expression values for TLRs1-10 and HPRT were determined based on serial 10-fold dilutions containing known copy numbers of the respected gene. The absolute expression values for TLRs1-10 were divided by the absolute expression value of HPRT.

## **2.12. Statistical analyses**

Results were analyzed by paired or unpaired Student's-t test, where applicable, using GraphPad Prism software (Graph Pad Software Inc., San Diego, California). A paired t-test was used when analyzing TLR1-10 expression in livers, and hepatocytes derived from those livers. Differences between experimental conditions were considered to be significant when two-sided P values were less than 0.05. Data bars marked with \* were significant at  $P < 0.05$ , \*\* at  $P \leq 0.01$ , \*\*\* at  $P \leq 0.001$ , and \*\*\*\* at  $P \leq 0.0001$ .

## **Chapter 3 - Results**

### **3.1. General Study Design**

The results of this study will be presented in chronological order of data collection. Using TLR primers designed based on interspecies sequence compatibility (Table 2.1), the amplification of woodchuck TLRs1-10 gene fragments was achieved. The resulting amplicons were cloned and sequenced to confirm the identity of the woodchuck gene fragment amplified. Following confirmation by automated DNA sequencing, the primer sequences were adjusted to be entirely woodchuck TLR sequence compatible (Table 2.2) and real-time RT-qPCR tests for quantification of expression of individual woodchuck TLRs1-10 were developed. When sensitivity of detection, melting curves, or amplification curves were undesirable using a specific TLR primer pair, primers were redesigned, synthesized, and tested again. Once all the real-time RT-qPCR assays were adjusted in such a way that all woodchuck TLRs could be quantified under identical amplification conditions, expression analysis was performed. Woodchuck livers, hepatocytes isolated from these livers, sequential liver biopsies and PBMCs derived from animals with different forms and stages of WHV infection were analyzed for the expression levels of TLRs1-10. To establish baseline expression, liver, hepatocytes and PBMCs from healthy woodchucks were investigated and the results from these evaluations are presented first. After establishing baseline, TLR expression throughout the course of WHV infection is presented in representative samples of woodchuck liver and paired hepatocytes, liver biopsies, and PBMC samples.

### **3.2. Woodchuck TLR1-10 Gene Fragment Identification and Their Sequence Confirmation**

TLR primer pairs designed based on interspecies homology (Table 2.1) were used to amplify fragments of the woodchuck TLR using cDNA from liver and spleen samples from healthy woodchucks. EB-agarose gel electrophoresis was used to identify the amplification product of the RT-PCR reaction for each TLR primer set. TLR1-5 and TLR7-10 primer pairs yielded bands of the predicted molecular size (Figures 3.1A – 3.5A and 3.7A – 3.10A). TLR6 primer set amplified a gene fragment of predicted base pair size from liver cDNA but not from spleen cDNA (Figure 3.6A).

The amplified gene fragments for each TLR were excised from LMP-agarose and DNA cloned using a TOPO TA cloning kit. Mini-scale preparations of the resulting plasmids were digested with *EcoRI* to determine if they contained the fragments carrying the woodchuck TLR sequences of interest. Many plasmid digests for each TLR transcript produced bands of predicted size (Figures 3.1B – 3.10B). However, TLR1 and TLR7 plasmid digests yielded additional bands of unexpected size. Clone 2 of the TLR1 digest yielded a band of approximately 400-bp, while clone 8 yielded a band of about 300-bp (Figure 3.1B). Similarly, clone 3 of the TLR7 digest yielded a band of approximately 500-bp, while clone 5 yielded a band of about 400-bp (Figure 3.7B). Clones with inserts of unexpected base pair size were excluded from further downstream processing and analysis.

**Figure 3.1. Initial PCR amplification of woodchuck-specific TLR1, analysis of minipreps of TLR1 plasmid DNA, and sequence confirmation.**

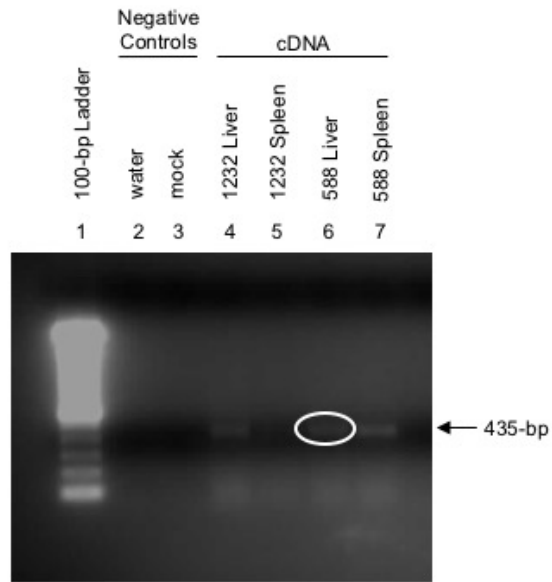
**A.** EB-agarose gel electrophoresis of PCR products amplified using TLR1 primers. 500 ng of cDNA, generated using DNase-treated RNA samples from liver and spleen tissue of two woodchucks, were used as templates. Lane 1, 100-bp ladder; lane 2, water (negative PCR control); lane 3, RT mock (negative cDNA control); lane 4, liver sample (cDNA from woodchuck 1232); lane 5, spleen sample (cDNA from 1232); lane 6, liver sample (cDNA from woodchuck 588); lane 7, spleen sample (cDNA from 588). Arrows indicate the 435 bp-specific amplicon. The white circle indicates the band that was purified and inserted into plasmid DNA.

**B.** Analysis of *Eco*RI-digested minipreps of TLR1 plasmid DNA using EB-gel electrophoresis. Lane 1, 100-base pair ladder; lanes 2 - 11, clone #1 to clone #10. Multiple clones showed a band of 435-bp, while bands of approximately 400-bp were detected in lanes 3 and 9. The white circle indicates the clone that was sequenced.

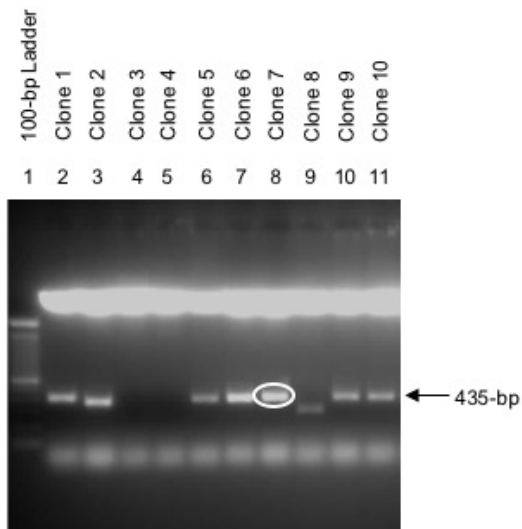
**C.** Woodchuck TLR1 gene fragment determined by automated DNA sequencing.

**D.** Nucleotide BLAST result comparing woodchuck TLR1 sequence homology with other mammalian species reported.

**A**



**B**



## C

### Woodchuck TLR1 435-bp fragment

```
1 5'- CATTGATGC CCTGCCTATA TGCAAAGAGT TTGGCAGCAT
41 GTCTCAGCTA AAATTTCTGG GATTGAGTGC TACACAGTTA
81 GAAAAATCTC GTGTGCAGCC AATTGCTCAT TTGAATATCA
121 GTAAGATTTT GCTAGTTTTA GGAGAGACTT ATGGGGAAAA
161 AGAAGATCCT GAGAGTCTTC AGGACTTTAA CACAGACAGT
201 CTGCATATTG TTTTCCCTGT GAAAAAGGTA TTCCATTTTA
241 TTTTGGATAT GTCAGTAAGC ACTGCGATAA GTTTGGAAct
281 GTCTAATATC AAATGTGTGC TAGACAGTGA GTGTTCTTAT
321 TTCCTAAGTG CTTTGGTAAA ACTTCAAAAC AATCCAAGGC
361 TATTGAATCT TACCTTGAAC AACATTGAAA CAACTTGGAA
401 TTCATTCATT AATATCCTCC AGCTGGTTTG GCATA - 3'
```

## D

---

Species	GenBank Accession Number	% Nucleotide Homology
Human	AB445617.1	86
Chimpanzee	KF319575.1	86
Gorilla	KF319525.1	86

---

**Figure 3.2. Initial PCR amplification of woodchuck-specific TLR2, analysis of minipreps of TLR2 plasmid DNA, and sequence confirmation.**

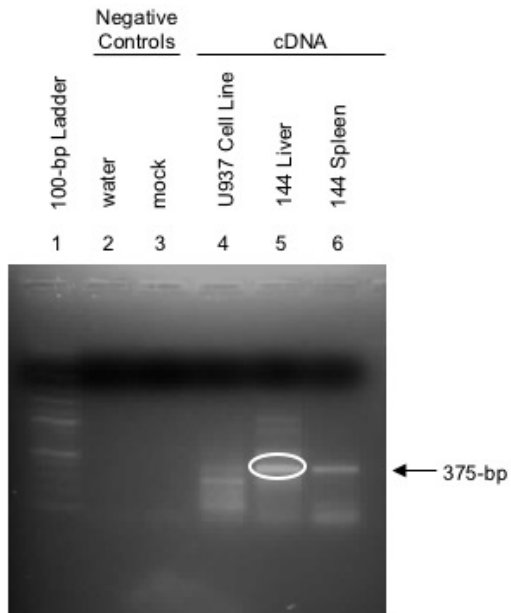
**A.** EB-agarose gel electrophoresis of PCR products amplified using TLR2 primers. 500 ng of cDNA that was generated using DNase-treated RNA from indicated cell or tissue samples were used as templates. Lane 1, 100-bp ladder; lane 2, water (negative PCR control); lane 3, mock (negative RT control); lane 4, human U937 cell line (macrophage cell line used as positive control); lane 5, liver sample from woodchuck 144; lane 6, spleen sample from woodchuck 144. Arrows indicate the 375 bp-specific amplicon. The white circle indicates the band that was purified and inserted into plasmid DNA.

**B.** EB-gel electrophoresis of miniprep products of TLR2 cloning reactions. Lane 1, 100-bp ladder; lanes 2 - 7, TLR2 clone #1 to clone #6. Clones #5 and #6 showed expected molecular size of bands. The white circle indicates clone that was processed for sequencing.

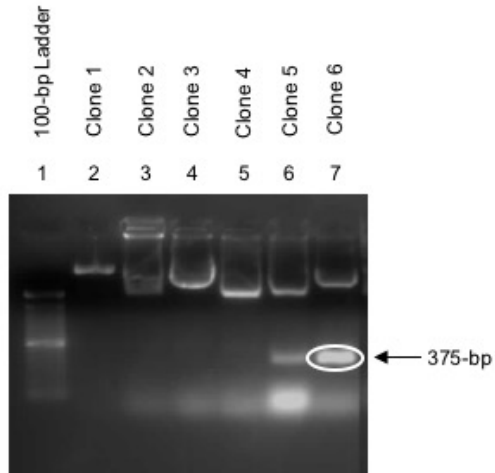
**C.** Woodchuck TLR2 gene fragment determined by automated DNA sequencing.

**D.** Nucleotide BLAST result comparing woodchuck TLR2 sequence homology with other mammalian species reported.

**A**



**B**



## C

### Woodchuck TLR2 375-bp fragment

```
1   5'- TGCTCCTGTG AATTCCTCTC CTTCACTCAG CAGCAGCCAG
41  CTCTGGCCCA GGTGCTGGTG GACTGGCCAG ACAGCTACCT
81  GTGTGACTCT CCCTCCCACG TGC GCGGCCA GCGGGTGCTC
121 GACGTCCGGC TCTCCGCCTC CGAGTGCCAC CGGGTGGCGC
161 TGGTGTCTGG CGTGTGCTGT GCCCTCTTCC TGTTGATCCT
201 GCTCACGGGG GGCCTGTGCC ACCGCTTCCA CGGTGTGTGG
241 TACCTGAAGA TGATGTGGGC CTGGCTCCAG GCCAAAAGGA
281 AGCCCCGGAA GGC GCCGTGC AGGGACATCT GCTACGACGC
321 GTTCGTCTCC TACAGCGAGC GGGACTCCCA CTGGGTGGAG
361 AACCTTATGG TCCAG - 3'
```

## D

---

Species	GenBank Accession Number	% Nucleotide Homology
Woodchuck	HQ446273.1*	98
Wild Pig	AY289531.1	86
Antelope	EU580541.1	86
Sheep	AY957613.1	85
Rhesus Macaque	EU204933.1	85
Gorilla	KF319742.1	84

---

\*Previously reported woodchuck TLR2 sequence (Unpublished Paper).

**Figure 3.3. Initial PCR amplification of woodchuck-specific TLR3, analysis of minipreps of TLR3 plasmid DNA, and sequence confirmation.**

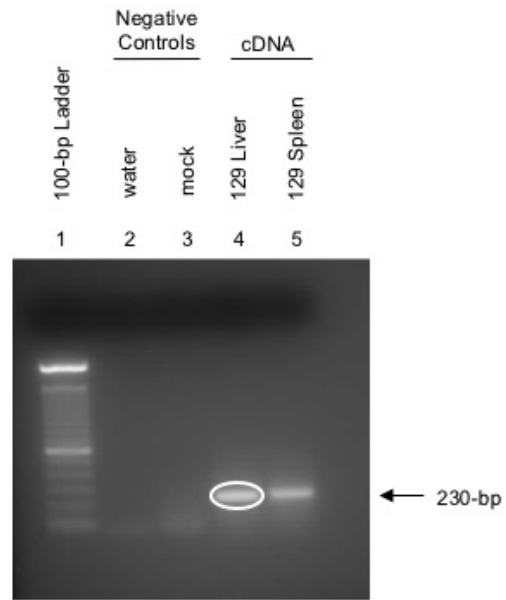
**A.** EB-agarose gel electrophoresis of PCR products amplified using TLR3 primers. 500 ng of cDNA, generated using DNase-treated RNA from liver and spleen tissue samples, were used as templates. Lane 1, 100-bp ladder; lane 2, water; lane 3, mock; lane 4, liver from woodchuck 129; lane 5, spleen from woodchuck 129). Arrows indicate the expected 230 bp amplicon. The white circle indicates the band that was purified and cloned.

**B.** EB-gel electrophoresis of miniprep products from TLR3 cloning reaction. Lane 1, 100-bp ladder; lane 2 - 11, TLR3 clone #1 to clone #10. Multiple clones demonstrated bands of expected molecular size of 230-bp. The white circle indicates the clone that was sequenced.

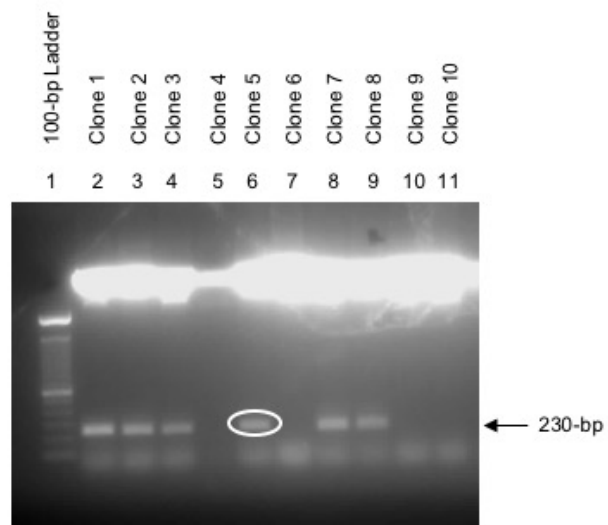
**C.** Woodchuck TLR3 gene fragment determined by automated DNA sequencing.

**D.** Nucleotide BLAST result comparing woodchuck TLR3 sequence identified with other mammalian species reported.

**A**



**B**



## C

### Woodchuck TLR3 230-bp fragment

```
1 5'- AGGGACTTTG AGGCAGGTGT CCTTGGACTT GAAGCAATTG
41 TTAATAGTAT TAAAAGGAGC AGAAAAATTA TTTTGTAT
81 TACACAGCAT CTATTAAG ATCCATTATG CAAAAGATTC
121 AAGGTGCACC ATGCAGTTCA GCAAGCAATT GAACAAAATC
161 TGGATTCCAT TATATTGATT TTTCTTGAGG AGATTCCGGA
201 TTATAAACTA AACCATGCAC TCTGTTTGCG - 3'
```

## D

Species	GenBank Accession Number	% Nucleotide Homology
Woodchuck	EU586552.1*	100
Wild Pig	KC011280.1	93
Yak	KF990165.1	93
Sheep	NM_001135928.1	93
Cow	AY124007.1	93

\*Primers used in this study were previously published in Zhang et al., 2009. Therefore, sequence identified has 100% homology with sequence previously reported.

**Figure 3.4. Initial PCR amplification of woodchuck-specific TLR4, analysis of minipreps of TLR4 plasmid DNA, and sequence confirmation.**

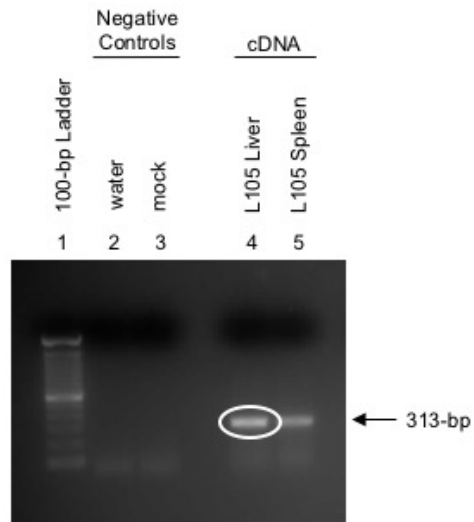
**A.** EB-agarose gel electrophoresis of PCR products amplified using TLR4 primers. 500 ng of cDNA, generated using DNase-treated RNA from liver and spleen tissue samples, were used as templates. Lane 1, 100-bp ladder; lane 2, water; lane 3, mock; lane 4, liver cDNA from woodchuck 105; lane 5, spleen cDNA from woodchuck 105. Arrows indicate the expected 313 bp amplicon. The white circle indicates the band that was purified and inserted into plasmid DNA.

**B.** EB-gel electrophoresis of miniprep products from TLR 4 cloning reaction. Lane 1, 100-bp ladder; lanes 2 - 9, TLR4 clone #1 to clone #8. Multiple clones showed the expected molecular size of 313-bp. The white circle indicates the clone that was subsequently sequenced.

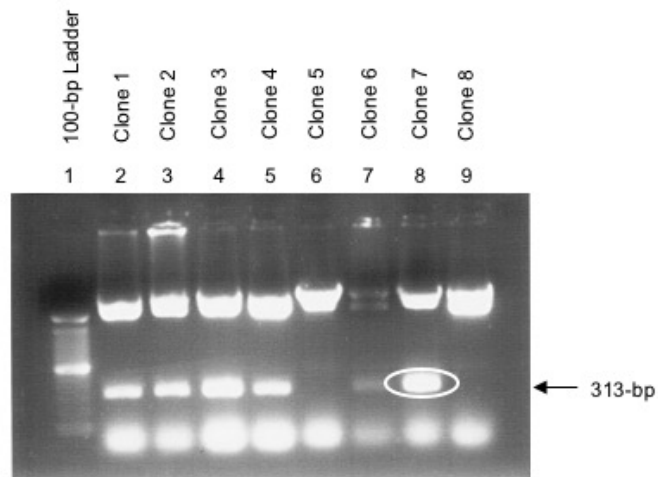
**C.** Woodchuck TLR4 gene fragment determined by automated DNA sequencing.

**D.** Nucleotide BLAST results comparing woodchuck TLR4 sequence with other mammalian species reported.

**A**



**B**



## C

### Woodchuck TLR4 313-bp fragment

```
1 5'- CTCTGCCTTC ACTACAGAGA CTTTATTCCT GGTGTGGCTA
41 TTGCAGCCAA CATCATCCAG GAAGGTTTCC ATAAAAGCCG
81 GAAGGCATA GTGGTGGTCT CTCAGCACTT CATCCAGAGC
121 CGCTGGTGTA TCTTTGAATA TGAGATTGCT CAGACCTGGC
161 AGTTCCTGAG CAGCCACGCT GGCATCATT TCATTGTCCT
201 GCAGAAGGTG GAGAAGTCCC TGCTCCGGCA GCAGGTGGAG
241 TTGTACCGCC TACTCAGCAG GAACACTTAC CTGGAATGGG
281 AGGACAGTGT CCTGGGGCGG CACATCTTCT GGA - 3
```

## D

---

Species	GenBank Accession Number	% Nucleotide Homology
Woodchuck	EU586553.1*	100
Human	NM_138557.2	93
Chimpanzee	KF320634.1	93
Gorilla	KF320567.1	93

---

\*Previously reported woodchuck TLR4 sequence (Zhang et al., 2009).

**Figure 3.5. Initial PCR amplification of woodchuck-specific TLR5, analysis of minipreps of TLR5 plasmid DNA, and sequence confirmation.**

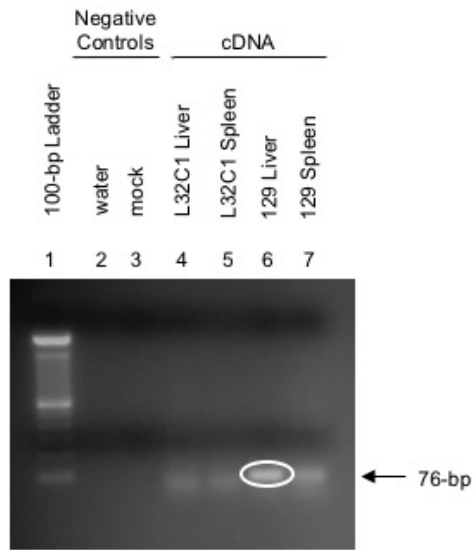
**A.** EB-agarose gel electrophoresis of PCR products amplified using TLR5 primers. 500 ng of cDNA was generated after DNase treatment of isolated RNA and used as a template. Lane 1, 100-bp ladder; lane 2, water (negative PCR control); lane 3, mock (negative RT control); lane 4, liver cDNA from woodchuck 32C1; lane 5, spleen cDNA from woodchuck 32C1; lane 6, liver cDNA from woodchuck 129; lane 7, spleen cDNA from woodchuck 129. Arrows indicate the 76 bp-specific amplicon. The white circle indicates the band that was purified and inserted into plasmid DNA.

**B.** EB-gel electrophoresis of miniprep products from TLR5 cloning reaction. Lane 1, 100-bp ladder; lanes 2 - 16, TLR5 clone #1 to clone #15. Clone #12 and clone #14 showed expected molecular size of the bands observed. Both clones were sequenced (marked by white circles).

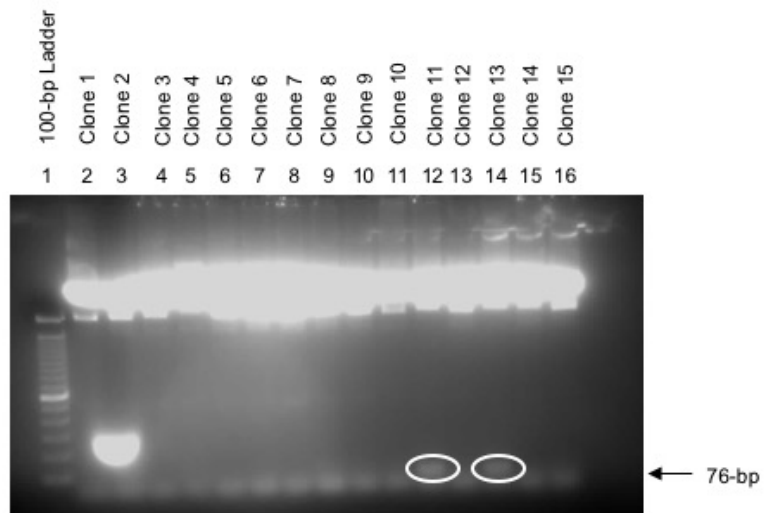
**C.** Woodchuck TLR5 gene fragment determined by automated DNA sequencing.

**D.** Nucleotide BLAST result comparing TLR5 sequence homology with other mammalian species reported.

**A**



**B**



## C

### Woodchuck TLR5 76-bp fragment

1    5'- GCCTTGAAGC CTTCAGTTAT GCCCAGAGCA GGTGCCTCTC  
41    TGACCTCAGC AGTGCCTCA TCATGGTGGT GGTTGG - 3'

## D

---

Species	GenBank Accession Number	% Nucleotide Homology
Water Buffalo	NM_001290918.1	89
Yak	KJ101606.1	88
Cattle	GQ866979.1	88

---

**Figure 3.6. Initial PCR amplification of woodchuck-specific TLR6, analysis of minipreps of TLR6 plasmid DNA, and sequence confirmation.**

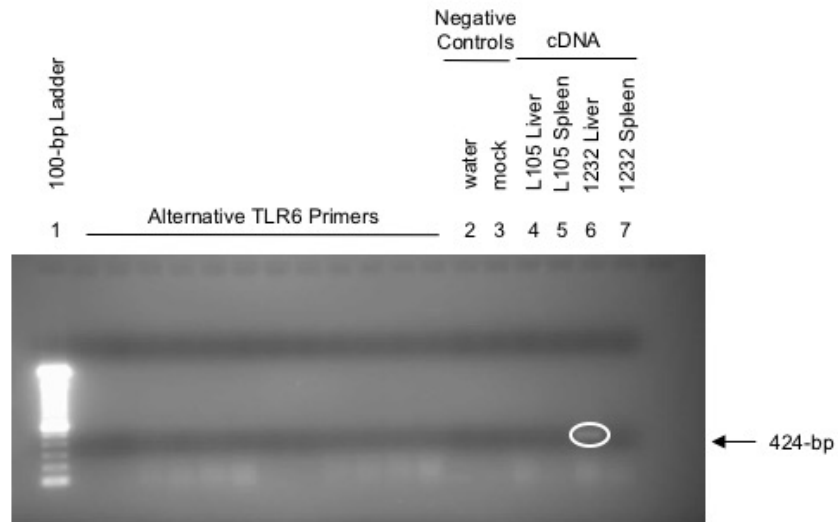
**A.** EB-agarose gel electrophoresis of PCR products amplified using TLR6 primers. 500 ng of cDNA, generated using DNase-treated RNA from liver and spleen tissue samples indicated, were used as templates. Lane 1, 100-bp ladder; lane 2, water (negative PCR control); lane 3, mock (negative RT control); lane 4, liver cDNA from woodchuck 105; lane 5, spleen cDNA from woodchuck 105; lane 6, liver cDNA from woodchuck 1232; lane 7, spleen cDNA from woodchuck 1232. Arrows indicate the 424 bp-specific amplicon. The white circle indicates the band that was purified and inserted into plasmid DNA.

**B.** EB-gel electrophoresis of miniprep products from TLR6 cloning reaction. Lane 1, 100-bp ladder; lanes 2 - 10, TLR6 clone #1 to clone #9. Multiple clones showed expected molecular size of bands. The white circle indicates clone that was sequenced.

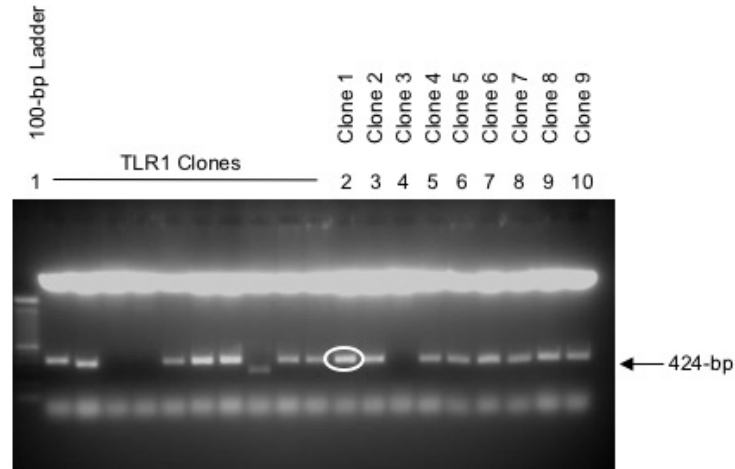
**C.** Woodchuck TLR6 gene fragment determined by automated DNA sequencing.

**D.** Nucleotide BLAST result comparing woodchuck TLR6 sequence identified in this study with other mammalian species reported.

**A**



**B**



## C

### Woodchuck TLR6 424-bp fragment

```
1   5'- GCCCAAACCT GTGGAATATC TCAATATTTA CAATTTAACA
41  ATAGTCGAAA GCATTAATGA AGAAGATTTT GCTTATTCTG
81  AAACAGCACT GAAAGCATT A AAATAGAAC ATATTA AAAA
121 CCAAGTTTTT ATCTTCTCAC AGACAGCGTT GTACACAGTG
161 TTTTCTGAGA TGAACATTAT GATGTTAACC ATATCAGACA
201 CACCTTTTAT TCATATGCTT TGTCCTCAAG CACCAAGCAC
241 ATTTAAATTT TTGAACTTTA CCCAGAATGT GTTCACAGAT
281 AGTGTTTTTC AAAACTGTTC CACTTTAGTG CAATTGGAGA
321 CACTTATCTT GCAAAAAAAT GGATTAAAAA ACCTTTGTAA
361 AGTATCTCTC ATGACAAAGA ATATGCCGTC CTTGGAATTC
401 CTGGATGTTA GCTGGAATTC TTTG - 3'
```

## D

---

Species	GenBank Accession Number	% Nucleotide Homology
Long-tailed Macaque	NM_001319617.1	90
Rhesus Macaque	NM_001130430.1	90
Chimpanzee	KF320918.2	89
Gorilla	KF320867.1	89
Human	AB445652.1	89

---

**Figure 3.7. Initial PCR amplification of woodchuck-specific TLR7, analysis of minipreps of TLR7 plasmid DNA, and sequence confirmation.**

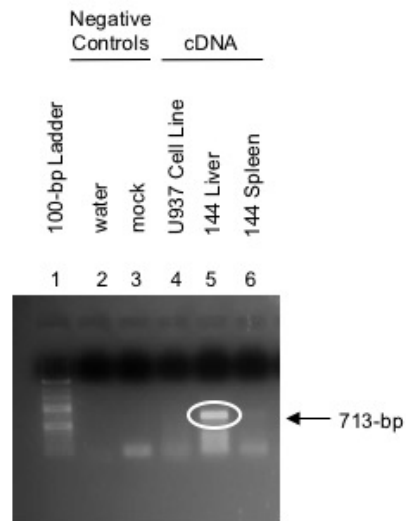
**A.** EB-agarose gel electrophoresis of PCR products amplified using TLR7 primers. 500 ng of cDNA, generated using DNase-treated RNA from cell and tissue samples, were used as templates. Lane 1, 100-bp ladder; lane 2, water; lane 3, mock; lane 4, human U937 cell line cDNA (macrophage cell line used as expected positive control); lane 5, liver cDNA from woodchuck 144; lane 6, spleen cDNA from woodchuck 144. Arrows indicate the 713 bp-specific amplicon. The white circle indicates the band that was purified and inserted into plasmid DNA.

**B.** EB-gel electrophoresis of miniprep products from TLR7 cloning reaction. Lane 1, 100-bp ladder; lane 2 - 7, TLR7 clone #1 to clone #6. Clone #2 band showed expected molecular size of 713-bp. Clone #2 DNA was processed and sent for sequencing.

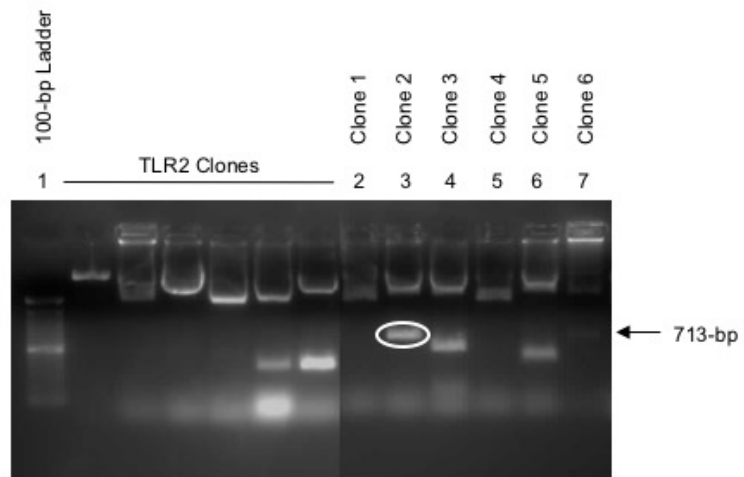
**C.** Woodchuck TLR7 gene fragment determined by automated DNA sequencing.

**D.** Nucleotide BLAST result comparing woodchuck TLR7 sequence identified in this study with other mammalian species reported.

**A**



**B**



## C

### Woodchuck TLR7 713-bp fragment

```

1   5'- GCTGTATGGT TTGTCTGGTG GGTAAATCAC ACGGAGGTGA
41  CTATTCCTTA CCTGGCCACA GAAGTGA CTT GTGTGGGGCC
81  AGGAGCACAC AAAGGCCAGA GTGTGGTCTC TCTGGATCTG
121 TATACCTGTG AGTTAGATCT CACTAACTTG ATTCTGTTCT
161 CATTTTCCAT ATCTACAGCT CTCTTTCTGA TGGTGGTTAT
201 GACAGCAAGT CACCTCTATT TCTGGGATGT ATGGTATTTT
241 TACCATTTCT GTAAGGCCAA GATAAGGGGG TATCAGCATC
281 TGCTATCAAC AGGTTCTTGC TATGATGCTT TTATTGTATA
321 TGACACTAAA GATCCAGCTG TGACAGAATG GGTTTTTGAG
361 GAGTTGGTGG CCCAATTAGA AGATCCACGA GAGAAACATT
401 TTAATTTATG TCTGGAGGAG AGAGACTGGC TACCAGGGCA
441 GCCAGTTCTG GAAAATCTTT CCCAGAGCAT ACAGCTTAGC
481 AAAAAAGACAG TGTTTGTGAT GACAGACAAG TACGCAAAGA
521 CTGAAAATTT CAAGATAGCA TTTTACTTGT CCCATCAGAG
561 GTCATGGAT GAAAAAGTAG ATGTGATTAT CTTGATATTC
601 CTTGAGAAGC CCCTTAAGAA GTCCAAGTTT CTCCAGCTCC
641 GGAAGAGGCT CTGTGGGAGT TCTGTCCTTG AGTGGCCAAC
681 AAATCCACAG GCTCACCCAT ACTTCTGGCA GTG - 3'

```

## D

Species	GenBank Accession Number	% Nucleotide Homology
Woodchuck	KT013099.1*	99
Orangutan	AB445663.1	92
Chimpanzee	KF321069.1	92
Gorilla	KF321036.1	92
Human	AB445659.1	92

\*Previously reported woodchuck TLR4 sequence (Menne et al., 2015).

**Figure 3.8. Initial PCR amplification of woodchuck-specific TLR8, analysis of minipreps of TLR8 plasmid DNA, and sequence confirmation.**

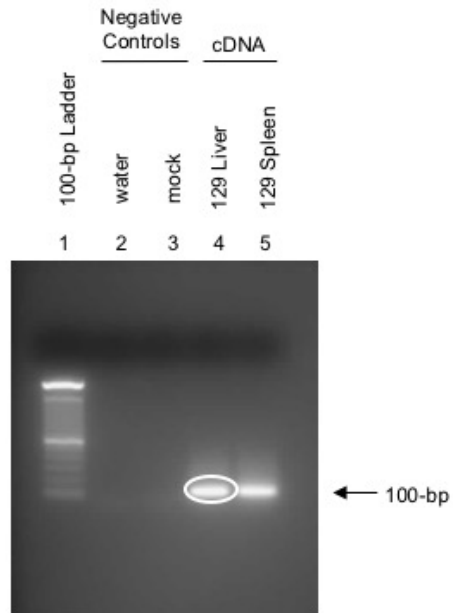
**A.** EB-agarose gel electrophoresis of PCR products amplified using TLR8 primers. 500 ng of cDNA, generated using DNase-treated RNA from liver and spleen tissue samples, were used as templates. Lane 1, 100-bp ladder; lane 2, water; lane 3, mock; lane 4, liver cDNA from woodchuck 129; lane 5, spleen cDNA from woodchuck 129. Arrows indicate the 100 bp-specific amplicon. The white circle indicates the band that was purified and inserted into plasmid DNA.

**B.** EB-gel electrophoresis of miniprep products from TLR8 cloning reaction. Lane 1, 100-bp ladder; lanes 2 - 11, TLR8 clone #1 to clone #10. Several clones produced expected molecular size of 100-bp. The white circle indicates the clone that was sequenced.

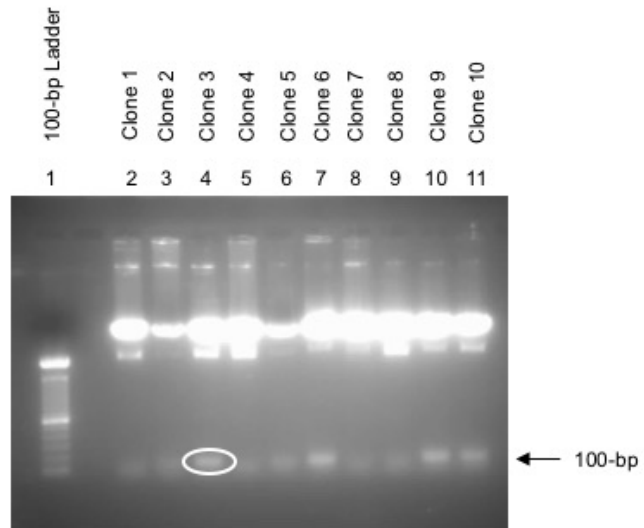
**C.** Woodchuck TLR8 gene fragment determined by automated DNA sequencing.

**D.** Nucleotide BLAST result comparing woodchuck TLR8 sequence homology with other mammalian species reported.

**A**



**B**



## C

### Woodchuck TLR8 100-bp fragment

1 5'- CACATCCCAA ACTTTCTATG ATGCTTACAT TTCTTATGAC  
41 ACCAAAGATG CCTCTGTTAC TGATTGGGTA ATCAATGAGC  
81 TCGCTACCA CCTTGAAGAG - 3'

## D

---

Species	GenBank Accession Number	% Nucleotide Homology
Human	DQ023140.1	97
Chimpanzee	KF321313.1	97
Gorilla	KF321278.1	97
Rhesus Macaque	NM_001130427.1	97

---

**Figure 3.9. Initial PCR amplification of woodchuck-specific TLR9, analysis of minipreps of TLR9 plasmid DNA, and sequence confirmation.**

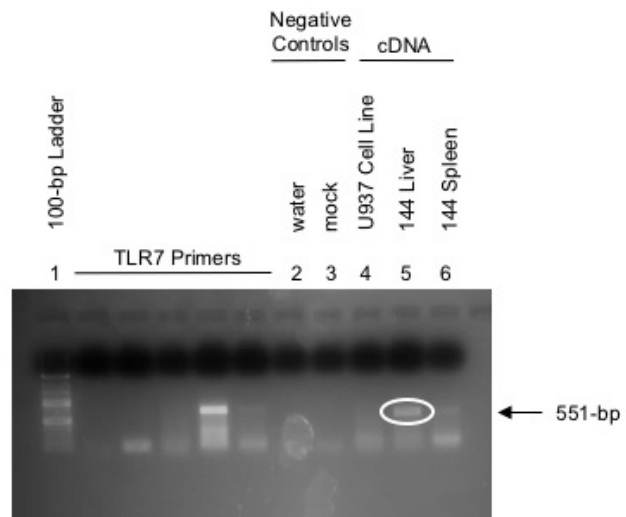
**A.** EB-agarose gel electrophoresis of PCR products amplified using TLR9 primers. 500 ng of cDNA, generated using DNase-treated RNA from cell line and tissue samples, were used as templates. Lane 1, 100-bp ladder; lane 2, water; lane 3, mock; lane 4, human U937 cell line cDNA (macrophage cell line used as expected positive control); lane 5, liver cDNA from woodchuck 144; lane 6, spleen cDNA from woodchuck 144. Arrows indicate the 551 bp-specific amplicon. The white circle indicates the band that was purified and inserted into plasmid DNA.

**B.** EB-gel electrophoresis of miniprep products from TLR9 cloning reaction. Lane 1, 100-bp ladder; lane 2 - 7, TLR9 clone #1 to clone #6. Three clones demonstrated bands of expected molecular size of about 551-bp. The white circle indicates the clone that was sequenced.

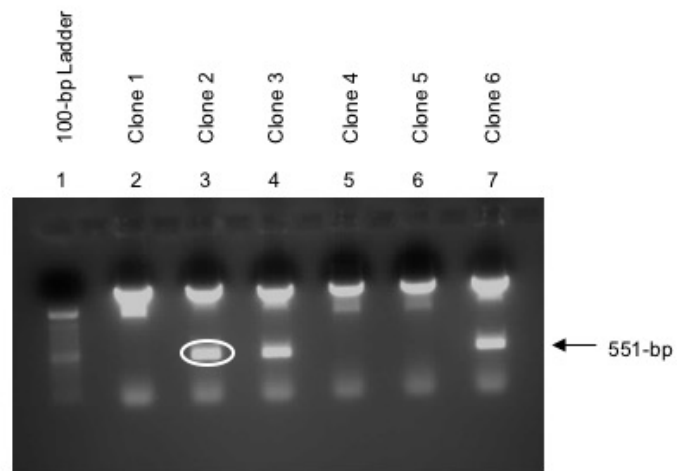
**C.** Woodchuck TLR9 gene fragment determined by DNA sequencing.

**D.** Nucleotide BLAST result comparing woodchuck TLR9 sequence identified in this study with other mammalian species reported.

**A**



**B**



# C

## Woodchuck TLR9 551-bp fragment

```
1   5'- CTCTGCGGCT GGGACGTCTG GTACTGCTTC CACCTGGGCC
41  TGGCCTGGCT TCCCTTGCGG CGCGGCACCC GCGCCCTGCC
81  CTACGATGCC TTCGTGGTCT TCGACAAGGC GCAGAACGCG
121 GTGGCTGACT GGGTGTACAA TGAGCTGCGG GTGAGGCTAG
161 AGGAGCGTCG CGGACGCCGC GCGCTCCGTC TTTGCCTGGA
201 GGAGCGGGAT TGGCTGCCGG GCAAATCACT CTTCGAGAAC
241 CTGTGGGCCT CGGTCTATGG CAGCCGAAAG ACTCTCTTTG
281 TGCTGGACCA CACGGATCGG GTCAGTGGCC TCTTGCGCAC
321 CAGCTTCCTG CTAGCCCGGC AGCGCCTGCT GGAGGACCGC
361 AAGGATGTCG TGGTGTGGT GATCCTGCGC CCGGACGCCC
401 GCCGCTCCCG CTACGTGCGG CTGCGCCAGC GCCTCTGCCG
441 CCAGAGCGTC CTCTTTTGGC CCCACCAGCC CAGTGGTCAG
481 GGCAGCTTCT GGGCTCAGTT GAGCACGGCC CTGACCAGGG
521 ACAACCGCCA CTTCTATAAC CGGAACTTCT G - 3'
```

# D

---

Species	GenBank Accession Number	% Nucleotide Homology
Human	NM_017442.3	87
Cat	AY859724.1	87
Chimpanzee	KF321433.1	87
Sheep	NM_001011555.1	86

---

**Figure 3.10. Initial PCR amplification of woodchuck-specific TLR10, analysis of minipreps of TLR10 plasmid DNA, and sequence confirmation.**

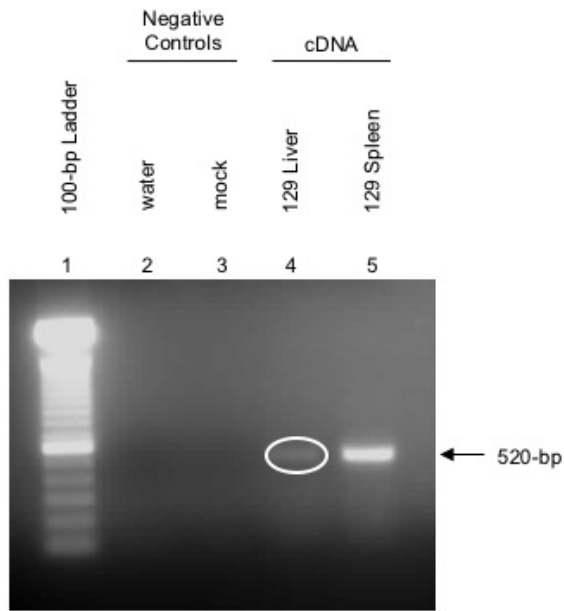
**A.** EB-agarose gel electrophoresis of PCR products amplified using TLR10 primers. 500 ng of cDNA, generated using DNase-treated RNA from liver and spleen tissue samples indicated, were used as templates. Lane 1, 100-bp ladder; lane 2, water; lane 3, mock; lane 4, liver cDNA from woodchuck 129; lane 5, spleen cDNA from woodchuck 129. Arrows indicate the 520 bp-specific amplicon. The white circle indicates the band that was purified and inserted into plasmid DNA.

**B.** EB-gel electrophoresis of miniprep products from TLR10 cloning reaction. Lane 1, 100-bp ladder; lane 2 - 11, TLR10 clone #1 to clone #10. Several clones showed expected molecular size of bands. The white circle indicates the clone that was sequenced.

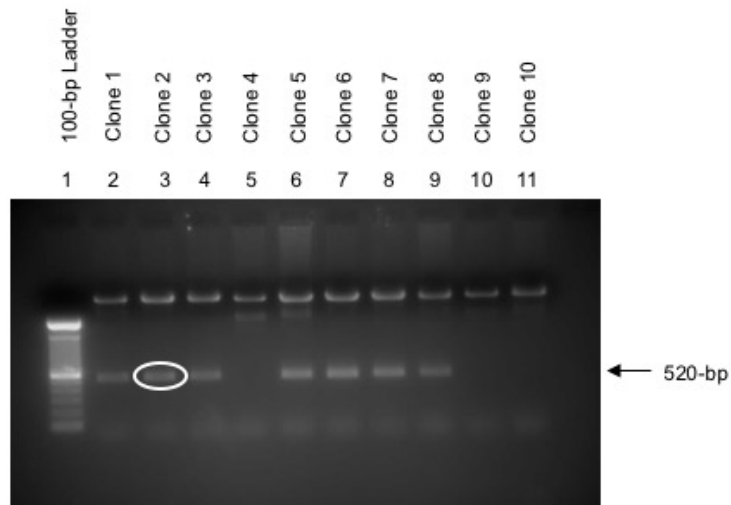
**C.** Woodchuck TLR10 gene fragment determined by automated DNA sequencing.

**D.** Nucleotide BLAST result comparing woodchuck TLR10 sequence homology with other mammalian species reported.

**A**



**B**



# C

## Woodchuck TLR10 520-bp fragment

```
1 5'- ATCCATTCCG GTGTAATTGT GAATTAAGAG ATTCATTCA
41 GCTTGAAAAA TATTCAGAGG GCATGATGAT TGGATGGTCA
81 GATTCATACA TCTGTGAATA CCCTTTGAAT GTAAAGGGGA
121 CTCGGTTGAA AGATGTTGAT CTTCTGAAT TGTCTTGCAA
161 CACAGCTTTG TTGGTTGTCA CCATTGTGGC CATCATGACC
201 ATTCTGGGGG TGACCGTGGC CTTCTGCTAC CTTGCTTGG
241 ATCTGCTTTG GTACTTCAGG ATGCCAGTTC AATGGGCACA
281 AACCTGTCAC AGGGTTAGGA GGACAGCACA AGAACAACTT
321 AAGAGCAATG TCCAATTCCA GGCATTTATT TCCTACAGTG
361 AACATGATTC TCTCTGGGTG AAGAATGAAT TGATCCCCAA
401 TCTAGAGAAA GAAGATGGTT CTGTTTTGAT TTGTCTTCT
441 GAGAGAACT TTGACCCTGG CAAGAGCATT GCTGAAAATA
481 TCATAAGGTG CATTGAGAAA AGCTATAAGT CCATCTTTGT - 3'
```

# D

---

Species	GenBank Accession Number	% Nucleotide Homology
Rhesus Macaque	NM_001130434.1	87
Chimpanzee	KF321589.1	86

---

Mini-scale preparations of the plasmids carrying inserts of the expected base-pair size yielded a sufficient amount of material to perform sequencing, thus providing validation that the bands of interest were indeed woodchuck TLRs. Automated sequencing of the amplified fragments yielded a 435-bp sequence for woodchuck TLR1 (calculated molecular mass of 268.61 kDa), 375-bp sequence specific for TLR2 (calculated molecular mass of 231.64 kDa), 230-bp sequence specific for TLR3 (calculated molecular mass of 141.96 kDa), 313-bp sequence specific for TLR4 (calculated molecular mass of 193.29 kDa), 76-bp sequence specific for TLR5 (calculated molecular mass of 46.84 kDa), 424-bp sequence specific for TLR6 (calculated molecular mass of 261.80 kDa), 713-bp sequence specific for TLR7 (calculated molecular mass of 440.40 kDa), 100-bp sequence specific for TLR8 (calculated molecular mass of 61.66 kDa), 551-bp sequence specific for TLR9 (calculated molecular mass of 340.43 kDa) and a 520-bp sequence specific for TLR10 (calculated molecular mass of 321.15 kDa) (Figure 3.1C – 3.10C). Alignment of each TLR sequence with published sequences deposited in GenBank using the basic local alignment search tool (BLAST) allowed for comparison (by percent homology in the nucleotide sequence) between woodchuck TLRs and those of other mammalian species. All woodchuck TLRs1-10 gene fragments shared a nucleotide homology equal to or greater than 84% with either human, other higher primates, or even-toed hoofed animals, such as the sheep or cow (Figure 3.1D – 3.10D).

Once it was confirmed that each woodchuck TLR was amplified, large quantities of each plasmid were produced. By performing maxipreps of the plasmids, woodchuck

specific TLRs1-10 sequences are now available in Dr. Michalak's laboratory for use in further applications.

### **3.3. Optimization of Real-time RT-qPCR Conditions for Absolute Quantification of Woodchuck TLRs1-10**

#### **3.3.1. Primer Specificity**

To ensure specificity of real-time RT-qPCR amplification, it was important to perform  $T_m$  (melting temperature) calling analysis (Roche Life Sciences, LightCycler® 480 Software, Version 1.5). A  $T_m$  calling analysis determines the temperature at which amplified dsDNA product melts or dissociates into ssDNA. As the reaction temperature increases, the sample fluorescence decreases due to dsDNA product separation; the fluorescent DNA binding dye (SYBR® green) is specific for dsDNA and will separate from the amplicon as it denatures. The resulting fluorescent profile will identify the characteristic melting peak of a product. The melting temperature of a given amplification product depends on nucleotide sequence, the length of the sequence, and guanine-cytosine to adenine-thymine (GC/AT) ratio (Roche Life Sciences, 2008). If the primers are specific, the melting profile will show only a single peak indicating the presence of a single product. A  $T_m$  calling analysis was performed on all TLRs amplified with primer pairs designed in this study (see Table 2).

The specificity of TLR1-10 primer pairs was determined by analyzing melting curves and melting peaks. Figures 3.11A and 3.12A illustrate melting peaks obtained

**Figure 3.11. An example of real-time RT-qPCR optimization and determination of the assay sensitivity for detection of woodchuck TLR4.**

**A.** cDNA from PBMC samples (n=20) and 10-fold serial dilutions of known concentrations of TLR4 plasmid ( $10^6$  –  $10^1$  copies) were amplified using woodchuck TLR4-specific primers. The resulting melting peaks for TLR4 plasmid standards (top) and both standards and amplicons of test PBMCs (bottom) are displayed. Single peaks obtained indicate that TLR4-specific products were amplified using both the plasmid standards and PBMC samples.

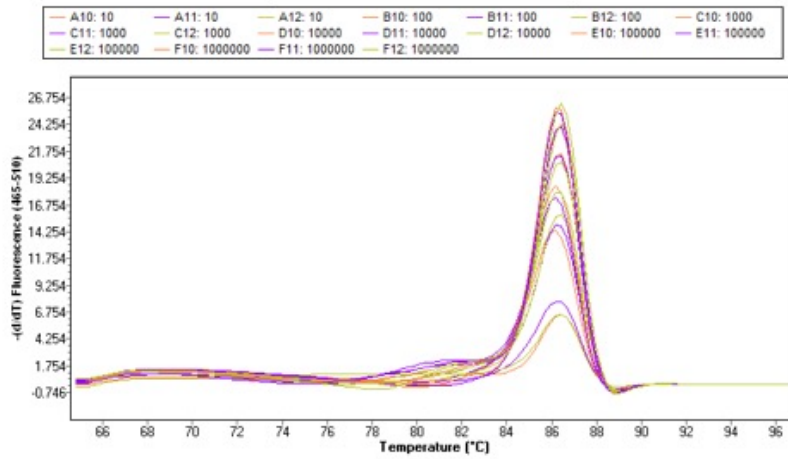
**B.** Amplification curves for TLR4 plasmid standard dilutions showing amplification of  $10^6$  copies down to  $10^1$  copies per reaction (left to right).

**C.** The resulting plot generated from amplification of TLR4 plasmid standards. The standard curve had an error of 0.0160, efficiency of 1.979 and a slope of -3.374.

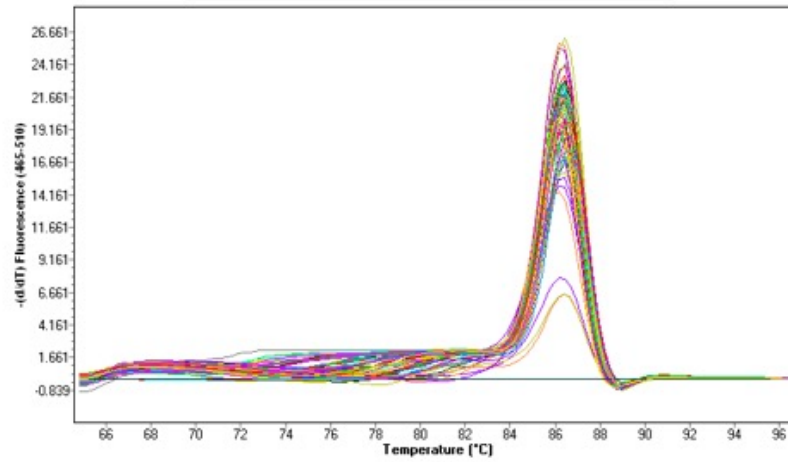
**D.** Overlay of amplification curves for both TLR4 plasmid standards and tested PBMC samples. PBMC cDNA samples were amplified and produced amplification curves within the range of the standard curve, thus, allowing for absolute TLR4 quantification in PBMCs based on known copy numbers of the TLR4 plasmid standards.

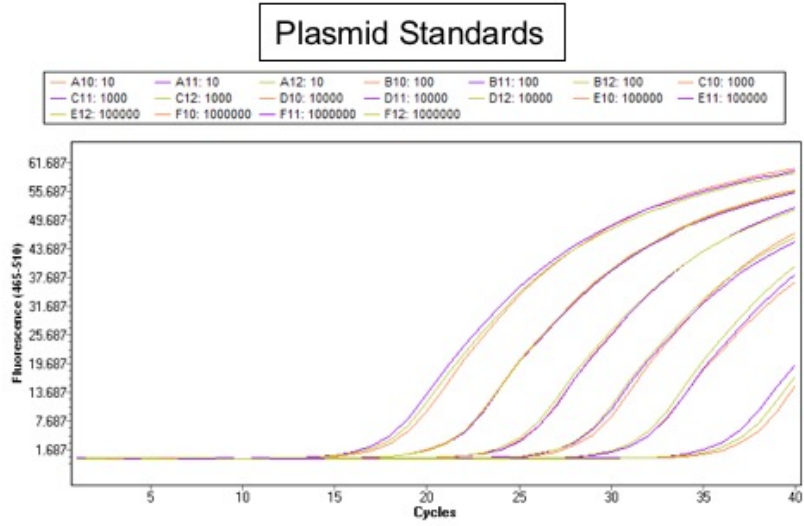
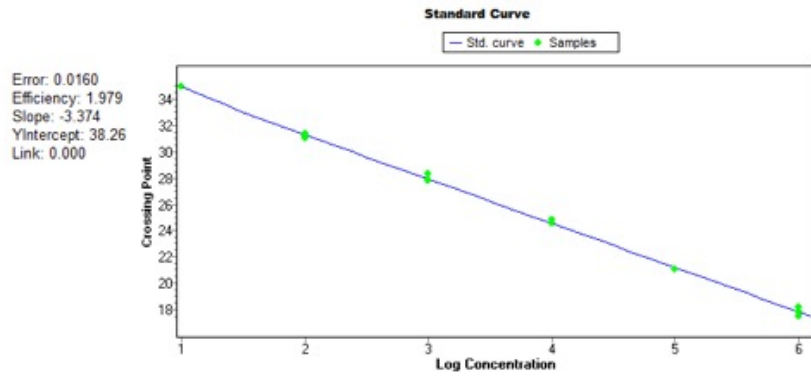
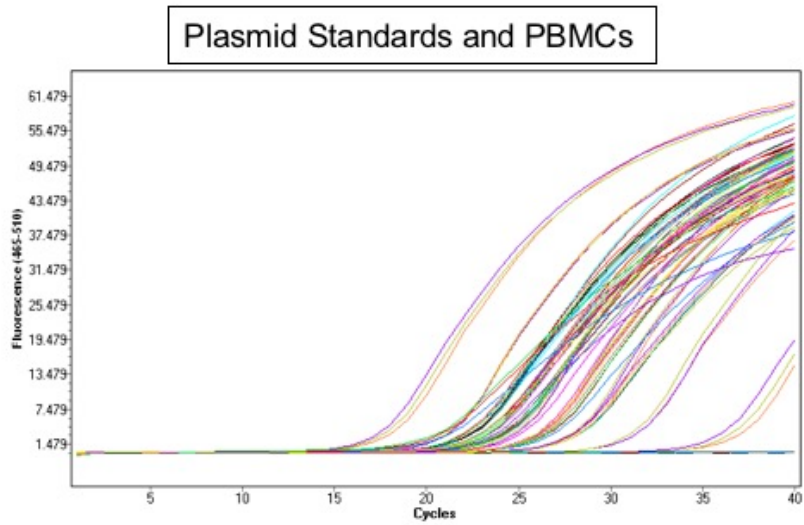
A

### Plasmid Standards



### Plasmid Standards and PBMCs



**B****C****D**

**Figure 3.12. An example of real-time RT-qPCR optimization and determination of the assay sensitivity for detection of woodchuck TLR10.**

**A.** cDNA from liver tissue (n=20) and 10-fold serial dilutions of known concentrations of TLR10 plasmid standards ( $10^6$  –  $10^1$  copies) were amplified using woodchuck TLR10-specific primers. The resulting melting peaks for TLR10 plasmid standards (top) and both standards and amplicons of test liver tissue samples (bottom) are displayed. Single peaks obtained indicate that TLR10-specific products were amplified in both the plasmid standards and liver samples.

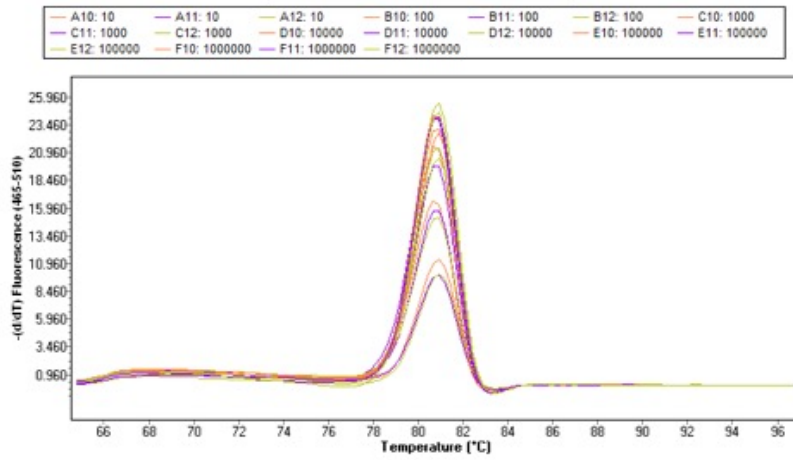
**B.** Amplification curves for TLR10 plasmid standard dilutions showing amplification of  $10^6$  copies down to  $10^1$  copies per reaction (left to right).

**C.** The resulting plot generated from amplification of TLR10 plasmid standards. The standard curve had an error of 0.0193, efficiency of 1.914 and a slope of -3.547.

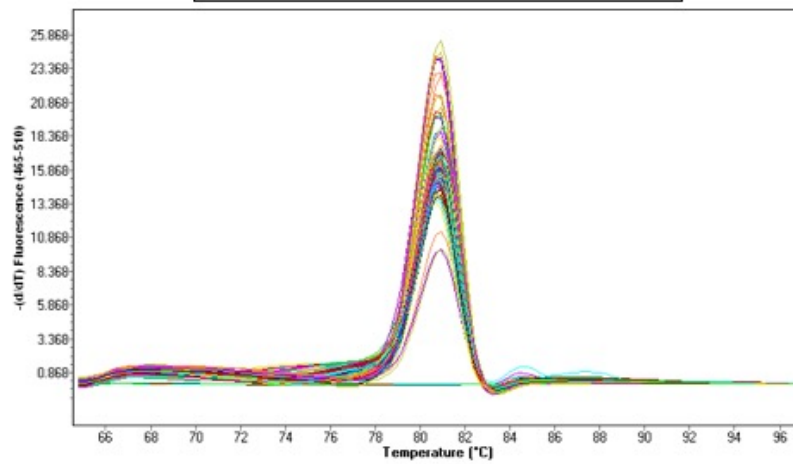
**D.** Overlay of amplification curves for both TLR10 plasmid standards and test liver cDNA samples. Liver cDNA samples were amplified and produced amplification curves within the range of the standard curve, thus, allowing for absolute TLR10 quantification.

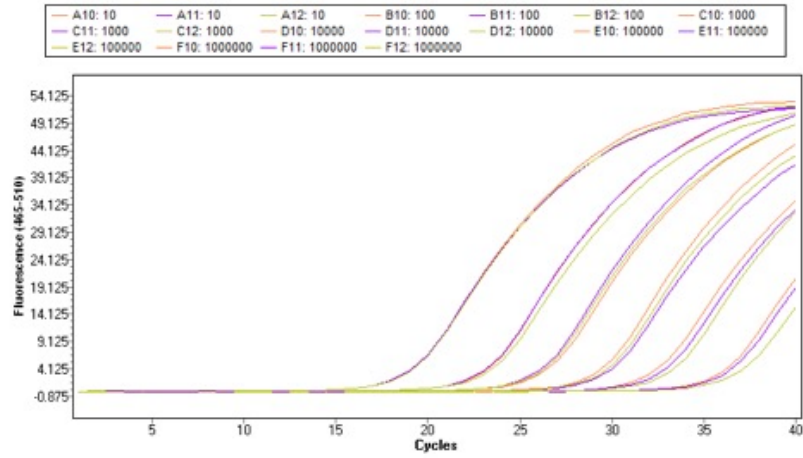
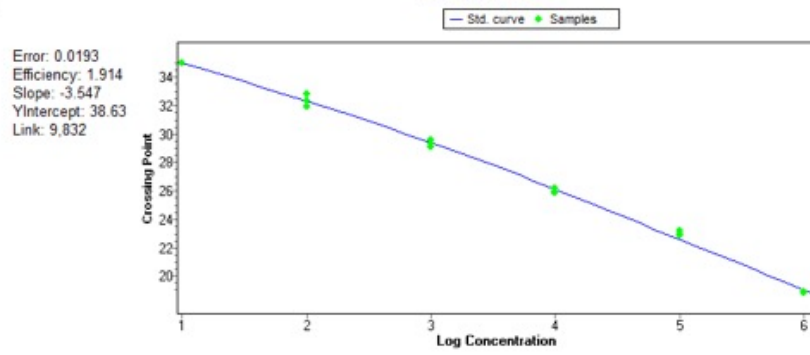
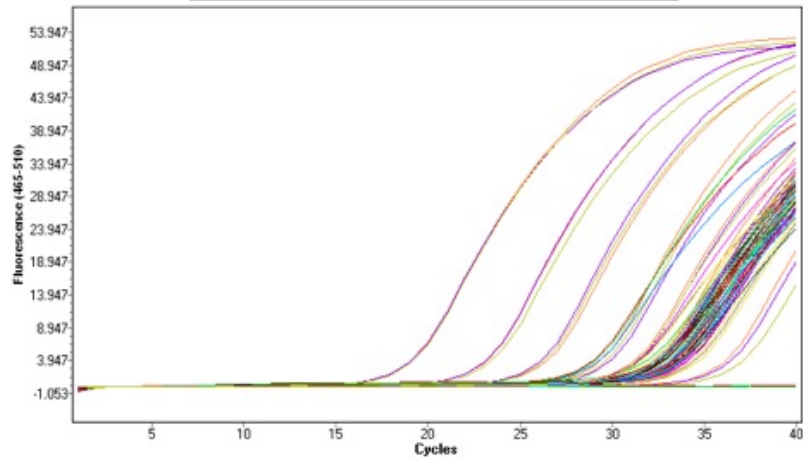
A

### Plasmid Standards



### Plasmid Standards and PBMCs



**B****Plasmid Standards****C****Standard Curve****D****Plasmid Standards and PBMCs**

after amplification with TLR4-specific or TLR10-specific primers, respectively. As shown, primer pairs generated single melting peaks indicating a high specificity of the primers to the amplicons generated. Ultimately, a multiplex approach was designed; *i.e.*, all TLR primer pairs amplified their target sequences optimally under the same PCR cycling conditions.

### **3.3.2. Quantification Standard Curve Optimization**

Absolute quantification analysis allows for the quantification of an amplification product based on an absolute value (*i.e.*, copy number). For this purpose, 10-fold serial dilutions of known concentrations of quantification standards were amplified to produce amplification curves. From these amplification curves, standard curves were derived. The slope of the standard curve describes the kinetics of the reaction and is directly related to the efficiency (E). Ideally, the perfect standard curve will have a slope of -3.3 and, thus, an efficiency of 2 ( $E=10^{-1/\text{slope}}$ ). This means that the amount of nucleic acid in the reaction is doubling with each amplification cycle (Light Cycler480® Software Applications Manual, 2008). An error value is assigned to each standard curve and is a direct measure of the accuracy of the quantification based on the standard curve (error values < 0.2 are acceptable). Based on the crossing points of the unknown test samples within the standard curve, a value can be generated relative to the copy number of the target DNA present. The absolute quantification method provides utmost accuracy when analyzing expressional changes of target genes.

In this study, standard curves for absolute quantification of woodchuck TLRs1-10 were generated. For example, amplification curves for TLR4 and TLR10 quantification

standards (Figures 3.11B and 3.12B, respectively) and the resulting standard curves (Figure 3.11C and 3.12C) produced efficiency values very close to 2, with acceptable error ( $< 0.2$ ). All test sample amplification curves were within the standard curve (Figure 3.11D and 3.12D) allowing for accurate quantification.

### **3.4. Housekeeping Gene Expression Profiles in Liver, Hepatocytes and PBMCs from Healthy and WHV-Infected Woodchucks**

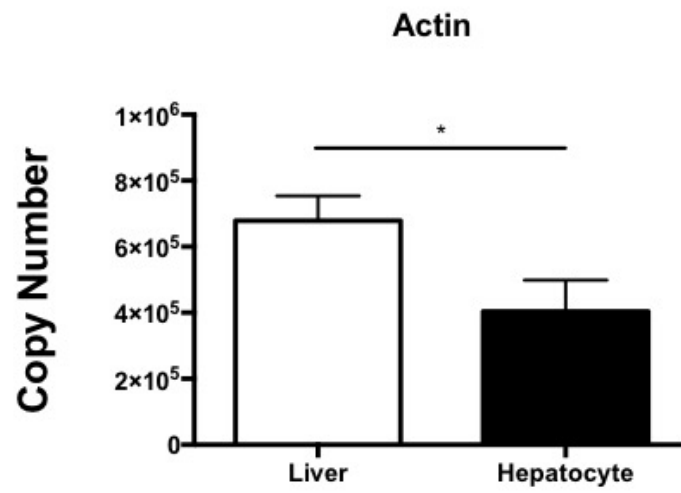
It was important to investigate the expression level of the housekeeping  $\beta$ -actin gene to ensure that it is expressed at comparable levels in tissue samples being evaluated. Expression of  $\beta$ -actin was assessed in livers ( $n=26$ ) and hepatocytes isolated from these livers ( $n=26$ ) in healthy ( $n=5$ ) and WHV-infected ( $n=21$ ) woodchucks. Interestingly,  $\beta$ -actin was expressed at significantly higher levels in liver samples ( $P=0.028$ ) when compared to hepatocytes (Figure 3.13A). Due to this difference in expression, along with reasons outlined previously (Section 2.7.3), it was necessary to test the reliability of other housekeeping genes. HPRT was expressed similarly among liver samples ( $n=87$ ) and hepatocytes ( $n=26$ ). However, HPRT expression was significantly higher in PBMCs ( $n=51$ ) than in both liver ( $P<0.0001$ ) and hepatocytes ( $P<0.0001$ ) (Figure 3.13B) (for rough copy numbers see Appendix Tables A1 – A3). Therefore, TLR expression levels in livers and hepatocytes were only compared to those in PBMCs of healthy woodchucks.

**Figure 3.13. HPRT is a more reliable housekeeping gene than  $\beta$ -actin when comparing gene expression in woodchuck livers and hepatocytes derived from these livers.**

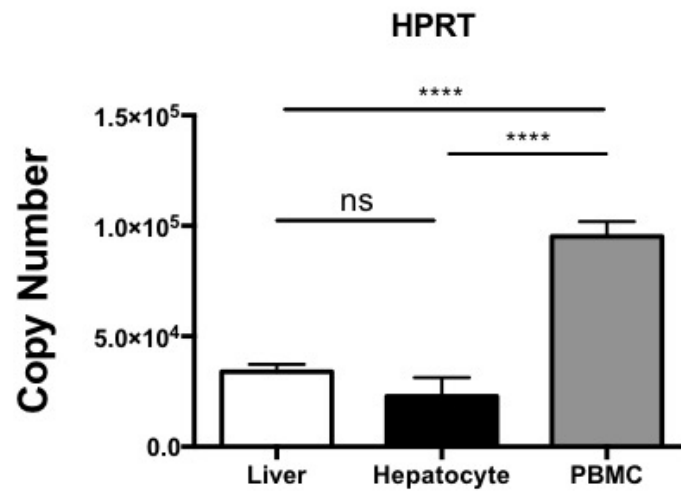
**A.** Liver samples (n=26) and derived hepatocytes were obtained from 26 woodchucks with different forms of WHV infection.  $\beta$ -actin housekeeping gene is expressed at significantly higher levels in livers than in hepatocytes isolated from these livers.

**B.** Liver samples (n=87), hepatocytes (n=26), and PBMCs (n=51) were isolated from woodchucks prior to and during WHV infection. HPRT housekeeping gene was expressed at similar levels in livers and derived hepatocytes, while the gene transcription levels were significantly higher in PBMCs.  $\beta$ -actin and HPRT expression were quantified by real-time RT-qPCR. 50 ng of RNA equivalent for each sample was tested in triplicate. Results are shown as mean values  $\pm$  SEM. Differences between data bars marked with \* are significant at  $P < 0.05$ , and \*\*\*\* at  $P \leq 0.0001$  by two-tailed Student's t-test.

**A**



**B**



### **3.5. TLR Expression Levels in Normal Woodchuck Livers, Hepatocytes and PBMCs**

To establish baseline expression levels of woodchuck TLRs1-10, liver (n=25), hepatocyte (n=5) and PBMC (n=11) samples from healthy, WHV-naïve woodchucks were evaluated for expression of individual TLRs using specific real-time RT-qPCR assays. Except for TLR2 ( $P=0.0422$ ) and TLR10 ( $P=0.0069$ ), TLRs were equally expressed in hepatocyte and liver tissue (Figure 3.14). When compared to PBMCs, hepatocytes and liver tissue demonstrated significantly upregulated gene transcription of TLR3 ( $P=0.0188$  and  $P=0.018$ , respectively) and TLR7 ( $P<0.0001$  and  $P=0.0139$ , respectively). Moreover, hepatocytes were found to transcribe significantly higher levels of TLR4 ( $P=0.0271$ ) and TLR5 ( $P=0.0015$ ) than PBMCs. In contrast, TLR6 ( $P=0.0015$ ), TLR8 ( $P=0.0001$ ) and TLR9 ( $P<0.0001$ ) expression was significantly greater in PBMCs than in liver tissue. Interestingly, TLR1 was not expressed in hepatocytes or liver tissue, but was detected in PBMCs (Figure 3.14). For rough copy numbers detected in livers, hepatocytes and PBMCs from healthy animals see Appendix Tables A1 – A3.

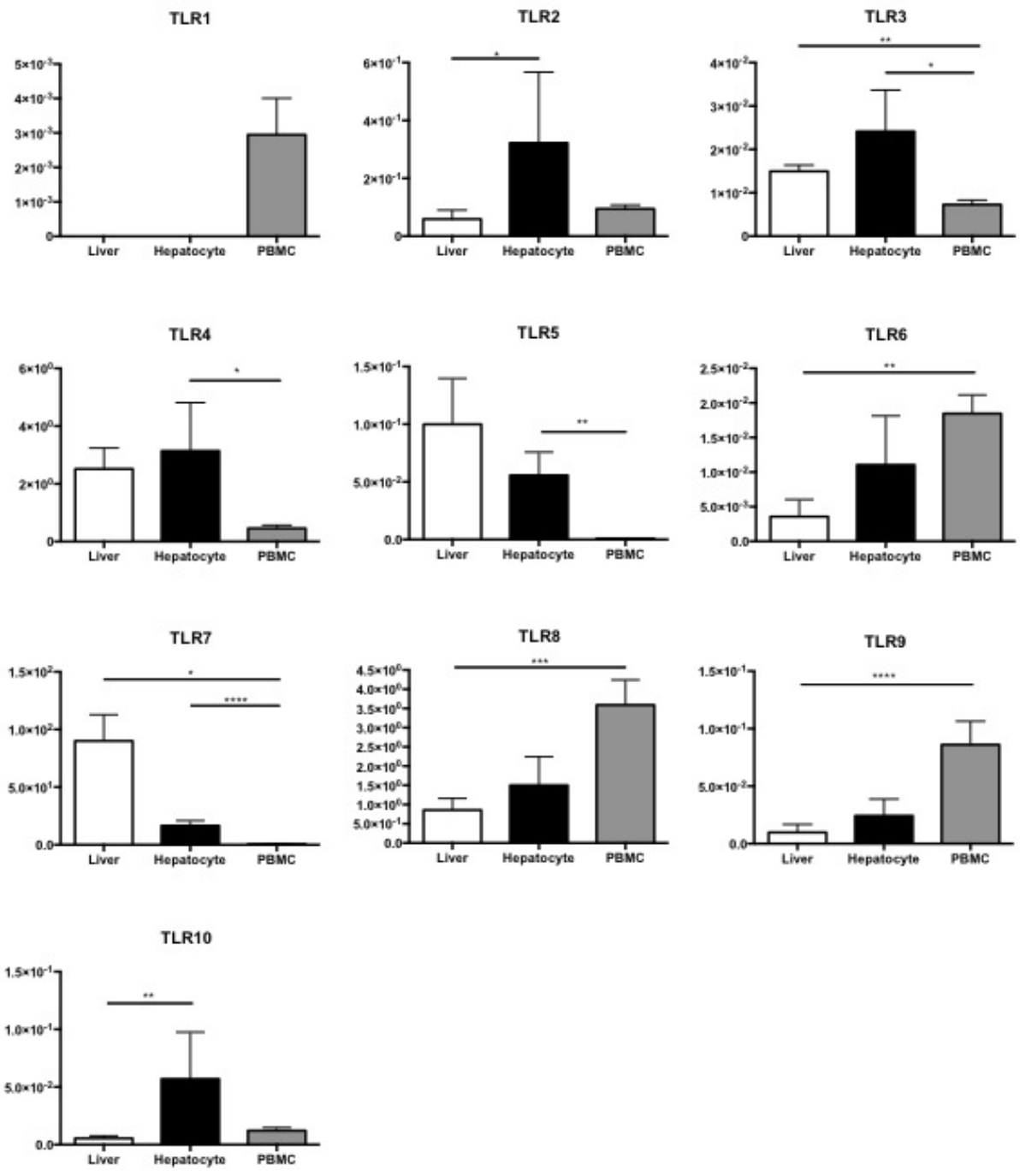
### **3.6. Transcription of Individual TLRs in Livers and Hepatocytes Isolated from These Livers of Healthy Woodchucks and Animals with Different Stages of WHV Infection**

To delineate possible differences of TLR expression levels in the livers of animals with different stages of WHV infection, hepatic TLR expression was compared among all study groups. Analysis showed that TLR5 transcriptional levels

**Figure 3.14. Baseline expression levels of TLRs1-10 in healthy woodchuck livers, hepatocytes and PBMCs.**

Real-time RT-qPCR quantification of woodchuck TLR1-10 transcription in healthy liver tissue samples (n=25), hepatocytes derived from healthy woodchuck livers (n=5) and PBMCs (n=11). TLR1 expression was evaluated but not detected in liver or hepatocytes. Gene transcription was normalized against woodchuck HPRT expression in respective tissue or cells and presented as relative expression values. Total RNA equivalent of 50 ng was tested in each sample in triplicate. Results are presented as mean values  $\pm$  SEM. Differences between data bars marked with \* are significant at  $P < 0.05$ , \*\* at  $P < 0.01$ , \*\*\* at  $P < 0.001$ , and \*\*\*\* at  $P < 0.0001$  by two-tailed Student's t-test.

Relative Expression



were significantly greater in livers of healthy ( $P=0.0082$ ) and SLAH ( $P=0.0035$ ) animals when compared to those from woodchucks with CH (Figure 3.15). While livers from healthy woodchucks ( $P=0.0005$ ) and animals with PreAH ( $P=0.0107$ ) showed significantly lower transcription levels of TLR9 when compared to those from animals with POI. Lastly, TLR8 expression was upregulated in livers of animals with PreAH ( $P=0.0493$ ) in comparison to those from woodchucks with SLAH (for additional information see Appendix Table A1)

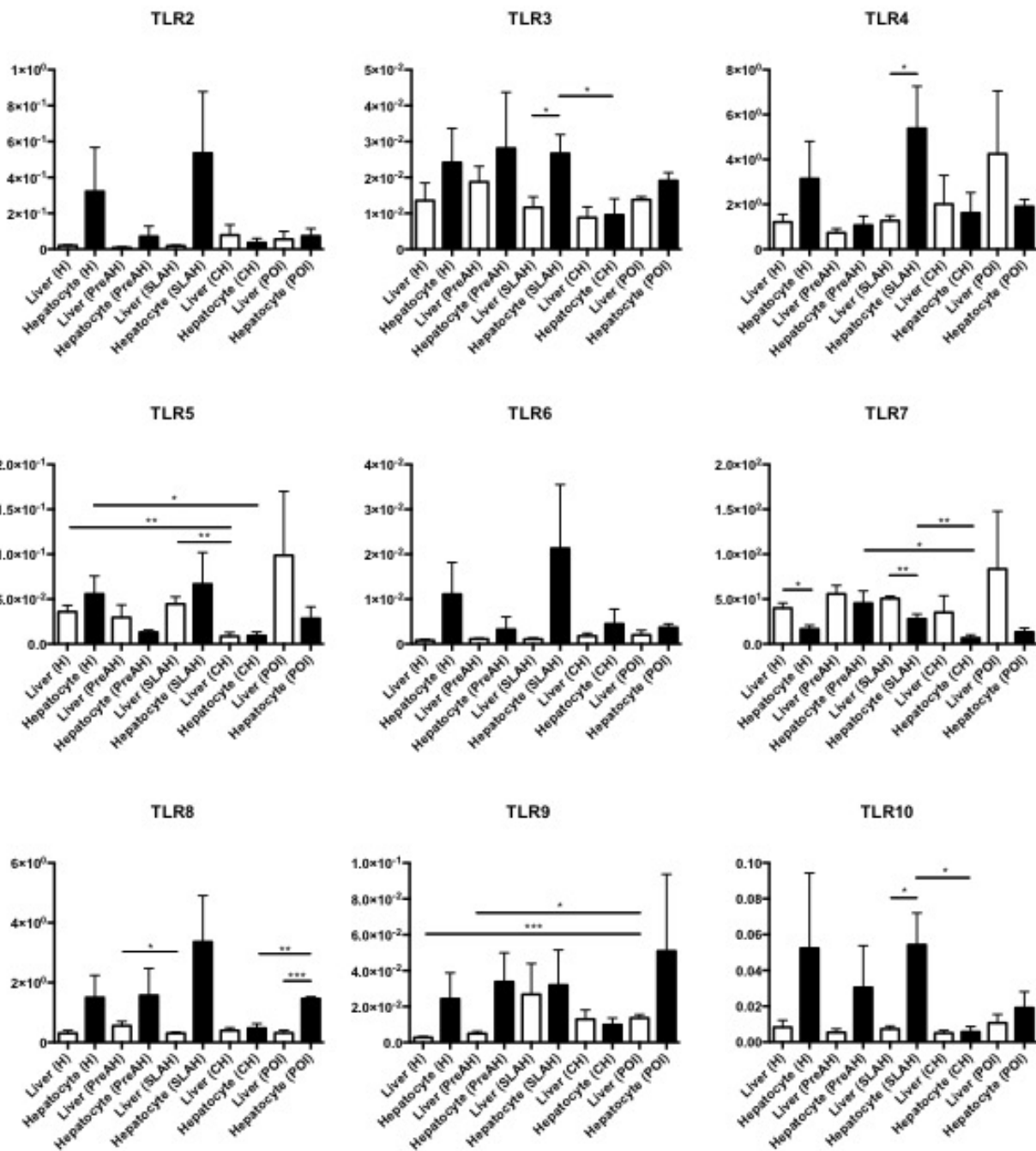
In hepatocytes, transcriptional levels of TLR1-10 were also evaluated across all study groups. When compared to CH, hepatocytes from healthy animals had significantly higher levels of TLR5 ( $P=0.0350$ ), while those from SLAH animals displayed upregulated expression of TLR3 ( $P=0.0352$ ), TLR7 ( $P=0.0096$ ) and TLR10 ( $P=0.0379$ ) (Figure 3.15). Hepatocytes from woodchucks with CH also showed downregulated expression of TLR7 and TLR8 when compared to woodchucks with PreAH ( $P=0.0106$ ) or POI ( $P=0.0038$ ). It became apparent that hepatocyte TLR expression in CH was characterized by distinctive downregulation of TLR3, TLR5, TLR7, TLR8, and TLR10 in comparison to hepatocytes from healthy animals and those from woodchucks with other stages of WHV infection. For rough copy numbers detected in hepatocytes see Appendix Table A2.

Transcription levels of TLR1-10 were compared between livers and hepatocytes derived from these livers from healthy and WHV-infected woodchucks. The livers of healthy woodchucks ( $P=0.012$ ) and animals with SLAH ( $P=0.002$ ) showed significantly

**Figure 3.15. TLRs1-10 expression profiles in livers and hepatocytes purified from these livers from healthy and WHV-infected woodchucks**

Transcriptional levels of TLRs1-10 in livers from healthy animals (n=5), woodchucks with PreAH (n=4), SLAH (n=8), CH (n=6) or POI (n=3) and hepatocytes isolated from these livers. Expression was quantified by real-time RT-qPCR. TLR1 expression was evaluated but not detected in livers or hepatocytes. TLR transcription in livers and hepatocytes were only compared within the same study group (*i.e.*, form of WHV infection), while expression in livers were compared with livers, and hepatocytes with hepatocytes across the study groups. TLR transcription was normalized against HPRT expression and presented as relative expression values. Total RNA equivalent of 50 ng was tested for each sample in triplicate. Results are shown as mean values  $\pm$  SEM. Differences between data bars marked with \* are significant at  $P < 0.05$ , \*\* at  $P < 0.01$ , and \*\*\* at  $P < 0.001$ , by two-tailed Student's t-test.

Relative Expression



upregulated levels of TLR7 when compared to hepatocytes from the same study groups (Figure 3.15). Conversely, livers from woodchucks with SLAH demonstrated significantly downregulated gene expression of TLR3 ( $P=0.0253$ ), TLR4 ( $P=0.0478$ ), and TLR10 ( $P=0.0193$ ) when compared to hepatocytes derived from these livers. TLR8 expression was also found to have significantly lower levels in the livers than hepatocytes ( $P=0.0005$ ) in animals with POI (Figure 3.15). These results clearly indicated that there are significant differences in expression of individual TLRs between livers and high purity hepatocytes isolated from these livers. Furthermore, these differences were influenced by the status of WHV infection and they were most evident in animals with SLAH.

There were no significant differences seen in expression of TLR2 and TLR6 in livers and hepatocytes from healthy and WHV-infected woodchucks. Again, TLR1 was undetected in both liver and hepatocytes samples.

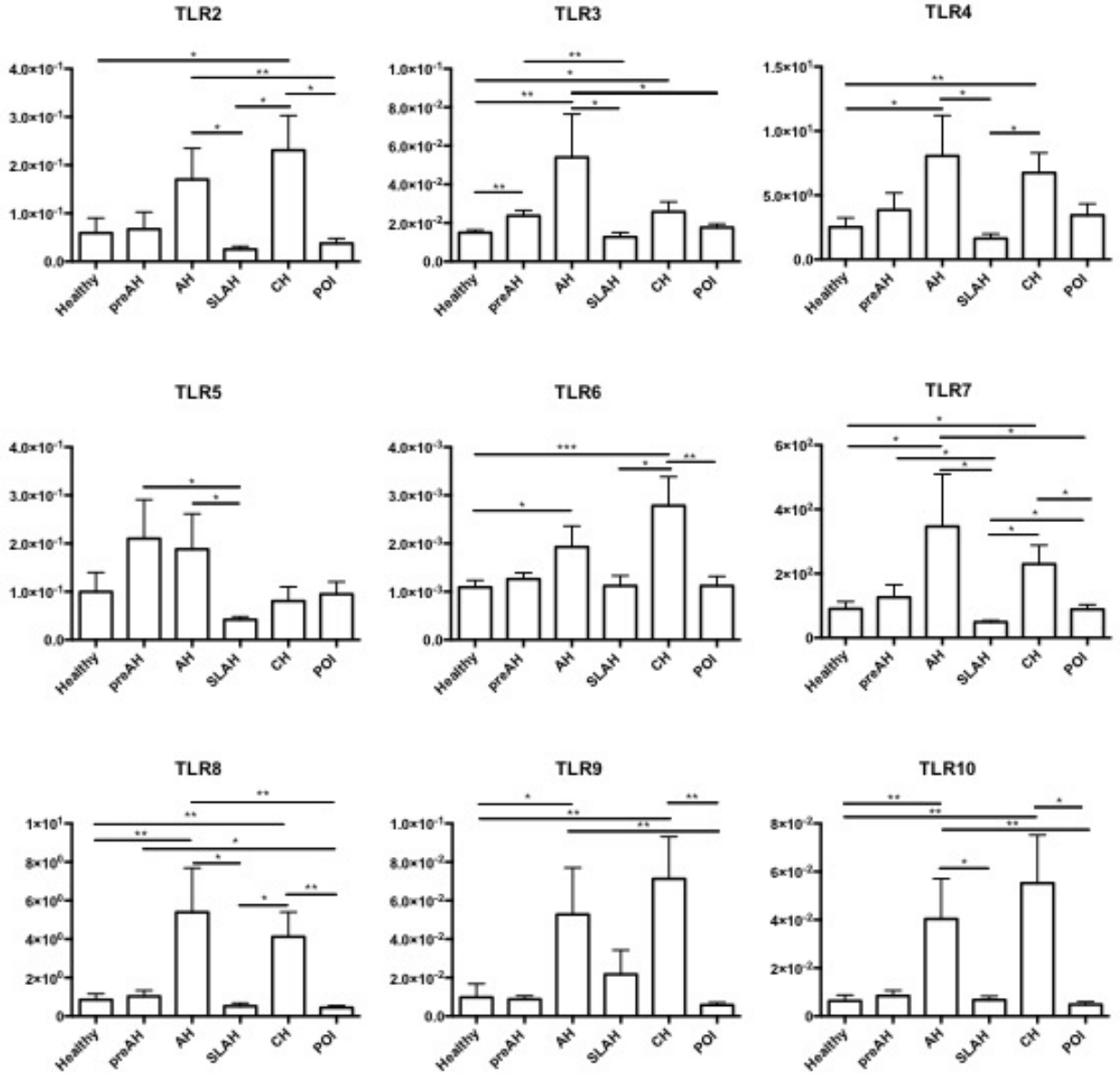
### **3.7. Expression Profiles of TLRs1-10 in Sequential Liver Biopsies Obtained Prior to and During WHV Infection**

Woodchuck liver tissue collected at biopsies throughout the course of WHV infection and during follow-up autopsy were investigated. When compared to the healthy state, the PreAH phase was characterized by significantly higher expression levels of TLR3 ( $P=0.0060$ ) (Figure 3.16). Livers in the PreAH stage also had higher transcription levels of TLR3 ( $P=0.0074$ ), TLR5 ( $P=0.0251$ ) and TLR7 ( $P=0.0329$ ) when compared to the SLAH phase, while TLR8 ( $P=0.0276$ ) was upregulated when compared

**Figure 3.16. Transcription levels of TLRs1-10 in sequential liver biopsy samples collected from woodchucks with different forms of WHV infection.**

Liver tissue samples from healthy woodchucks (n=25) and animals with PreAH (n=8), AH (n=8), SLAH (n=11), CH (n=18) phases of WHV hepatitis or POI (n=17) were analyzed for expression of TLR1-10. Liver samples analyzed were a combination of biopsy and autopsy samples collected prior to and during different phases of hepatitis or SLAH or POI. Quantification of mRNA was performed by RT-qPCR. TLR1 expression was evaluated but not detected. Gene transcription levels were normalized against woodchuck HPRT expression and presented as relative expression values. Total RNA equivalent of 50 ng was tested from each test sample in triplicate. Results are shown as mean values  $\pm$  SEM. Differences between data bars marked with \* are significant at  $P < 0.05$ , \*\* at  $P < 0.01$ , and \*\*\* at  $P < 0.001$ , by two-tailed Student's t-test.

Relative Expression



to livers with POI. Conversely, POI livers had significantly higher expression levels of hepatic TLR7 ( $P=0.0395$ ) when compared to the SLAH phase. Analysis of liver biopsies from the AH phase showed significant upregulation of TLR genes, more specifically, TLR3 ( $P=0.0039$ ), TLR4 ( $P=0.0148$ ), TLR6 ( $P=0.0312$ ), TLR7 ( $P=0.0132$ ), TLR8 ( $P=0.0024$ ), TLR9 ( $P=0.0244$ ) and TLR10 ( $P=0.0020$ ) when compared to their expression in healthy liver tissue (Figure 3.16). Upregulated transcriptional levels of hepatic TLRs were continued when comparing AH with both SLAH and POI forms of the infection. AH stage livers had significantly higher transcripts for TLR2 ( $P=0.0175$ ), TLR3 ( $P=0.0455$ ), TLR4 ( $P=0.0283$ ), TLR5 ( $P=0.0312$ ), TLR7 ( $P=0.0447$ ), TLR8 ( $P=0.0229$ ), and TLR10 ( $P=0.0302$ ) compared to the SLAH stage. When compared to POI, AH livers showed higher expression of TLR3 ( $P=0.0254$ ), TLR7 ( $P=0.0291$ ), TLR8 ( $P=0.0040$ ), TLR9 ( $P=0.0083$ ) and TLR10 ( $P=0.0045$ ). In a similar manner, CH livers transcribed significantly more TLR2 ( $P=0.0201$ ), TLR3 ( $P=0.0265$ ), TLR4 ( $P=0.0098$ ), TLR6 ( $P=0.0006$ ), TLR7 ( $P=0.0176$ ), TLR8 ( $P=0.0066$ ), TLR9 ( $P=0.0041$ ), and TLR10 ( $P=0.0068$ ) than livers of healthy animals. Liver biopsies from woodchucks with CH also had significantly greater transcriptional levels of TLR2 ( $P=0.0353$ ), TLR4 ( $P=0.0170$ ), TLR6 ( $P=0.0133$ ), TLR7 ( $P=0.0247$ ) and TLR8 ( $P=0.0386$ ) when compared to the SLAH stage. TLR2 ( $P=0.0143$ ), TLR6 ( $P=0.0064$ ), TLR7 ( $P=0.0300$ ), TLR8 ( $P=0.0090$ ), TLR9 ( $P=0.0065$ ) and TLR10 ( $P=0.0201$ ) were transcribed at significantly higher levels, again in the CH phase, when compared to the liver tissue collected during POI (Figure 3.16). Again, TLR1 was undetectable in liver biopsies throughout the course of WHV infection. There was a trend towards a global increase in hepatic TLR expression when comparing healthy, SLAH, and POI phases directly to both AH and CH

stages. The increase in TLR expression could be related to active liver inflammation characterizing both AH and CH. For rough copy numbers detected see Appendix Table A1.

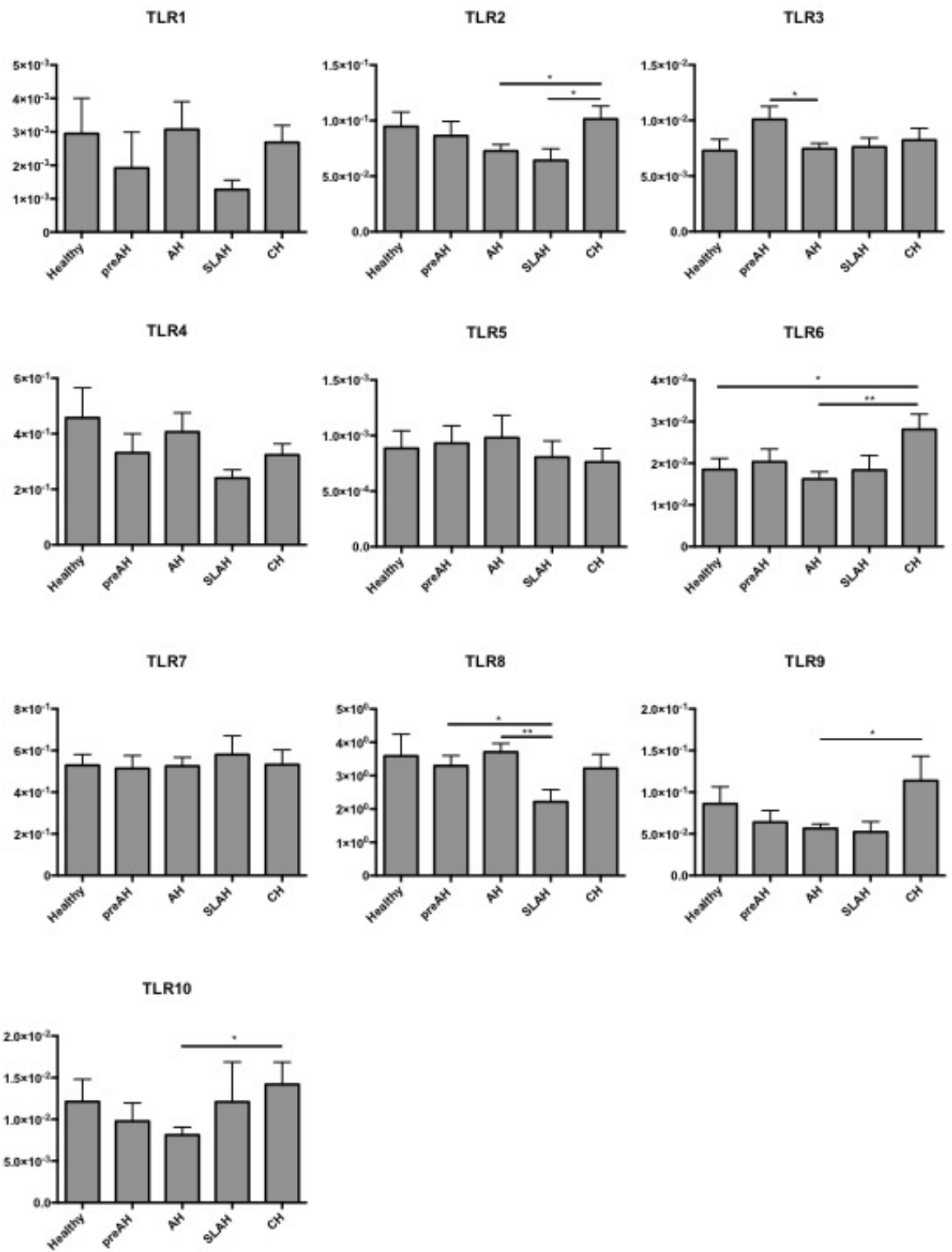
### **3.8. Expression of TLRs1-10 in Sequential PBMC Samples of Healthy Animals and Those with Different Stages of Experimental WHV Infection**

Sequential PBMC samples collected from healthy and infected woodchucks during the course of WHV infection progression were evaluated for TLR1-10 transcription levels. As seen with liver tissue, woodchucks with CH showed upregulated expression of TLR genes in their PBMCs when compared to the PBMCs from healthy woodchucks and from other study groups (Figure 3.17). When comparing cells from healthy animals and those with SLAH, PBMCs from CH had significantly higher expression levels of TLR6 ( $P=0.0452$ ) and TLR2 ( $P=0.0420$ ). Additionally, PBMCs from CH transcribed greater levels of TLR2 ( $P=0.0209$ ), TLR6 ( $P=0.0029$ ), TLR9 ( $P=0.0110$ ) and TLR10 ( $P=0.0129$ ) in comparison to those from AH (Figure 3.17). TLR8 was significantly downregulated in the cells from SLAH when compared to PBMCs from PreAH ( $P=0.0423$ ) and AH ( $P=0.0066$ ). Whereas TLR3 had higher expression levels in PBMCs from PreAH phase ( $P=0.0213$ ) when compared to the cells from AH. For rough copy numbers detected in PBMCs see Appendix Table A3.

**Figure 3.17. Profiles of TLRs1-10 expression in sequential PBMC Samples isolated from healthy woodchucks and those with different forms of WHV infection.**

Transcriptional levels of TLRs1-10 in PBMCs from healthy animals (n=11) and woodchucks during the course of different phases of WHV infection, including PreAH (n=8), AH (n=18), SLAH (n=6) and CH (n=8). Quantification of mRNA was performed by RT-qPCR. Gene transcriptional levels were normalized against woodchuck HPRT expression in individual PBMC samples. Total RNA equivalent of 50 ng was tested from each test sample in triplicate. Results are shown as mean values  $\pm$  SEM. Differences between data bars marked with \* are significant at  $P < 0.05$ , and \*\* at  $P < 0.01$ , by two-tailed Student's t-test.

Relative Expression



## Chapter 4 - Discussion

### 4.1. Summary of Findings

This study investigated the expression of TLRs1-10 in the liver, hepatocytes isolated from these livers, and PBMCs of healthy woodchucks and animals with different stages of experimental WHV infection and forms of WHV hepatitis. Due to the lack of recognition of the full spectrum of woodchuck TLRs, primers specific for TLRs1-2 and TLRs4-10 were generated. TLRs1-10 primers were used to amplify woodchuck TLR gene exon fragments, as confirmed by sequencing and interspecies homology comparisons. TLRs1-10 primers were optimized for RT-qPCR and a multiplex assay was designed that allowed for simultaneous absolute quantification of TLRs1-10 expression in a single PCR run with high specificity and sensitivity. Expression analysis revealed that TLRs1-10 transcription levels were comparable among healthy woodchuck livers and their derived hepatocytes, while PBMC expression differed. However, there were significant differences in TLR expression in livers and their derived hepatocytes when comparing healthy woodchucks and woodchucks with different stages of WHV-infection. Analysis of hepatocytes collected throughout different forms of WHV infection showed a trend towards decreased expression during CH, while liver biopsies showed a trend towards global increase in TLR expression during active liver inflammation (*i.e.*, AH and CH). Finally, sequential PBMC samples collected from healthy and WHV-infected woodchucks showed an increase in most TLR gene transcription during CH.

## 4.2. Timeline of Woodchuck TLRs1-10 Identification

A comparison of the woodchuck TLRs1-10 gene fragments identified in this study (Figures 3.1C – 3.10C) with previously published woodchuck TLRs revealed sequence fragments which were not previously reported, in addition to entirely new woodchuck TLRs sequences identified. In November of 2009 (when this study was already in progress), partial sequences for TLR3 (GenBank accession number EU586552.1), TLR4 (GenBank accession number EU586553.1), TLR7 (GenBank accession number EU586554.1), TLR8 (GenBank accession number EU586555.1), and TLR9 (GenBank accession number EU586556.1) were reported by another group (Zhang *et al.*, 2009). In December of 2010 and August of 2015, woodchuck TLR2 (GenBank accession number HQ446273.1) and the complete coding sequence for woodchuck TLR7 (GenBank accession number KT013099.1) were also reported to the National Center for Biotechnology Information (NCBI) GenBank. When compared to the TLR gene fragments identified in the current study (Figure 3.1A – 3.10A), all but TLR3 and TLR7 sequences were partially or fully unique and have not yet been previously reported (Table 2.1). It is important to note that I successfully identified all woodchuck TLR sequences, with the exception of TLR3, in the Michalak Lab prior to the reporting by other research groups. TLR2, TLR4, TLR7 and TLR9 were positively identified during my honors degree program in the summer semester in 2008. TLR1, TLR5, TLR6, TLR8 and TLR10 woodchuck sequences were identified during my Master's degree program which began in September of 2009.

### **4.3. Woodchuck TLR1-10 mRNA Protein Coding Sequence Compatibility with Human TLRs1-10**

Woodchuck TLRs1-10 partial gene sequences (Figure 3.1C – 3.10C) were aligned with complete mRNA protein coding sequences of human TLRs1-10 and then translated to their respective amino acid sequences. Based on the alignment position of the woodchuck amino acid sequence, it was possible to infer the region of the TLR protein that the partial woodchuck gene fragments represented. After analyzing woodchuck TLRs1-10 amino acid sequences it was apparent that all identified gene fragments, except for TLR1 and TLR6, coded for the TIR domain of the TLR protein. Woodchuck TLR3 (amino acids 790 – 870), TLR4 (amino acids 710 – 810), and TLR5 (amino acids 770 – 800) aligned with a region located directly within the TIR domain of human TLR3 (GenBank accession number ABC86910), TLR4 (GenBank accession number AAF05316), and TLR5 (GenBank accession number AAI09119). While TLR8 (amino acids 880 – 910) and TLR9 (amino acids 840 – 1030) spanned the cytoplasmic region prior to the TIR domain, as well as overlapping with the TIR domain of human TLR8 (GenBank accession number AAZ95441) and TLR9 (GenBank accession number AAZ95521). Furthermore, TLR2 (amino acids 540 – 670), TLR7 (amino acids 790 – 1030), and TLR10 (amino acids 520 – 693) corresponded to the extracellular, transmembrane and TIR domains of human TLR2 (GenBank accession number AAH33756), TLR7 (GenBank accession number AAZ99026), and TLR10 (GenBank accession number AAY78491). In contrast, TLR1 (amino acids 120 – 270) and TLR6 (amino acids 280 – 420) represent the cytoplasmic domain of human TLR1 (GenBank accession number AAH33756) and TLR6 (GenBank accession number BAA78631).

TLRs1-10 primers used in this study were designed based on a consensus sequence that incorporated multiple mammalian complete protein coding sequences for each TLR gene. The TIR domain is the most evolutionary conserved region of TLRs, thus, it is not surprising that most primers were located in this region due to high sequence homology when comparing multiple mammalian genes. As mentioned in Section 1.7.3.1.1, TLR2 can dimerize with both TLR1 and TLR6. It has been shown that the TIR domain of both TLR1 and TLR6 have high sequence homology, making it an undesirable region for primer development (Plain *et al.*, 2010). Therefore, primers for woodchuck TLR1 and TLR6 were designed to amplify the mRNA protein coding sequence for the cytoplasmic region, where the receptors share the least sequence homology. This allowed for specific amplification of woodchuck TLR1 and TLR6 in our study.

#### **4.4. Amplification Techniques Utilized in This Study**

This current work implemented multiple techniques that allowed for efficient and accurate quantification of TLRs1-10 in healthy and WHV-infected woodchucks with a very high degree of sensitivity. Firstly, a multiplex assay was developed that allowed for simultaneous amplification of TLRs1-10 in woodchuck tissue and cell samples in the same RT-qPCR run (Figure 2.2). This technique was highly valuable as it served as an efficient quantifying tool to determine the level of expression of different TLRs in the same tissue or cell sample. Most TLRs can recognize a wide range of PAMPs, thus, utilizing a multiplex approach helped quickly identify the TLR signaling pathway being activated in a given experimental group. In the same manner, TLRs1-10 expressional

changes were able to be quickly assessed in a single RT-qPCR reaction from multiple test samples.

The quantification techniques used in this study were designed to provide absolute quantification of TLR target genes with a high degree of accuracy and sensitivity. TLRs1-10 plasmid standards were developed that contained inserts of each TLR gene fragment of interest. Serial 10-fold dilutions of these quantification standards (Figure 3.11B and 3.12B) were included in each RT-qPCR run which allowed for absolute quantification of expression of the TLR target gene in test samples (Figure 3.11D and 3.12D). Additionally, each TLR primer pair designed in this study was able to successfully amplify its target gene sequence with a high degree of sensitivity (*i.e.*,  $10^1 - 10^2$  copies/reaction) (Table 2.2), allowing for the detection of TLR expressional changes at very low levels. Controls for each PCR reaction included a NTC that contained everything but the cDNA template. This was essential for excluding potential contamination in the PCR reagents (Figure 2.1). In addition, a mock was included to control for any contamination carryover from the RT step. In this control, water was used instead of RNA template when reverse transcribing RNA to cDNA. This would control for any contamination carryover from RT reagents. Further, ICs were included (IC#1 Liver, IC#1 Spleen, IC#2 Liver, IC#2 Spleen) that consisted of cDNA from both liver and spleen tissue samples from two healthy animals. The expression levels of TLRs1-10 were previously quantified for these samples. They were used to assess consistency of TLR quantification between RT-qPCR runs on different plates. Expression levels of the tested gene should be consistent from plate to plate. Thus, the amplification techniques utilized in this study included the proper specificity and

quantification controls to ensure accurate quantification of TLRs1-10 in healthy and WHV-infected woodchucks.

#### **4.5. TLRs1-10 Expression Profiles in Normal Woodchuck Livers and Isolated Hepatocytes Were Comparable, While PBMCs Displayed Different Patterns of TLRs1-10 Expression than in Hepatic Tissue**

To establish a baseline for TLRs1-10 expression, hepatocytes were isolated from the livers of normal woodchucks and both total hepatic tissue and their isolated hepatocytes were analyzed for expression of TLRs1-10. In addition to liver and hepatocytes, PBMCs isolated from healthy woodchucks were also analyzed for their TLRs1-10 expressional patterns. It was found that TLR transcription levels in normal woodchuck liver and isolated hepatocytes were, for the most part, equally expressed (Figure 3.14). In contrast, woodchuck PBMCs were found to express TLR6, TLR8, and TLR9 at significantly higher levels than the liver and isolated hepatocytes. While TLR3, TLR4, TLR5, and TLR7 were expressed at significantly lower levels in PBMCs than in the liver and hepatocytes (Figure 3.14). TLR1 expression was not detected in the liver or hepatocytes, but was identifiable in PBMCs of healthy woodchucks.

Studies investigating TLR expression in healthy human tissues have found that the liver contains the lowest mRNA levels of TLRs1-10 when compared to other organs in the body (Zarembler and Godowski, 2002; Nishimura and Naito, 2005). This decreased basal expression has been suggested to contribute to the high immune tolerance of the liver to intestinal microbes of which the liver is constantly exposed (Mencin *et al.*, 2009). In contrast, it has been shown that human PBMCs, along with the

spleen, have the highest mRNA levels of TLRs1-10, as they are most likely to encounter external pathogens in the blood and lymphoid system. One study comparing human PBMCs to hepatic tissue has found that all TLRs are expressed at higher levels in PBMCs when compared to hepatic tissue, except TLR3 (Zarembek and Godowski, 2002). Consistent with previous findings in human, the current study found that TLR3 mRNA was significantly higher in woodchuck livers when compared to woodchuck PBMCs (Figure 3.14). However, TLR4, TLR5, and TLR7 were found to be lower in woodchuck PBMCs than in hepatic tissue, while all other TLRs were expressed at comparable levels. The differences seen in basal (healthy state) expression patterns of TLRs between human and woodchuck may be attributed to species differences in expression of receptors involved in the innate immune response. Due to the limited availability of woodchuck TLR1-10 expressional studies in the literature, it was not possible to compare the basal TLR expression profiles found in this study with other woodchuck studies.

#### **4.6. There Are Significant Differences in TLR Expression Profiles in the Liver and Isolated Hepatocytes During the Course of WHV Infection**

Activation of the innate immune system through TLR signaling has been a recent focus for the development of treatments for hepadnaviral infection. In the woodchuck model of HBV infection, the majority of peer-reviewed articles have been focused on manipulation of TLR signaling with a lack of expressional analysis of individual TLR genes. Furthermore, due to the difficulties in obtaining liver biopsies during the course of infection, woodchuck studies have been limited to experiments involving *in vitro*

manipulations (*i.e.*, cultured hepatocyte cell lines and PWHs) and analysis of PBMC populations. Our study is the first to evaluate TLRs1-10 transcriptional levels in the liver and isolated hepatocytes of healthy woodchucks and those with different stages of WHV infection. Similarly, this study is the first to investigate TLR1-10 expressional changes in woodchuck liver biopsies throughout the course of WHV infection.

Firstly, when comparing woodchuck livers and their isolated hepatocytes across stages of infection, there was a common trend towards significant downregulation of TLRs (*i.e.*, TLR3, TLR5, TLR7, TLR8 and TLR10) in hepatocytes from CH when compared to hepatocytes from healthy animals and those with PreAH, SLAH, and POI (Figure 3.15). WHV has a tropism toward the liver, and with hepatocytes contributing to about 75-85% of the liver total cell number, WHV productively infects nearly 100% of hepatocytes by the time CH develops. Studies in HBV-transgenic mice have shown that HBV is able to suppress innate immune receptor signaling in hepatocytes and nonparenchymal liver cells (Wu *et al.*, 2009). Additionally, it has been well documented that HBV and its associated antigens and nucleic acids have the ability to augment TLR2 (Visvanathan *et al.*, 2007), TLR3 (An *et al.*, 2007; Li *et al.*, 2009), and TLR9 (Vincent *et al.*, 2011; Martinet *et al.*, 2012) expression in patients with CHB, thus, potentially diminishing immune control of the virus and contributing to establishment of CHB. The downregulation of TLR expression observed in the hepatocytes of woodchucks with CH may be due to WHV's ability to evade/suppress TLR signaling.

When comparing liver and hepatocytes within the same study group it was observed that SLAH animals have significantly lower levels of TLR3, TLR4 and TLR10

in the liver when compared with isolated hepatocytes (Figure 3.15). SLAH is defined as the resolution of AH, accompanied by a reduction of liver inflammation while virus replication persists at low level. In the woodchuck model, AH is characterized by immune infiltrations that, in some cases, can reach a high histological degree of hepatitis (Guy *et al.*, 2008). Immune infiltrations, consisting mainly of CD4+ (T<sub>h</sub>) and CD8+ T cells (CTLs), will increase overall TLR expression in the liver. Previous studies have confirmed that CD4+ and CD8+ T cells express mRNA and protein of most TLRs (Rahman *et al.*, 2009). In addition to T cells, hepatic immune infiltrations consist of B cells, monocytes/macrophages, and NK cells that all express TLRs at relatively high levels (Zarembek and Godowski, 2002; Tu *et al.*, 2008; Hua and Hou, 2013). With the resolution of AH (*i.e.*, SLAH), periods of normal or near normal liver morphology are observed (Michalak *et al.*, 1999; Guy *et al.*, 2008). Thus, it is not surprising that SLAH animals have decreased expression of TLR3 and TLR4 in the liver, as the number of immune cells expressing TLRs has decreased. As seen in Figure 3.14, TLR10 expression is significantly lower in the normal liver when compared to isolated hepatocytes, thus, lower levels of TLR10 in the liver of SLAH is closer to the situation characterizing the normal liver.

To gain a better understanding of the transcriptional regulation of TLRs during the progression of WHV-infection, liver biopsies taken throughout the course of infection were evaluated. When comparing healthy, SLAH, and POI stages of infection to AH and CH, there was significant upregulation of TLRs2-10 in the livers of woodchucks with AH and CH (Figure 3.16). HBV is a noncytopathic virus that causes intrahepatic inflammatory infiltrations during both AH and CH stages of infection. HBV-specific CTL

responses are generally too weak to eliminate the virus from infected hepatocytes, as observed in woodchucks with SLAH (Michalak *et al.*, 1999). However, the immune response is sufficient enough to induce acute and chronic liver inflammation (Rehermann, 2000). As mentioned, lymphocytic infiltration (*i.e.*, T<sub>h</sub> cells, CTLs, B cells, monocyte/macrophages, and NK cells) peaks during AH and can continue engaging the liver throughout the course of CH (Guy *et al.*, 2008). One study reported that immune infiltrates in a liver biopsy from a patient with CHB contained around 75% T cells, 10% B cells, and 10% NK cells (Mani and Kleiner, 2009). Therefore, the observed global increase in TLR expression in the liver during AH and CH stages of WHV infection may be directly related to intrahepatic inflammatory infiltration resulting in a global increase in cells expressing TLRs. As previously mentioned, hepatocyte TLR expression is downregulated during CH, which may be attributed to active suppression of the innate responses by the virus. Thus, it can be deduced that since the increase in TLR expression in the liver of woodchucks with CH is not due to an increase in hepatocyte TLR expression, it must be directly related to intrahepatic inflammatory infiltration.

When analyzing woodchuck liver biopsies from animals with PreAH it was apparent that TLR3, TLR5, and TLR7 transcriptional levels were upregulated when compared to the SLAH phase, while TLR8 expression was increased when compared to livers from woodchucks with POI (Figure 3.16). Previous studies in the Michalak lab have shown that WHV mRNA transcripts are detectable in hepatic tissue starting from one hour post infection, while molecular markers of the innate immune responses are detectable within the first few hours post-infection (Guy *et al.*, 2008). By 3 dpi, WHV-induced activation of intrahepatic APCs, NK and NKT cells is observed, which coincides

with a reduction in liver WHV virus load (Guy *et al.*, 2008). Additionally, hepatocytes have been shown to actively contribute to intrahepatic immune regulation and likely moderation of the local inflammatory response in WHV-infected woodchucks (Guy *et al.*, 2010; Guy *et al.*, 2011). Thus, the upregulation of TLRs observed in the livers of animals with PreAH is likely due to an increase in hepatocyte innate immune receptor expression in attempt control WHV levels within the infected cells. Similarly, the activation of intrahepatic APCs, NK and NKT cells in the early stages of infection likely adds to the overall increase in innate immune responses.

#### **4.7. Selective TLRs are Upregulated in PBMCs Isolated from Woodchucks with CH**

In the recent past, hepadnaviral infection of the lymphatic system was considered controversial. As of late, there has been accumulating data to support the idea that hepadnaviruses are both hepatotropic and lymphotropic in nature (Michalak, 2000; Michalak *et al.*, 2004; Mulrooney-Cousins and Michalak, 2015). Studies in WHV-infected woodchucks and HBV-infected humans have shown that PBMCs provide a place for hepadnaviruses to replicate and persist and they also play a role in the transmission of the virus from mother to child (Coffin and Michalak, 1999; Shao *et al.*, 2013). Due to the relatively non-invasiveness of blood collection, the majority of TLR investigations in the HBV field have been largely PBMC based. Most studies have focused on manipulation of TLR signaling to control virus replication, however, gene expression analysis of TLRs throughout the course of infection was usually absent or limited to a specific TLR (Zhang *et al.*, 2012; Meng *et al.*, 2016). Our study is the first to

investigate the expression profiles of TLRs1-10 in PBMCs isolated from woodchucks during the course of WHV infection and in different stages of WHV hepatitis.

Consistent with the findings in liver tissue, woodchuck PBMCs from animals with CH showed significant upregulation of TLR2, TLR6, TLR9 and TLR10 transcripts when compared to healthy and other stages WHV infection (Figure 3.17). These findings support the previous argument that immune cell infiltrates contribute to the increase in TLR expression observed in the liver of animals with AH and CH (Figure 3,16). Immune cells ( $T_h$  cells, CTLs, B cells, monocyte/macrophages, and NK cells) not only have higher basal expression levels of TLRs, they likely also have upregulated TLR expression during CH on cells forming intrahepatic inflammatory infiltrates.

The expression patterns of both TLR2 and TLR9 in woodchuck PBMCs observed in this study somehow differs from what was seen in previous reports describing findings in WHV-infected woodchucks. One study investigating TLR2 expression in PBMCs of healthy woodchucks and those with AH and CH found that TLR2 was significantly downregulated in both AH and CH stages of infection (Zhang *et al.*, 2012). Additionally, the authors found that mRNA expression of TLR2 was negatively correlated with WHV viral loads in the sera of animals with AH, and it was suggested that TLR2 expression may be actively suppressed by the virus. In the current study, an upregulation of TLR2 was seen in the PBMCs of woodchucks with CH when compared to animals with AH and SLAH (Figure 3.17). More investigation is needed to conclusively elucidate TLR2's role during WHV infection. Finally, it has been previously shown that TLR9 signaling in human pDCs and B cells is diminished in patients with

CHB, thus potentially contributing to establishment of CHB (Vincent *et al.*, 2011; Martinet *et al.*, 2012). Although it was observed in the current study that TLR9 was upregulated in PBMCs during CH (Figure 3.17), it is possible that its ability to induce an antiviral response is diminished. An increase in mRNA for a particular gene may not always correlate into an increase in functional activity of transcribed protein. Functional studies are needed to confirm that TLR9 antiviral response was affected by WHV-induced CH.

It is interesting to note that TLR1 was detectable in woodchuck PBMCs but not in the liver or isolated hepatocytes. There were no significant differences in TLR1 expression observed during the course of WHV-infection, however, it is possible that TLR1 may be more functionally active as an innate immune receptor in the periphery than in the intrahepatic inflammatory infiltrates.

## Chapter 5 – Conclusions and Significance

### 5.1. Summary and Conclusions

1. Primers for woodchuck TLRs1-2 and TLRs4-10 were designed and used to successfully amplify woodchuck TLRs1-10 gene exon fragments.
2. With the exception of TLR2 and TLR10, expression of TLRs in livers (n=25) and hepatocytes isolated from healthy woodchucks (n=5) was not different. However, comparing pairs of livers and hepatocytes isolated from them (n=5), significant upregulation of TLR7 was found.
3. An upregulation of several TLRs (*i.e.*, TLR3, TLR5, TLR7) in the liver was characteristic of animals with PreAH when compared to woodchucks with SLAH. TLR3 and TLR8 transcription was also significantly higher in PreAH livers when compared to healthy animals and those with POI, respectively. No difference in liver TLRs2-10 transcription was evident between animals with PreAH and those with AH or CH. Comparing pairs of livers and hepatocytes obtained during PreAH (n=4), there was no difference in TLRs expression. The results suggest that upregulated TLR transcription during PreAH may be related to an increase in hepatic innate immune response in attempt to control WHV during early infection. Interestingly, the level of this response appeared to be comparable to that characterizing AH and CH despite of the absence of inflammatory cell infiltrations in PreAH.
4. Livers from woodchucks with SLAH demonstrated significant downregulation of TLR2, TLR3, TLR4, TLR5, TLR7, TLR8 and TLR10 when compared to livers

from animals with AH, while TLR2, TLR4, TLR6, TLR7 and TLR8 transcription was significantly lower when compared to livers from CH. Furthermore, TLR7 was downregulated in the livers of SLAH woodchucks when compared to animals with PreAH and POI. There were no significant differences in expression of liver TLRs2-10 when comparing SLAH to healthy animals. Hepatocytes from animals with SLAH showed a significant reduction in gene transcription of TLR3, TLR7 and TLR10 when compared to hepatocytes from CH. When comparing liver and hepatocyte pairs (n=8), SLAH animals have significantly higher TLR3, TLR4 and TLR10 expression levels in their hepatocytes than livers, while TLR7 was downregulated. Taken together, livers from SLAH transcribed significantly less TLRs than livers in AH and CH, but similar levels as in healthy woodchucks. This is consistent with resolution of liver inflammation. However, upregulated expression of some TLRs in hepatocytes from SLAH suggests that WHV persisting in these cells was recognized by the innate immune system.

5. In the livers of woodchucks with CH, an upregulation of TLRs2-4 and TLRs6-10 was evident when compared to healthy animals and those with SLAH or POI, but not to those with AH. In contrast, a downregulation of TLR expression (*i.e.*, TLR3, TLR5, TLR7, TLR8 and TLR10) in hepatocytes was seen in CH when compared to healthy animals and those with PreAH, SLAH and POI. Taken together, this may suggest active suppression of TLR expression in hepatocytes during CH due to WHV's potential ability to evade or suppress TLR signaling. When comparing pairs of livers with their isolated hepatocytes (n=6), no differences were observed in CH.

6. Liver tissue obtained at biopsies, that encompasses both hepatocytes and other liver cells, showed significant upregulation of expression of TLRs during AH (*i.e.*, TLR2-10) and CH (*i.e.*, TLR2-4 and TLR6-10). The increase in TLR expression appeared not to be related to an increase in hepatocyte TLR expression in CH and, thus, was likely related to intrahepatic inflammatory infiltration alone.
7. Expression of TLR2, TLR3, TLR6, TLR7, TLR8, TLR9 and TLR10 was found to be significantly downregulated in the livers of POI animals when compared to AH and CH. TLR8 transcription was also downregulated in the livers of POI woodchucks when compared to PreAH, while TLR7 was upregulated when compared to SLAH. There were no differences seen between TLRs2-10 transcription in POI livers when compared to healthy hepatic tissue. When considering hepatocytes, TLR8 transcription was significantly upregulated in comparison to the livers they were isolated from and it was also upregulated in relation to hepatocytes from animals with CH. POI is characterized by the absence of classical serological markers of WHV infection, WHV DNA in the liver and liver inflammation, therefore it is not surprising that there was no induction of TLR expression in hepatic tissue.
8. Woodchuck PBMCs significantly upregulated TLR expression (*i.e.*, TLR2, TLR6, TLR9 and TLR10) during CH and this may coincide with the increased TLR expression observed during active liver inflammation.
9. Overall, this study uncovered that hepatic TLR expression is significantly modulated in the course of WHV infection and coinciding hepatitis, and that

analysis of TLRs expression in circulating lymphoid cells (PBMC) does not reflect the liver profiles of TLR transcription.

### **5.1.1. Comments**

This study was the first to investigate TLRs1-10 expression patterns over the course of hepadnaviral infection and in different forms of hepatitis in the woodchuck model. Primers were designed to successfully amplify woodchuck TLRs1-2, and TLRs4-10 gene exon fragments. These primers and their target gene sequences are now available to further TLR research in the WHV-woodchuck system. Ultimately, a multiplex assay was developed allowing for the amplification of TLRs1-10 in test woodchuck tissue or cell samples in a single PCR run.

Expression analysis of livers and isolated hepatocytes revealed that TLR expression from normal woodchucks were comparable, while PBMCs differentially expressed TLRs1-10 in relation to hepatic tissue. In WHV-infected woodchucks, an upregulation of several TLRs, namely TLR3, TLR5, TLR7 and TLR8, was discovered in the livers of animals with PreAH when compared to healthy animals and those with SLAH and POI. This might be due to an increase in hepatic innate immune response in attempt to control WHV during early infection. The activation of intrahepatic APCs, NK and NKT cells has been observed in the early stages of infection. In contrast, a downregulation of TLR expression (*i.e.*, TLR3, TLR5, TLR7, TLR8 and TLR10) in hepatocytes was identified in animals with CH when compared to hepatocytes from healthy animals and those with PreAH, SLAH, and POI. The observed suppression of TLR expression may be due to WHV's ability to evade/suppress TLR signaling. On the

other hand, liver biopsies demonstrated significant upregulation of TLR gene transcripts during AH (*i.e.*, TLRs2-10) and CH (*i.e.*, TLRs2-4 and TLRs6-10), when there is active cell inflammatory infiltration in the liver. Therefore, it can be deduced that the increase in TLR expression in the liver of woodchucks with AH and CH must be related to inflammatory infiltration. This is supported by the fact that woodchuck PBMCs (*i.e.*, T<sub>h</sub> cells, CTLs, B cells, monocyte/macrophages, and NK cells) have higher expression levels of TLR2, TLR6, TLR9 and TLR10 during CH.

## **5.2. Significance of Findings**

Taken together, it can be concluded that the liver TLR expression is significantly altered in the course of hepadnaviral infection. Although binding of hepadnaviral antigens to TLRs has not yet been directly confirmed, there is accumulating evidence strongly indicating TLR involvement in the immune response to HBV infection. The findings in my study suggest that restoration of hepatocyte TLR expression may be important in resolving CH. Restoring hepatocyte TLR function may promote viral clearance. In consequence, this should limit intrahepatic immune cell infiltration and coinciding damage to the liver. The findings of this study contribute to a better understanding of the role of TLRs during hepadnaviral infection in the woodchuck model of hepatitis B. They may contribute to the development of novel antiviral treatments to allow for better control of the virus through activation of a stronger intrahepatocyte immune response during CH. Assessment of hepatic TLR expression could serve as an important biomarker to predict the efficacy of test antiviral drugs and their effectiveness in resolving CH.

## Chapter 6 – Future Directions

1. To assess the histological degree of inflammatory infiltrations and relate to the TLRs1-10 expression levels identified in the livers and hepatocytes in the course of this study.
2. To investigate the expression of TLRs1-10 at the protein level in the liver, isolated hepatocytes, and PBMCs of healthy woodchucks and woodchucks infected with WHV.
3. To carry out functional studies using TLR ligands and inhibitors in cell cultures of PWH and PBMCs isolated from woodchucks with different stages of WHV-infection and assess their effects on WHV replication and production of cytokines.
4. To carry out *in vivo* studies on the effects of selected TLR inhibitors, particularly those differentially expressed in hepatocyte and in whole liver tissue, on the progression and outcomes of CH in woodchucks.

## References Cited

- Akira, S., Uematsu, S. & Takeuchi, O. 2006. Pathogen recognition and innate immunity. *Cell*, 124, 783-801.
- Akira, S., Yamamoto, M. & Takeda, K. 2003. Role of adapters in Toll-like receptor signalling. *Biochem Soc Trans*, 31, 637-42.
- Alexopoulou, L., Holt, A. C., Medzhitov, R. & Flavell, R. A. 2001. Recognition of double-stranded RNA and activation of NF-kappaB by Toll-like receptor 3. *Nature*, 413, 732-8.
- An, B. Y., Xie, Q., Lin, L. Y., Shen, H. C., Jia, N. N., Wang, H., Guo, S. M., Yu, H. & Guo, Q. 2007. [Expression of Toll-like receptor 3 on peripheral blood dendritic cells in HBeAg positive patients with chronic hepatitis B]. *Zhonghua Gan Zang Bing Za Zhi*, 15, 729-33.
- Ank, N., Iversen, M. B., Bartholdy, C., Staeheli, P., Hartmann, R., Jensen, U. B., Dagnaes-Hansen, F., Thomsen, A. R., Chen, Z., Haugen, H., Klucher, K. & Paludan, S. R. 2008. An important role for type III interferon (IFN-lambda/IL-28) in TLR-induced antiviral activity. *J Immunol*, 180, 2474-85.
- Barchet, W., Cella, M. & Colonna, M. 2005. Plasmacytoid dendritic cells--virus experts of innate immunity. *Semin Immunol*, 17, 253-61.
- Blondot, M. L., Bruss, V. & Kann, M. 2016. Intracellular transport and egress of hepatitis B virus. *J Hepatol*, 64, S49-59.
- Blumberg, B. S., Alter, H. J. & Visnich, S. 1965. A "New" Antigen in Leukemia Sera. *JAMA*, 191, 541-6.
- Boland, G., Beran, J., Lievens, M., Sasadeusz, J., Dentico, P., Nothdurft, H., Zuckerman, J. N., Genton, B., Steffen, R., Loutan, L., Van Hattum, J. & Stoffel, M. 2004. Safety and immunogenicity profile of an experimental hepatitis B vaccine adjuvanted with AS04. *Vaccine*, 23, 316-20.
- Boule, M. W., Broughton, C., Mackay, F., Akira, S., Marshak-Rothstein, A. & Rifkin, I. R. 2004. Toll-like receptor 9-dependent and -independent dendritic cell activation by chromatin-immunoglobulin G complexes. *J Exp Med*, 199, 1631-40.
- Bowie, A. G. & Unterholzner, L. 2008. Viral evasion and subversion of pattern-recognition receptor signalling. *Nat Rev Immunol*, 8, 911-22.
- Broz, P. & Monack, D. M. 2013. Newly described pattern recognition receptors team up against intracellular pathogens. *Nat Rev Immunol*, 13, 551-65.

- Busch, K. & Thimme, R. 2015. Natural history of chronic hepatitis B virus infection. *Med Microbiol Immunol*, 204, 5-10.
- Chen, J., Rider, D. A. & Ruan, R. 2006. Identification of valid housekeeping genes and antioxidant enzyme gene expression change in the aging rat liver. *J Gerontol A Biol Sci Med Sci*, 61, 20-7.
- Churchill, N. D. & Michalak, T. I. 2004. Woodchuck hepatitis virus hepatocyte culture models. *Methods Mol Med*, 96, 175-87.
- Coffin, C. S. & Michalak, T. I. 1999. Persistence of infectious hepadnavirus in the offspring of woodchuck mothers recovered from viral hepatitis. *J Clin Invest*, 104, 203-12.
- Cooper, A., Tal, G., Lider, O. & Shaul, Y. 2005. Cytokine induction by the hepatitis B virus capsid in macrophages is facilitated by membrane heparan sulfate and involves TLR2. *J Immunol*, 175, 3165-76.
- Cote, P. J., Korba, B. E., Miller, R. H., Jacob, J. R., Baldwin, B. H., Hornbuckle, W. E., Purcell, R. H., Tennant, B. C. & Gerin, J. L. 2000. Effects of age and viral determinants on chronicity as an outcome of experimental woodchuck hepatitis virus infection. *Hepatology*, 31, 190-200.
- Cova, L., Duflot, A., Prave, M. & Trepo, C. 1993. Duck hepatitis B virus infection, aflatoxin B1 and liver cancer in ducks. *Arch Virol Suppl*, 8, 81-7.
- Dandri, M., Volz, T. K., Lutgehetmann, M. & Petersen, J. 2005. Animal models for the study of HBV replication and its variants. *J Clin Virol*, 34 Suppl 1, S54-62.
- Dane, D. S., Cameron, C. H. & Briggs, M. 1970. Virus-like particles in serum of patients with Australia-antigen-associated hepatitis. *Lancet*, 1, 695-8.
- De Kok, J. B., Roelofs, R. W., Giesendorf, B. A., Pennings, J. L., Waas, E. T., Feuth, T., Swinkels, D. W. & Span, P. N. 2005. Normalization of gene expression measurements in tumor tissues: comparison of 13 endogenous control genes. *Lab Invest*, 85, 154-9.
- Dheda, K., Huggett, J. F., Bustin, S. A., Johnson, M. A., Rook, G. & Zumla, A. 2004. Validation of housekeeping genes for normalizing RNA expression in real-time PCR. *Biotechniques*, 37, 112-4, 116, 118-9.
- Diebold, S. S., Kaisho, T., Hemmi, H., Akira, S. & Reis E Sousa, C. 2004. Innate antiviral responses by means of TLR7-mediated recognition of single-stranded RNA. *Science*, 303, 1529-31.

- Edelmann, K. H., Richardson-Burns, S., Alexopoulou, L., Tyler, K. L., Flavell, R. A. & Oldstone, M. B. 2004. Does Toll-like receptor 3 play a biological role in virus infections? *Virology*, 322, 231-8.
- Egli, A., Santer, D. M., O'shea, D., Tyrrell, D. L. & Houghton, M. 2014. The impact of the interferon-lambda family on the innate and adaptive immune response to viral infections. *Emerg Microbes Infect*, 3, e51.
- Enders, G. H., Ganem, D. & Varmus, H. E. 1987. 5'-terminal sequences influence the segregation of ground squirrel hepatitis virus RNAs into polyribosomes and viral core particles. *J Virol*, 61, 35-41.
- Fosdick, A., Zheng, J., Pflanz, S., Frey, C. R., Hesselgesser, J., Halcomb, R. L., Wolfgang, G. & Tumas, D. B. 2014. Pharmacokinetic and pharmacodynamic properties of GS-9620, a novel Toll-like receptor 7 agonist, demonstrate interferon-stimulated gene induction without detectable serum interferon at low oral doses. *J Pharmacol Exp Ther*, 348, 96-105.
- Gane, E. J., Lim, Y. S., Gordon, S. C., Visvanathan, K., Sicard, E., Fedorak, R. N., Roberts, S., Massetto, B., Ye, Z., Pflanz, S., Garrison, K. L., Gaggar, A., Mani Subramanian, G., Mchutchison, J. G., Kottlil, S., Freilich, B., Coffin, C. S., Cheng, W. & Kim, Y. J. 2015. The oral toll-like receptor-7 agonist GS-9620 in patients with chronic hepatitis B virus infection. *J Hepatol*, 63, 320-8.
- Gerlich, W. H. 2013. Medical virology of hepatitis B: how it began and where we are now. *Virology*, 10, 239.
- Gerritsen, B. & Pandit, A. 2016. The memory of a killer T cell: models of CD8(+) T cell differentiation. *Immunol Cell Biol*, 94, 236-41.
- Gotthardt, D., Riediger, C., Weiss, K. H., Encke, J., Schemmer, P., Schmidt, J. & Sauer, P. 2007. Fulminant hepatic failure: etiology and indications for liver transplantation. *Nephrol Dial Transplant*, 22 Suppl 8, viii5-viii8.
- Guan, Y., Ranao, D. R., Jiang, S., Mutha, S. K., Li, X., Baudry, J. & Tapping, R. I. 2010. Human TLRs 10 and 1 share common mechanisms of innate immune sensing but not signaling. *J Immunol*, 184, 5094-103.
- Guo, J., Loke, J., Zheng, F., Hong, F., Yea, S., Fukata, M., Tarocchi, M., Abar, O. T., Huang, H., Sninsky, J. J. & Friedman, S. L. 2009. Functional linkage of cirrhosis-predictive single nucleotide polymorphisms of Toll-like receptor 4 to hepatic stellate cell responses. *Hepatology*, 49, 960-8.
- Guy, C. S., Mulrooney-Cousins, P. M., Churchill, N. D. & Michalak, T. I. 2008. Intrahepatic expression of genes affiliated with innate and adaptive immune

- responses immediately after invasion and during acute infection with woodchuck hepadnavirus. *J Virol*, 82, 8579-91.
- Guy, C. S., Rankin, S. L. & Michalak, T. I. 2011. Hepatocyte cytotoxicity is facilitated by asialoglycoprotein receptor. *Hepatology*, 54, 1043-50.
- Guy, C. S., Wang, J. & Michalak, T. I. 2010. Hepadnaviral infection augments hepatocyte cytotoxicity mediated by both CD95 ligand and perforin pathways. *Liver Int*, 30, 396-405.
- Halperin, S. A., Dobson, S., Mcneil, S., Langley, J. M., Smith, B., Mccall-Sani, R., Levitt, D., Nest, G. V., Gennevois, D. & Eiden, J. J. 2006. Comparison of the safety and immunogenicity of hepatitis B virus surface antigen co-administered with an immunostimulatory phosphorothioate oligonucleotide and a licensed hepatitis B vaccine in healthy young adults. *Vaccine*, 24, 20-6.
- Halperin, S. A., Van Nest, G., Smith, B., Abtahi, S., Whiley, H. & Eiden, J. J. 2003. A phase I study of the safety and immunogenicity of recombinant hepatitis B surface antigen co-administered with an immunostimulatory phosphorothioate oligonucleotide adjuvant. *Vaccine*, 21, 2461-7.
- Halperin, S. A., Ward, B., Cooper, C., Predy, G., Diaz-Mitoma, F., Dionne, M., Embree, J., Mcgeer, A., Zickler, P., Moltz, K. H., Martz, R., Meyer, I., Mcneil, S., Langley, J. M., Martins, E., Heyward, W. L. & Martin, J. T. 2012. Comparison of safety and immunogenicity of two doses of investigational hepatitis B virus surface antigen co-administered with an immunostimulatory phosphorothioate oligodeoxyribonucleotide and three doses of a licensed hepatitis B vaccine in healthy adults 18-55 years of age. *Vaccine*, 30, 2556-63.
- Hashimoto, C., Hudson, K. L. & Anderson, K. V. 1988. The Toll gene of *Drosophila*, required for dorsal-ventral embryonic polarity, appears to encode a transmembrane protein. *Cell*, 52, 269-79.
- Hawn, T. R., Verbon, A., Lettinga, K. D., Zhao, L. P., Li, S. S., Laws, R. J., Skerrett, S. J., Beutler, B., Schroeder, L., Nachman, A., Ozinsky, A., Smith, K. D. & Aderem, A. 2003. A common dominant TLR5 stop codon polymorphism abolishes flagellin signaling and is associated with susceptibility to legionnaires' disease. *J Exp Med*, 198, 1563-72.
- Heil, F., Hemmi, H., Hochrein, H., Ampenberger, F., Kirschning, C., Akira, S., Lipford, G., Wagner, H. & Bauer, S. 2004. Species-specific recognition of single-stranded RNA via toll-like receptor 7 and 8. *Science*, 303, 1526-9.
- Hirahara, K. & Nakayama, T. 2016. CD4<sup>+</sup> T-cell subsets in inflammatory diseases: beyond the Th1/Th2 paradigm. *Int Immunol*, 28, 163-71.

- Hochrein, H., Schlatter, B., O'keeffe, M., Wagner, C., Schmitz, F., Schiemann, M., Bauer, S., Suter, M. & Wagner, H. 2004. Herpes simplex virus type-1 induces IFN-alpha production via Toll-like receptor 9-dependent and -independent pathways. *Proc Natl Acad Sci U S A*, 101, 11416-21.
- Hodgson, P. D. & Michalak, T. I. 2001. Augmented hepatic interferon gamma expression and T-cell influx characterize acute hepatitis progressing to recovery and residual lifelong virus persistence in experimental adult woodchuck hepatitis virus infection. *Hepatology*, 34, 1049-59.
- Hou, J., Liu, Z. & Gu, F. 2005. Epidemiology and Prevention of Hepatitis B Virus Infection. *Int J Med Sci*, 2, 50-57.
- Hua, Z. & Hou, B. 2013. TLR signaling in B-cell development and activation. *Cell Mol Immunol*, 10, 103-6.
- Huang, X., Li, H., Wang, J., Huang, C., Lu, Y., Qin, X. & Li, S. 2015a. Genetic polymorphisms in Toll-like receptor 3 gene are associated with the risk of hepatitis B virus-related liver diseases in a Chinese population. *Gene*, 569, 218-24.
- Huang, Z., Ge, J., Pang, J., Liu, H., Chen, J., Liao, B., Huang, X., Zuo, D., Sun, J., Lu, M., Zhang, X. & Hou, J. 2015b. Aberrant expression and dysfunction of TLR2 and its soluble form in chronic HBV infection and its regulation by antiviral therapy. *Antiviral Res*, 118, 10-9.
- Hui, C. K., Leung, N., Yuen, S. T., Zhang, H. Y., Leung, K. W., Lu, L., Cheung, S. K., Wong, W. M., Lau, G. K. & Hong Kong Liver Fibrosis Study, G. 2007. Natural history and disease progression in Chinese chronic hepatitis B patients in immune-tolerant phase. *Hepatology*, 46, 395-401.
- Isogawa, M., Robek, M. D., Furuichi, Y. & Chisari, F. V. 2005. Toll-like receptor signaling inhibits hepatitis B virus replication in vivo. *J Virol*, 79, 7269-72.
- Jin, M. S., Kim, S. E., Heo, J. Y., Lee, M. E., Kim, H. M., Paik, S. G., Lee, H. & Lee, J. O. 2007. Crystal structure of the TLR1-TLR2 heterodimer induced by binding of a tri-acylated lipopeptide. *Cell*, 130, 1071-82.
- Jo, J., Tan, A. T., Ussher, J. E., Sandalova, E., Tang, X. Z., Tan-Garcia, A., To, N., Hong, M., Chia, A., Gill, U. S., Kennedy, P. T., Tan, K. C., Lee, K. H., De Libero, G., Gehring, A. J., Willberg, C. B., Klenerman, P. & Bertolotti, A. 2014. Toll-like receptor 8 agonist and bacteria trigger potent activation of innate immune cells in human liver. *PLoS Pathog*, 10, e1004210.
- Kariko, K., Ni, H., Capodici, J., Lamphier, M. & Weissman, D. 2004. mRNA is an endogenous ligand for Toll-like receptor 3. *J Biol Chem*, 279, 12542-50.

- Kawai, T., Adachi, O., Ogawa, T., Takeda, K. & Akira, S. 1999. Unresponsiveness of MyD88-deficient mice to endotoxin. *Immunity*, 11, 115-22.
- Kawasaki, K., Akashi, S., Shimazu, R., Yoshida, T., Miyake, K. & Nishijima, M. 2000. Mouse toll-like receptor 4.MD-2 complex mediates lipopolysaccharide-mimetic signal transduction by Taxol. *J Biol Chem*, 275, 2251-4.
- Koblansky, A. A., Jankovic, D., Oh, H., Hieny, S., Sungnak, W., Mathur, R., Hayden, M. S., Akira, S., Sher, A. & Ghosh, S. 2013. Recognition of profilin by Toll-like receptor 12 is critical for host resistance to *Toxoplasma gondii*. *Immunity*, 38, 119-30.
- Korba, B. E., Wells, F. V., Baldwin, B., Cote, P. J., Tennant, B. C., Popper, H. & Gerin, J. L. 1989. Hepatocellular carcinoma in woodchuck hepatitis virus-infected woodchucks: presence of viral DNA in tumor tissue from chronic carriers and animals serologically recovered from acute infections. *Hepatology*, 9, 461-70.
- Krug, A., French, A. R., Barchet, W., Fischer, J. A., Dzionek, A., Pingel, J. T., Orihuela, M. M., Akira, S., Yokoyama, W. M. & Colonna, M. 2004. TLR9-dependent recognition of MCMV by IPC and DC generates coordinated cytokine responses that activate antiviral NK cell function. *Immunity*, 21, 107-19.
- Kugelberg, E. 2014. Innate immunity: Making mice more human the TLR8 way. *Nat Rev Immunol*, 14, 6.
- Kumar, S., Ingle, H., Prasad, D. V. & Kumar, H. 2013. Recognition of bacterial infection by innate immune sensors. *Crit Rev Microbiol*, 39, 229-46.
- Lanford, R. E., Guerra, B., Chavez, D., Giavedoni, L., Hodara, V. L., Brasky, K. M., Fosdick, A., Frey, C. R., Zheng, J., Wolfgang, G., Halcomb, R. L. & Tumas, D. B. 2013. GS-9620, an oral agonist of Toll-like receptor-7, induces prolonged suppression of hepatitis B virus in chronically infected chimpanzees. *Gastroenterology*, 144, 1508-17, 1517 e1-10.
- Lavanchy, D. 2012. Viral hepatitis: global goals for vaccination. *J Clin Virol*, 55, 296-302.
- Leadbetter, E. A., Rifkin, I. R., Hohlbaum, A. M., Beaudette, B. C., Shlomchik, M. J. & Marshak-Rothstein, A. 2002. Chromatin-IgG complexes activate B cells by dual engagement of IgM and Toll-like receptors. *Nature*, 416, 603-7.
- Lee, S. M., Kok, K. H., Jaume, M., Cheung, T. K., Yip, T. F., Lai, J. C., Guan, Y., Webster, R. G., Jin, D. Y. & Peiris, J. S. 2014. Toll-like receptor 10 is involved in induction of innate immune responses to influenza virus infection. *Proc Natl Acad Sci U S A*, 111, 3793-8.

- Lemaitre, B., Nicolas, E., Michaut, L., Reichhart, J. M. & Hoffmann, J. A. 1996. The dorsoventral regulatory gene cassette *spatzle/Toll/cactus* controls the potent antifungal response in *Drosophila* adults. *Cell*, 86, 973-83.
- Lester, S. N. & Li, K. 2014. Toll-like receptors in antiviral innate immunity. *J Mol Biol*, 426, 1246-64.
- Levie, K., Gjorup, I., Skinhoj, P. & Stoffel, M. 2002. A 2-dose regimen of a recombinant hepatitis B vaccine with the immune stimulant AS04 compared with the standard 3-dose regimen of Engerix-B in healthy young adults. *Scand J Infect Dis*, 34, 610-4.
- Li, N., Li, Q., Qian, Z., Zhang, Y., Chen, M. & Shi, G. 2009. Impaired TLR3/IFN-beta signaling in monocyte-derived dendritic cells from patients with acute-on-chronic hepatitis B liver failure: relevance to the severity of liver damage. *Biochem Biophys Res Commun*, 390, 630-5.
- Liang, T. J. 2009. Hepatitis B: the virus and disease. *Hepatology*, 49, S13-21.
- Livingston, B. D., Alexander, J., Crimi, C., Oseroff, C., Celis, E., Daly, K., Guidotti, L. G., Chisari, F. V., Fikes, J., Chesnut, R. W. & Sette, A. 1999. Altered helper T lymphocyte function associated with chronic hepatitis B virus infection and its role in response to therapeutic vaccination in humans. *J Immunol*, 162, 3088-95.
- Livingston, B. D., Crimi, C., Grey, H., Ishioka, G., Chisari, F. V., Fikes, J., Grey, H., Chesnut, R. W. & Sette, A. 1997. The hepatitis B virus-specific CTL responses induced in humans by lipopeptide vaccination are comparable to those elicited by acute viral infection. *J Immunol*, 159, 1383-92.
- Locarnini, S. & Zoulim, F. 2010. Molecular genetics of HBV infection. *Antivir Ther*, 15 Suppl 3, 3-14.
- Lu, M., Klaes, R., Menne, S., Gerlich, W., Stahl, B., Dienes, H. P., Drebber, U. & Roggendorf, M. 2003. Induction of antibodies to the PreS region of surface antigens of woodchuck hepatitis virus (WHV) in chronic carrier woodchucks by immunizations with WHV surface antigens. *J Hepatol*, 39, 405-13.
- Lund, J. M., Alexopoulou, L., Sato, A., Karow, M., Adams, N. C., Gale, N. W., Iwasaki, A. & Flavell, R. A. 2004. Recognition of single-stranded RNA viruses by Toll-like receptor 7. *Proc Natl Acad Sci U S A*, 101, 5598-603.
- Lv, S., Wang, J., Dou, S., Yang, X., Ni, X., Sun, R., Tian, Z. & Wei, H. 2014. Nanoparticles encapsulating hepatitis B virus cytosine-phosphate-guanosine induce therapeutic immunity against HBV infection. *Hepatology*, 59, 385-94.
- Maccallum, F. O. 1946. Homologous serum hepatitis. *Proc R Soc Med*, 39, 655-7.

- Maire, M., Parent, R., Morand, A. L., Alotte, C., Trepo, C., Durantel, D. & Petit, M. A. 2008. Characterization of the double-stranded RNA responses in human liver progenitor cells. *Biochem Biophys Res Commun*, 368, 556-62.
- Mancuso, G., Gambuzza, M., Midiri, A., Biondo, C., Papasergi, S., Akira, S., Teti, G. & Beninati, C. 2009. Bacterial recognition by TLR7 in the lysosomes of conventional dendritic cells. *Nat Immunol*, 10, 587-94.
- Mani, H. & Kleiner, D. E. 2009. Liver biopsy findings in chronic hepatitis B. *Hepatology*, 49, S61-71.
- Marion, P. L., Oshiro, L. S., Regnery, D. C., Scullard, G. H. & Robinson, W. S. 1980. A virus in Beechey ground squirrels that is related to hepatitis B virus of humans. *Proc Natl Acad Sci U S A*, 77, 2941-5.
- Martinet, J., Dufeu-Duchesne, T., Bruder Costa, J., Larrat, S., Marlu, A., Leroy, V., Plumas, J. & Aspod, C. 2012. Altered functions of plasmacytoid dendritic cells and reduced cytolytic activity of natural killer cells in patients with chronic HBV infection. *Gastroenterology*, 143, 1586-1596 e8.
- McMahon, B. J. 2008. Natural history of chronic hepatitis B - clinical implications. *Medscape J Med*, 10, 91.
- Medzhitov, R. & Janeway, C., Jr. 2000. The Toll receptor family and microbial recognition. *Trends Microbiol*, 8, 452-6.
- Mencin, A., Kluwe, J. & Schwabe, R. F. 2009. Toll-like receptors as targets in chronic liver diseases. *Gut*, 58, 704-20.
- Meng, Z., Zhang, X., Pei, R., Zhang, E., Kemper, T., Vollmer, J., Davis, H. L., Glebe, D., Gerlich, W., Roggendorf, M. & Lu, M. 2016. Combination therapy including CpG oligodeoxynucleotides and entecavir induces early viral response and enhanced inhibition of viral replication in a woodchuck model of chronic hepadnaviral infection. *Antiviral Res*, 125, 14-24.
- Menne, S. & Cote, P. J. 2007. The woodchuck as an animal model for pathogenesis and therapy of chronic hepatitis B virus infection. *World J Gastroenterol*, 13, 104-24.
- Menne, S., Tumas, D. B., Liu, K. H., Thampi, L., Aldeghaither, D., Baldwin, B. H., Bellezza, C. A., Cote, P. J., Zheng, J., Halcomb, R., Fosdick, A., Fletcher, S. P., Daffis, S., Li, L., Yue, P., Wolfgang, G. H. & Tennant, B. C. 2015. Sustained efficacy and seroconversion with the Toll-like receptor 7 agonist GS-9620 in the Woodchuck model of chronic hepatitis B. *J Hepatol*, 62, 1237-45.

- Michalak, T. 1978. Immune complexes of hepatitis B surface antigen in the pathogenesis of periarteritis nodosa. A study of seven necropsy cases. *Am J Pathol*, 90, 619-32.
- Michalak, T. I. 2000. Occult persistence and lymphotropism of hepadnaviral infection: insights from the woodchuck viral hepatitis model. *Immunol Rev*, 174, 98-111.
- Michalak, T. I., Churchill, N. D., Codner, D., Drover, S. & Marshall, W. H. 1995. Identification of woodchuck class I MHC antigens using monoclonal antibodies. *Tissue Antigens*, 45, 333-42.
- Michalak, T. I., Hodgson, P. D. & Churchill, N. D. 2000. Posttranscriptional inhibition of class I major histocompatibility complex presentation on hepatocytes and lymphoid cells in chronic woodchuck hepatitis virus infection. *J Virol*, 74, 4483-94.
- Michalak, T. I. & Lin, B. 1994. Molecular species of hepadnavirus core and envelope polypeptides in hepatocyte plasma membrane of woodchucks with acute and chronic viral hepatitis. *Hepatology*, 20, 275-86.
- Michalak, T. I., Mulrooney, P. M. & Coffin, C. S. 2004. Low doses of hepadnavirus induce infection of the lymphatic system that does not engage the liver. *J Virol*, 78, 1730-8.
- Michalak, T. I., Pardoe, I. U., Coffin, C. S., Churchill, N. D., Freake, D. S., Smith, P. & Trelogan, C. L. 1999. Occult lifelong persistence of infectious hepadnavirus and residual liver inflammation in woodchucks convalescent from acute viral hepatitis. *Hepatology*, 29, 928-38.
- Michalak, T. I., Pasquinelli, C., Guilhot, S. & Chisari, F. V. 1994. Hepatitis B virus persistence after recovery from acute viral hepatitis. *J Clin Invest*, 94, 907.
- Michalak, T. I., Snyder, R. L. & Churchill, N. D. 1989. Characterization of the incorporation of woodchuck hepatitis virus surface antigen into hepatocyte plasma membrane in woodchuck hepatitis and in the virus-induced hepatocellular carcinoma. *Hepatology*, 10, 44-55.
- Minuk, G. Y., Shaffer, E. A., Hoar, D. I. & Kelly, J. 1986. Ground squirrel hepatitis virus (GSHV) infection and hepatocellular carcinoma in the Canadian Richardson ground squirrel (*Spermophilus richardsonii*). *Liver*, 6, 350-6.
- Mogensen, T. H. 2009. Pathogen recognition and inflammatory signaling in innate immune defenses. *Clin Microbiol Rev*, 22, 240-73, Table of Contents.
- Mulrooney-Cousins, P. M., Chauhan, R., Churchill, N. D. & Michalak, T. I. 2014. Primary seronegative but molecularly evident hepadnaviral infection engages liver and

- induces hepatocarcinoma in the woodchuck model of hepatitis B. *PLoS Pathog*, 10, e1004332.
- Mulrooney-Cousins, P. M. & Michalak, T. I. 2007. Persistent occult hepatitis B virus infection: experimental findings and clinical implications. *World J Gastroenterol*, 13, 5682-6.
- Mulrooney-Cousins, P. M. & Michalak, T. I. 2015. Asymptomatic Hepadnaviral Persistence and Its Consequences in the Woodchuck Model of Occult Hepatitis B Virus Infection. *J Clin Transl Hepatol*, 3, 211-9.
- Nagai, Y., Akashi, S., Nagafuku, M., Ogata, M., Iwakura, Y., Akira, S., Kitamura, T., Kosugi, A., Kimoto, M. & Miyake, K. 2002. Essential role of MD-2 in LPS responsiveness and TLR4 distribution. *Nat Immunol*, 3, 667-72.
- Nishimura, M., Koeda, A., Suzuki, E., Shimizu, T., Kawano, Y., Nakayama, M., Satoh, T., Narimatsu, S. & Naito, S. 2006. Effects of prototypical drug-metabolizing enzyme inducers on mRNA expression of housekeeping genes in primary cultures of human and rat hepatocytes. *Biochem Biophys Res Commun*, 346, 1033-9.
- Nishimura, M. & Naito, S. 2005. Tissue-specific mRNA expression profiles of human toll-like receptors and related genes. *Biol Pharm Bull*, 28, 886-92.
- Notarangelo, L. D., Kim, M. S., Walter, J. E. & Lee, Y. N. 2016. Human RAG mutations: biochemistry and clinical implications. *Nat Rev Immunol*, 16, 234-46.
- O'Neill, L. A., Golenbock, D. & Bowie, A. G. 2013. The history of Toll-like receptors - redefining innate immunity. *Nat Rev Immunol*, 13, 453-60.
- Ohashi, K., Burkart, V., Flohe, S. & Kolb, H. 2000. Cutting edge: heat shock protein 60 is a putative endogenous ligand of the toll-like receptor-4 complex. *J Immunol*, 164, 558-61.
- Okamura, Y., Watari, M., Jerud, E. S., Young, D. W., Ishizaka, S. T., Rose, J., Chow, J. C. & Strauss, J. F., 3rd 2001. The extra domain A of fibronectin activates Toll-like receptor 4. *J Biol Chem*, 276, 10229-33.
- Owen, J. A., Punt, J., Stranford, S. A., Jones, P. P. & Kubly, J. 2013. *Kubly immunology*, New York, W.H. Freeman.
- Pandey, S. & Agrawal, D. K. 2006. Immunobiology of Toll-like receptors: emerging trends. *Immunol Cell Biol*, 84, 333-41.

- Plain, K. M., Purdie, A. C., Begg, D. J., De Silva, K. & Whittington, R. J. 2010. Toll-like receptor (TLR)6 and TLR1 differentiation in gene expression studies of Johne's disease. *Vet Immunol Immunopathol*, 137, 142-8.
- Popper, H., Shih, J. W., Gerin, J. L., Wong, D. C., Hoyer, B. H., London, W. T., Sly, D. L. & Purcell, R. H. 1981. Woodchuck hepatitis and hepatocellular carcinoma: correlation of histologic with virologic observations. *Hepatology*, 1, 91-8.
- Rahman, A. H., Taylor, D. K. & Turka, L. A. 2009. The contribution of direct TLR signaling to T cell responses. *Immunol Res*, 45, 25-36.
- Raimondo, G., Allain, J. P., Brunetto, M. R., Buendia, M. A., Chen, D. S., Colombo, M., Craxi, A., Donato, F., Ferrari, C., Gaeta, G. B., Gerlich, W. H., Levrero, M., Locarnini, S., Michalak, T., Mondelli, M. U., Pawlotsky, J. M., Pollicino, T., Prati, D., Puoti, M., Samuel, D., Shouval, D., Smedile, A., Squadrito, G., Trepo, C., Villa, E., Will, H., Zanetti, A. R. & Zoulim, F. 2008a. Statements from the Taormina expert meeting on occult hepatitis B virus infection. *J Hepatol*, 49, 652-7.
- Raimondo, G., Navarra, G., Mondello, S., Costantino, L., Colloredo, G., Cucinotta, E., Di Vita, G., Scisca, C., Squadrito, G. & Pollicino, T. 2008b. Occult hepatitis B virus in liver tissue of individuals without hepatic disease. *J Hepatol*, 48, 743-6.
- Rehermann, B. 2000. Intrahepatic T cells in hepatitis B: viral control versus liver cell injury. *J Exp Med*, 191, 1263-8.
- Rock, F. L., Hardiman, G., Timans, J. C., Kastelein, R. A. & Bazan, J. F. 1998. A family of human receptors structurally related to Drosophila Toll. *Proc Natl Acad Sci U S A*, 95, 588-93.
- Sankhyan, A., Sharma, C., Dutta, D., Sharma, T., Chosdol, K., Wakita, T., Watashi, K., Awasthi, A., Acharya, S. K., Khanna, N., Tiwari, A. & Sinha, S. 2016. Inhibition of preS1-hepatocyte interaction by an array of recombinant human antibodies from naturally recovered individuals. *Sci Rep*, 6, 21240.
- Schaefer, L., Babelova, A., Kiss, E., Hausser, H. J., Baliova, M., Krzyzankova, M., Marsche, G., Young, M. F., Mihalik, D., Gotte, M., Malle, E., Schaefer, R. M. & Grone, H. J. 2005. The matrix component biglycan is proinflammatory and signals through Toll-like receptors 4 and 2 in macrophages. *J Clin Invest*, 115, 2223-33.
- Schillie, S., Walker, T., Veselsky, S., Crowley, S., Dusek, C., Lazaroff, J., Morris, S. A., Onye, K., Ko, S., Fenlon, N., Nelson, N. P. & Murphy, T. V. 2015. Outcomes of infants born to women infected with hepatitis B. *Pediatrics*, 135, e1141-7.

- Schweitzer, A., Horn, J., Mikolajczyk, R. T., Krause, G. & Ott, J. J. 2015. Estimations of worldwide prevalence of chronic hepatitis B virus infection: a systematic review of data published between 1965 and 2013. *Lancet*, 386, 1546-55.
- Seeger, C., Baldwin, B., Hornbuckle, W. E., Yeager, A. E., Tennant, B. C., Cote, P., Ferrell, L., Ganem, D. & Varmus, H. E. 1991. Woodchuck hepatitis virus is a more efficient oncogenic agent than ground squirrel hepatitis virus in a common host. *J Virol*, 65, 1673-9.
- Seeger, C. & Mason, W. S. 2000. Hepatitis B virus biology. *Microbiol Mol Biol Rev*, 64, 51-68.
- Seeger, C. & Mason, W. S. 2015. Molecular biology of hepatitis B virus infection. *Virology*, 479-480, 672-86.
- Shahrakyvahed, A., Sanchooli, J., Sanadgol, N., Arababadi, M. K. & Kennedy, D. 2014. TLR9: an important molecule in the fight against hepatitis B virus. *Postgrad Med J*, 90, 396-401.
- Shao, Q., Zhao, X. & Yao Li, M. D. 2013. Role of peripheral blood mononuclear cell transportation from mother to baby in HBV intrauterine infection. *Arch Gynecol Obstet*, 288, 1257-61.
- Shibata, T., Motoi, Y., Tanimura, N., Yamakawa, N., Akashi-Takamura, S. & Miyake, K. 2011. Intracellular TLR4/MD-2 in macrophages senses Gram-negative bacteria and induces a unique set of LPS-dependent genes. *Int Immunol*, 23, 503-10.
- Slijepcevic, D., Kaufman, C., Wichers, C. G., Gilgioni, E. H., Lempp, F. A., Duijst, S., De Waart, D. R., Elferink, R. P., Mier, W., Stieger, B., Beuers, U., Urban, S. & Van De Graaf, S. F. 2015. Impaired uptake of conjugated bile acids and hepatitis b virus pres1-binding in na(+)-taurocholate cotransporting polypeptide knockout mice. *Hepatology*, 62, 207-19.
- Summers, J., Smolec, J. M. & Snyder, R. 1978. A virus similar to human hepatitis B virus associated with hepatitis and hepatoma in woodchucks. *Proc Natl Acad Sci U S A*, 75, 4533-7.
- Tabeta, K., Georgel, P., Janssen, E., Du, X., Hoebe, K., Crozat, K., Mudd, S., Shamel, L., Sovath, S., Goode, J., Alexopoulou, L., Flavell, R. A. & Beutler, B. 2004. Toll-like receptors 9 and 3 as essential components of innate immune defense against mouse cytomegalovirus infection. *Proc Natl Acad Sci U S A*, 101, 3516-21.
- Takeda, K. & Akira, S. 2005. Toll-like receptors in innate immunity. *Int Immunol*, 17, 1-14.

- Takeda, K. & Akira, S. 2015. Toll-like receptors. *Curr Protoc Immunol*, 109, 14 12 1-10.
- Takeda, K., Kaisho, T. & Akira, S. 2003. Toll-like receptors. *Annu Rev Immunol*, 21, 335-76.
- Takeda, K., Takeuchi, O. & Akira, S. 2002. Recognition of lipopeptides by Toll-like receptors. *J Endotoxin Res*, 8, 459-63.
- Takeuchi, O., Kawai, T., Muhlradt, P. F., Morr, M., Radolf, J. D., Zychlinsky, A., Takeda, K. & Akira, S. 2001. Discrimination of bacterial lipoproteins by Toll-like receptor 6. *Int Immunol*, 13, 933-40.
- Tang, H., Oishi, N., Kaneko, S. & Murakami, S. 2006. Molecular functions and biological roles of hepatitis B virus x protein. *Cancer Sci*, 97, 977-83.
- Termeer, C., Benedix, F., Sleeman, J., Fieber, C., Voith, U., Ahrens, T., Miyake, K., Freudenberg, M., Galanos, C. & Simon, J. C. 2002. Oligosaccharides of Hyaluronan activate dendritic cells via toll-like receptor 4. *J Exp Med*, 195, 99-111.
- Thoelen, S., Van Damme, P., Mathei, C., Leroux-Roels, G., Desombere, I., Safary, A., Vandepapeliere, P., Slaoui, M. & Meheus, A. 1998. Safety and immunogenicity of a hepatitis B vaccine formulated with a novel adjuvant system. *Vaccine*, 16, 708-14.
- Tian, T., Sun, D., Wang, P., Wang, H., Bai, X., Yang, X., Wang, Z. & Dong, M. 2015. Roles of Toll-like Receptor 7 and 8 in Prevention of Intrauterine Transmission of Hepatitis B Virus. *Cell Physiol Biochem*, 37, 445-53.
- Tsaur, I., Renninger, M., Hennenlotter, J., Oppermann, E., Munz, M., Kuehs, U., Stenzl, A. & Schilling, D. 2013. Reliable housekeeping gene combination for quantitative PCR of lymph nodes in patients with prostate cancer. *Anticancer Res*, 33, 5243-8.
- Tu, Z., Bozorgzadeh, A., Pierce, R. H., Kurtis, J., Crispe, I. N. & Orloff, M. S. 2008. TLR-dependent cross talk between human Kupffer cells and NK cells. *J Exp Med*, 205, 233-44.
- Vabulas, R. M., Ahmad-Nejad, P., Ghose, S., Kirschning, C. J., Issels, R. D. & Wagner, H. 2002. HSP70 as endogenous stimulus of the Toll/interleukin-1 receptor signal pathway. *J Biol Chem*, 277, 15107-12.
- Van Montfoort, N., Van Der Aa, E., Van Den Bosch, A., Brouwers, H., Vanwollegem, T., Janssen, H. L., Javanbakht, H., Buschow, S. I. & Woltman, A. M. 2016. Hepatitis B surface antigen activates myeloid dendritic cells via a soluble CD14-dependent mechanism. *J Virol*.

- Vijay-Kumar, M. & Gewirtz, A. T. 2009. Flagellin: key target of mucosal innate immunity. *Mucosal Immunol*, 2, 197-205.
- Vincent, I. E., Zannetti, C., Lucifora, J., Norder, H., Protzer, U., Hainaut, P., Zoulim, F., Tommasino, M., Trepo, C., Hasan, U. & Chemin, I. 2011. Hepatitis B virus impairs TLR9 expression and function in plasmacytoid dendritic cells. *PLoS One*, 6, e26315.
- Visvanathan, K., Skinner, N. A., Thompson, A. J., Riordan, S. M., Sozzi, V., Edwards, R., Rodgers, S., Kurtovic, J., Chang, J., Lewin, S., Desmond, P. & Locarnini, S. 2007. Regulation of Toll-like receptor-2 expression in chronic hepatitis B by the precore protein. *Hepatology*, 45, 102-10.
- Vos, Q., Lees, A., Wu, Z. Q., Snapper, C. M. & Mond, J. J. 2000. B-cell activation by T-cell-independent type 2 antigens as an integral part of the humoral immune response to pathogenic microorganisms. *Immunol Rev*, 176, 154-70.
- Wang, Y., Chen, K., Wu, Z., Liu, Y., Liu, S., Zou, Z., Chen, S. H. & Qu, C. 2014. Immunizations with hepatitis B viral antigens and a TLR7/8 agonist adjuvant induce antigen-specific immune responses in HBV-transgenic mice. *Int J Infect Dis*, 29, 31-6.
- Wieland, S. F. & Chisari, F. V. 2005. Stealth and cunning: hepatitis B and hepatitis C viruses. *J Virol*, 79, 9369-80.
- World Health Organization. 2016. *Hepatitis B* [Online]. Available: <http://www.who.int/mediacentre/factsheets/fs204/en/> [Accessed January 10 2016].
- Wu, J., Meng, Z., Jiang, M., Pei, R., Trippler, M., Broering, R., Bucchi, A., Sowa, J. P., Dittmer, U., Yang, D., Roggendorf, M., Gerken, G., Lu, M. & Schlaak, J. F. 2009. Hepatitis B virus suppresses toll-like receptor-mediated innate immune responses in murine parenchymal and nonparenchymal liver cells. *Hepatology*, 49, 1132-40.
- Xu, C. L., Hao, Y. H., Lu, Y. P., Tang, Z. S., Yang, X. C., Wu, J., Zheng, X., Wang, B. J., Liu, J. & Yang, D. L. 2015. Upregulation of toll-like receptor 4 on T cells in PBMCs is associated with disease aggravation of HBV-related acute-on-chronic liver failure. *J Huazhong Univ Sci Technolog Med Sci*, 35, 910-5.
- Xu, N., Yao, H. P., Lv, G. C. & Chen, Z. 2012. Downregulation of TLR7/9 leads to deficient production of IFN-alpha from plasmacytoid dendritic cells in chronic hepatitis B. *Inflamm Res*, 61, 997-1004.
- Yan, H., Zhong, G., Xu, G., He, W., Jing, Z., Gao, Z., Huang, Y., Qi, Y., Peng, B., Wang, H., Fu, L., Song, M., Chen, P., Gao, W., Ren, B., Sun, Y., Cai, T., Feng, X., Sui,

- J. & Li, W. 2012. Sodium taurocholate cotransporting polypeptide is a functional receptor for human hepatitis B and D virus. *Elife*, 1, e00049.
- Yan, H., Zhong, G., Xu, G., He, W., Jing, Z., Gao, Z., Huang, Y., Qi, Y., Peng, B., Wang, H., Fu, L., Song, M., Chen, P., Gao, W., Ren, B., Sun, Y., Cai, T., Feng, X., Sui, J. & Li, W. 2014. Sodium taurocholate cotransporting polypeptide is a functional receptor for human hepatitis B and D virus. *Elife*, 3.
- Yarovinsky, F. 2014. Innate immunity to *Toxoplasma gondii* infection. *Nat Rev Immunol*, 14, 109-21.
- Yarovinsky, F., Zhang, D., Andersen, J. F., Bannenberg, G. L., Serhan, C. N., Hayden, M. S., Hieny, S., Sutterwala, F. S., Flavell, R. A., Ghosh, S. & Sher, A. 2005. TLR11 activation of dendritic cells by a protozoan profilin-like protein. *Science*, 308, 1626-9.
- Zampino, R., Boemio, A., Sagnelli, C., Alessio, L., Adinolfi, L. E., Sagnelli, E. & Coppola, N. 2015. Hepatitis B virus burden in developing countries. *World J Gastroenterol*, 21, 11941-53.
- Zarembek, K. A. & Godowski, P. J. 2002. Tissue expression of human Toll-like receptors and differential regulation of Toll-like receptor mRNAs in leukocytes in response to microbes, their products, and cytokines. *J Immunol*, 168, 554-61.
- Zerbini, A., Pilli, M., Boni, C., Fiscicaro, P., Penna, A., Di Vincenzo, P., Giuberti, T., Orlandini, A., Raffa, G., Pollicino, T., Raimondo, G., Ferrari, C. & Missale, G. 2008. The characteristics of the cell-mediated immune response identify different profiles of occult hepatitis B virus infection. *Gastroenterology*, 134, 1470-81.
- Zhang, D., Zhang, G., Hayden, M. S., Greenblatt, M. B., Bussey, C., Flavell, R. A. & Ghosh, S. 2004. A toll-like receptor that prevents infection by uropathogenic bacteria. *Science*, 303, 1522-6.
- Zhang, E., Zhang, X., Liu, J., Wang, B., Tian, Y., Kosinska, A. D., Ma, Z., Xu, Y., Dittmer, U., Roggendorf, M., Yang, D. & Lu, M. 2011. The expression of PD-1 ligands and their involvement in regulation of T cell functions in acute and chronic woodchuck hepatitis virus infection. *PLoS One*, 6, e26196.
- Zhang, S. Y., Herman, M., Ciancanelli, M. J., Perez De Diego, R., Sancho-Shimizu, V., Abel, L. & Casanova, J. L. 2013. TLR3 immunity to infection in mice and humans. *Curr Opin Immunol*, 25, 19-33.
- Zhang, X., Ma, Z., Liu, H., Liu, J., Meng, Z., Broering, R., Yang, D., Schlaak, J. F., Roggendorf, M. & Lu, M. 2012. Role of Toll-like receptor 2 in the immune response against hepadnaviral infection. *J Hepatol*, 57, 522-8.

Zhang, X., Meng, Z., Qiu, S., Xu, Y., Yang, D., Schlaak, J. F., Roggendorf, M. & Lu, M. 2009. Lipopolysaccharide-induced innate immune responses in primary hepatocytes downregulates woodchuck hepatitis virus replication via interferon-independent pathways. *Cell Microbiol*, 11, 1624-37.

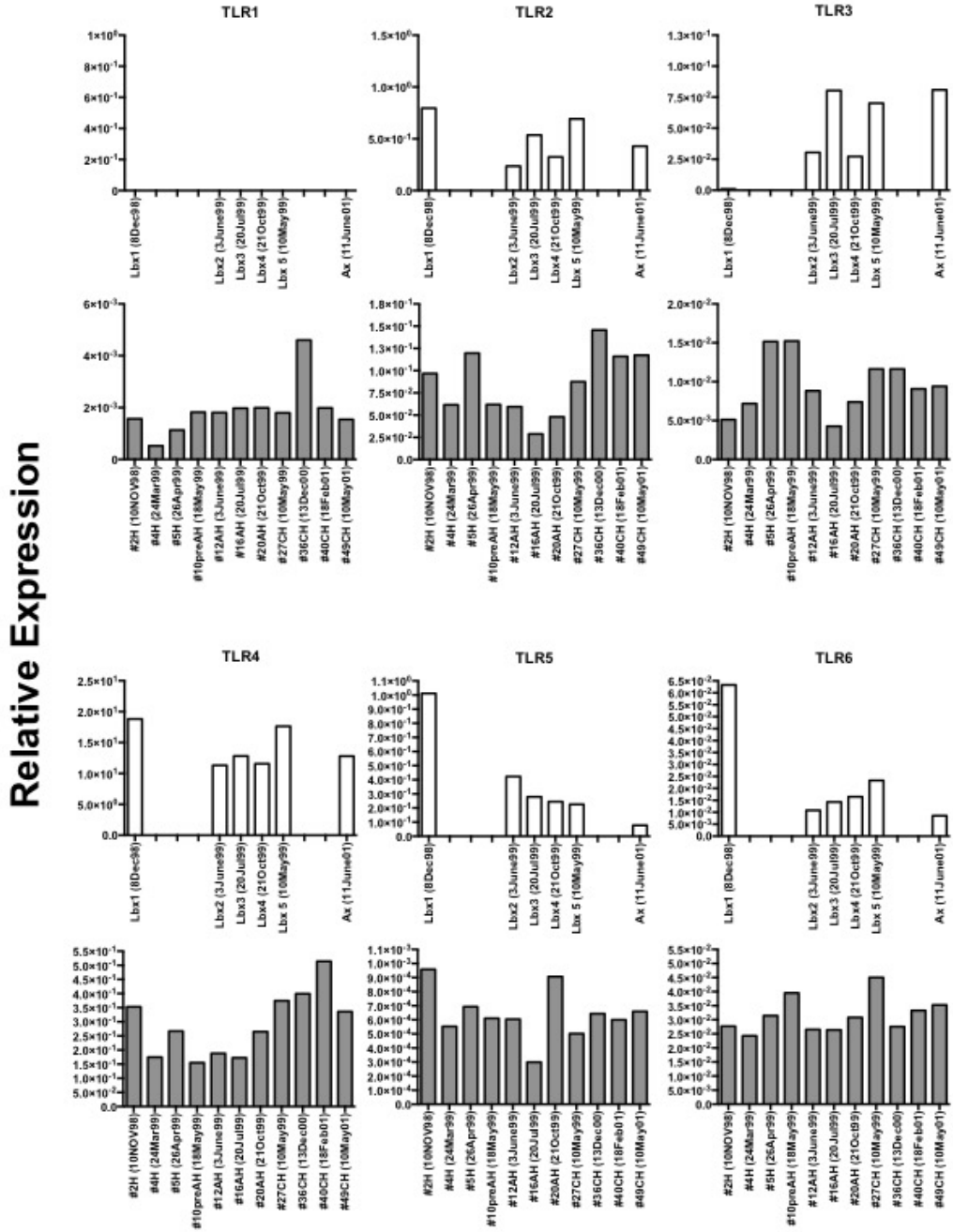
## Appendices

**Figure A1. Expression levels of TLRs1-10 in sequential liver biopsy samples and PBMCs during the course of hepadnaviral infection in woodchuck #1 that progressed from acute hepatitis (AH) to chronic hepatitis (CH).**

Liver biopsy tissue samples (top; white bars) and PBMCs (bottom; grey bars) isolated from woodchuck #1 during the progression of WHV infection (Healthy>AH>CH) were analyzed for expression of TLRs1-10. Quantification of TLR mRNA was performed by RT-qPCR. TLR1 expression was evaluated but not detected in the liver. Gene transcription levels were normalized against woodchuck HPRT expression. Total RNA equivalent of 50 ng was tested from each test sample in triplicate.

# Woodchuck #1

## Healthy > AH > CH



# Woodchuck #1

## Healthy > AH > CH

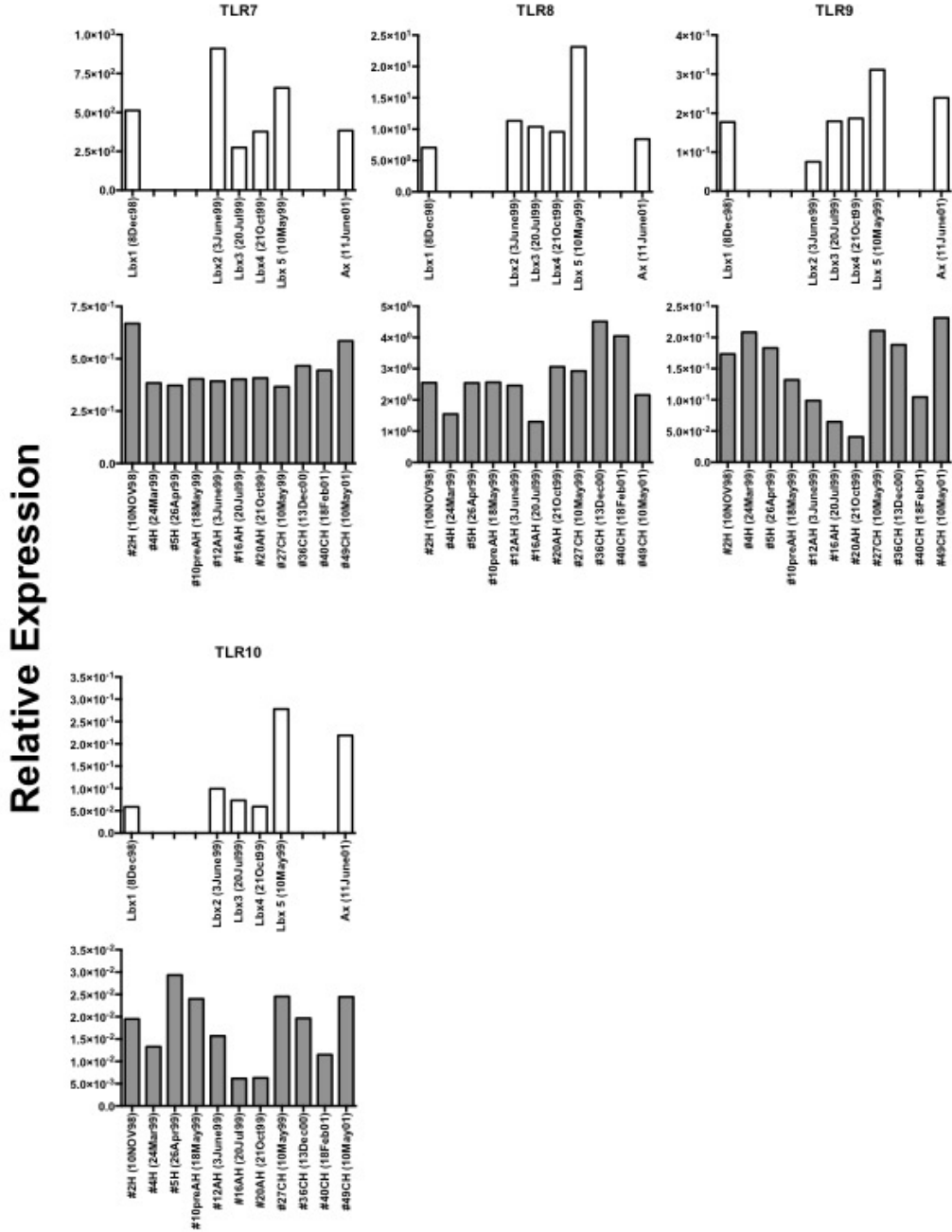
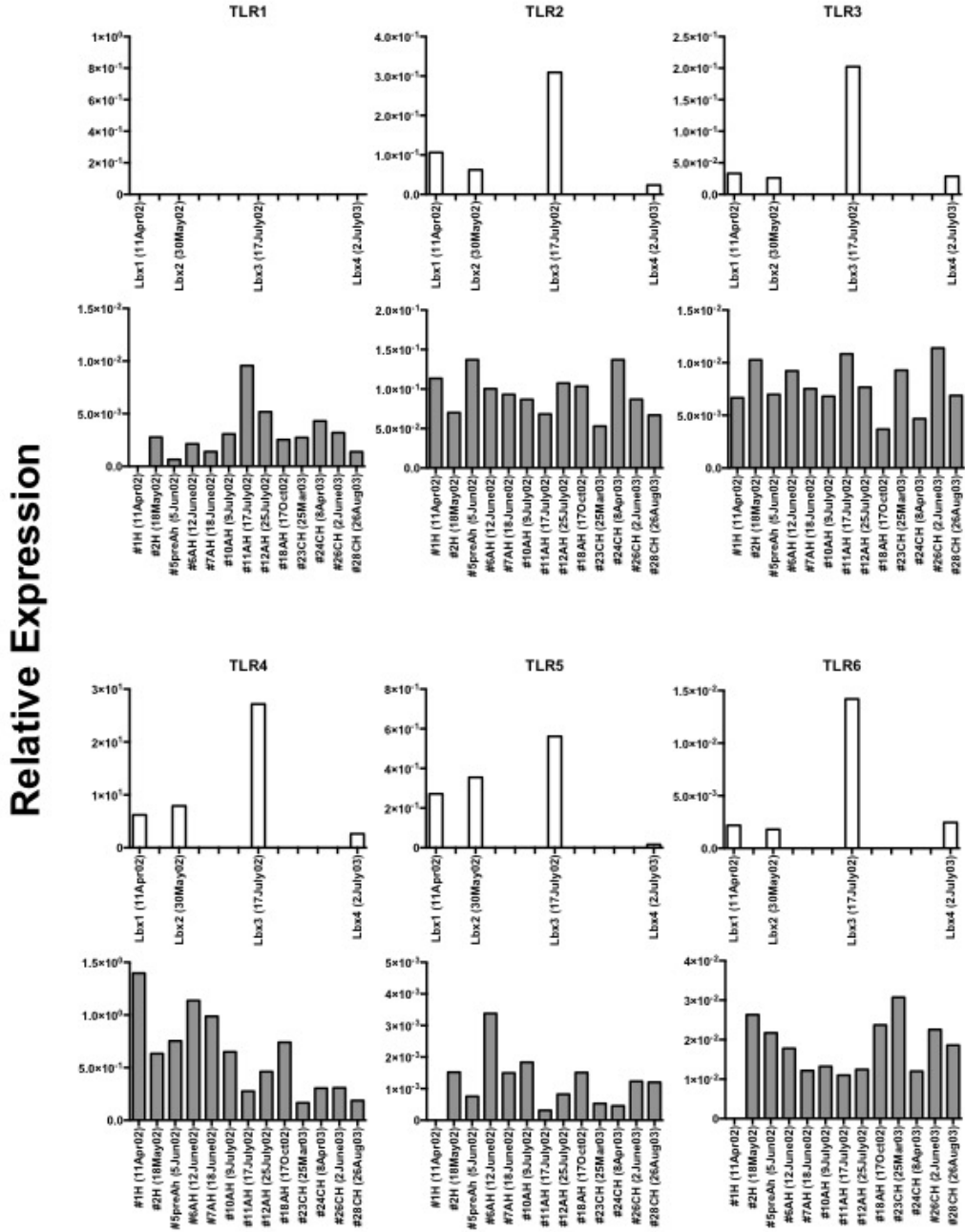


**Figure A2. Expression levels of TLRs1-10 in sequential liver biopsy samples and PBMCs during the course of hepadnaviral infection in woodchuck #2 that progressed from acute hepatitis (AH) to chronic hepatitis (CH).**

Liver biopsy tissue samples (top; white bars) and PBMCs (bottom; grey bars) isolated from woodchuck #2 during the progression of WHV infection (Healthy>PreAH>AH>CH) were analyzed for expression of TLRs1-10. Quantification of TLR mRNA was performed by RT-qPCR. TLR1 expression was evaluated but not detected in the liver. Gene transcription levels were normalized against woodchuck HPRT expression. Total RNA equivalent of 50 ng was tested from each test sample in triplicate.

## Woodchuck #2

### Healthy > PreAH > AH > CH



## Woodchuck #2

### Healthy > PreAH > AH > CH

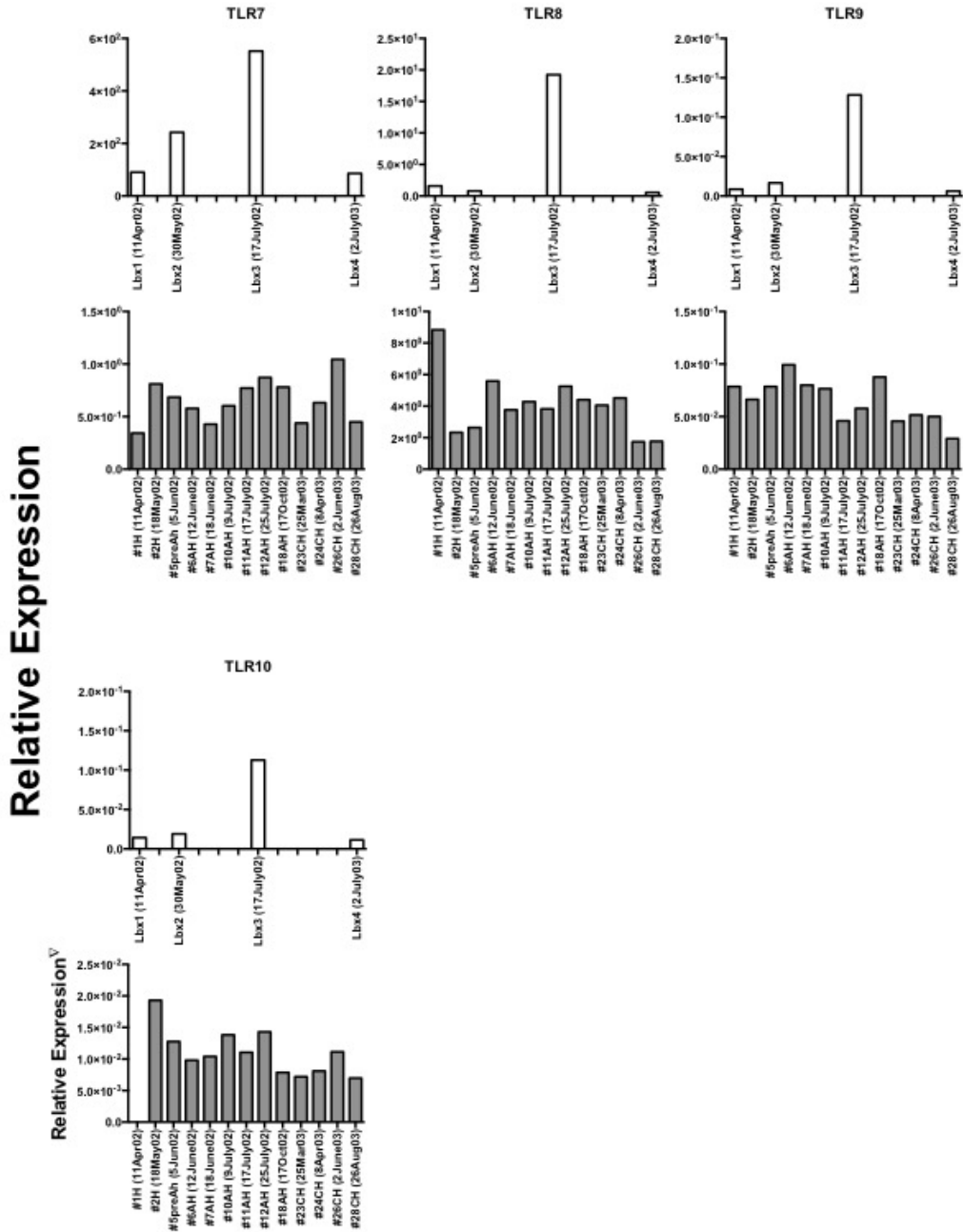


**Table A1. GenBank Accession Numbers of Woodchuck TLR1-10 Partial Gene Sequences Identified in This Study**

	<b>GenBank Accession Number</b>
<b>TLR1</b>	KY468972
<b>TLR2</b>	KY468973
<b>TLR3</b>	KY468974
<b>TLR4</b>	KY468975
<b>TLR5</b>	KY468976
<b>TLR6</b>	KY468977
<b>TLR7</b>	KY468978
<b>TLR8</b>	KY468979
<b>TLR9</b>	KY468980
<b>TLR10</b>	KY468981

**Table A2. Copy Number Values for the Housekeeping Gene HPRT and TLRs1-10 in Woodchuck Livers**

**Investigated in This Study**

	HPRT	TLR1	TLR2	TLR3	TLR4	TLR5	TLR6	TLR7	TLR8	TLR9	TLR10
<b>Healthy (n=25)</b>	41,208	0	964	610	58,341	1,790	38	2,349,408	20,849	86	101
	± 5,779	± 0	± 183	± 88	± 6,769	± 247	± 5	± 327,866	± 3,744	± 9	± 11
<b>PreAH (n=8)</b>	30,945	0	654	581	45,288	2,163	36	2,118,750	21,158	173	171
	± 9,226	± 0	± 165	± 135	± 6,315	± 402	± 10	± 308,004	± 5,580	± 33	± 44
<b>AH (n=8)</b>	18,662	0	913	451	50,250	928	38	1,513,875	17,145	132	124
	± 6,236	± 0	± 280	± 156	± 15,213	± 226	± 12	± 529,613	± 4,531	± 30	± 31
<b>SLAH (n=11)</b>	34,655	0	707	402	50,874	1,323	37	1,423,121	13,159	213	167
	± 9,810	± 0	± 184	± 106	± 13,011	± 377	± 9	± 256,761	± 2,996	± 96	± 31
<b>CH (n=18)</b>	32,896	0	1,140	364	46,082	259	90	1,476,543	26,276	350	264
	± 10,707	± 0	± 205	± 92	± 8,265	± 41	± 36	± 366,389	± 7,063	± 78	± 78
<b>POI (n=17)</b>	36,664	0	688	536	63,243	1,648	41	2,377,510	11,701	143	118
	± 5,783	± 0	± 78	± 67	± 7,035	± 254	± 8	± 371,466	± 2,176	± 44	± 25
<b>Mean</b>	32,505	0	844	491	52,346	1,352	47	1,876,534	18,381	183	158
	± 7923	± 0	± 182	± 107	± 9,435	± 258	± 13	± 360,017	± 4,348	± 49	± 37

**Table A3. Copy Number Values for the Housekeeping Gene HPRT and TLRs1-10 in Woodchuck Hepatocytes Investigated in This Study**

	HPRT	TLR1	TLR2	TLR3	TLR4	TLR5	TLR6	TLR7	TLR8	TLR9	TLR10
<b>Healthy (n=5)</b>	3,159	0	825	67	8,695	132	25	46,367	5,008	56	136
	± 985	± 0	± 528	± 22	± 3,723	± 27	± 16	± 12,071	± 2,296	± 31	± 88
<b>PreAH (n=4)</b>	22,851	0	551	324	16,985	358	22	1,230,983	17,108	508	237
	± 8,856	± 0	± 208	± 14	± 4,274	± 188	± 11	± 551,626	± 1,441	± 189	± 99
<b>SLAH (n=8)</b>	4,910	0	876	96	28,387	691	60	136,722	11,216	89	118
	± 1,919	± 0	± 399	± 35	± 18,881	± 627	± 47	± 85,963	± 5,265	± 34	± 27
<b>CH (n=6)</b>	66,871	0	225	225	48,638	90	34	98,700	21,504	650	43
	± 31,359	± 0	± 114	± 88	± 25,140	± 60	± 14	± 61,332	± 17,060	± 455	± 27
<b>POI (n=3)</b>	15,156	0	1,266	298	27,700	392	58	185,889	22,422	940	323
	± 1,975	± 0	± 838	± 75	± 2,283	± 176	± 20	± 42,563	± 3,948	± 822	± 190
<b>Mean</b>	22,589	0	749	202	26,081	333	40	339,732	15,452	449	172
	± 9,019	± 0	± 418	± 47	± 10,860	± 216	± 22	± 150,711	± 6,002	± 306	± 86

**Table A4. Copy Number Values for the Housekeeping Gene HPRT and TLRs1-10 in Woodchuck PBMCs Investigated in This Study**

	HPRT	TLR1	TLR2	TLR3	TLR4	TLR5	TLR6	TLR7	TLR8	TLR9	TLR10
<b>Healthy (n=11)</b>	93,458	130	7,712	715	41,878	86	1,737	43,231	310,421	9,320	1,118
	± 18,021	± 16	± 1,311	± 194	± 12,554	± 25	± 411	± 7,112	± 79,215	± 3,104	± 337
<b>PreAH (n=8)</b>	101,292	144	8,433	1,098	32,588	98	2,075	48,967	317,958	6,628	1,009
	± 13,708	± 56	± 1,466	± 261	± 7,746	± 22	± 418	± 6,715	± 40,233	± 1,743	± 266
<b>AH (n=18)</b>	80,694	175	6,183	595	34,366	78	1,389	42,188	282,926	4,736	646
	± 10,430	± 25	± 1,013	± 86	± 8,223	± 21	± 227	± 5,470	± 35,104	± 798	± 114
<b>SLAH (n=6)</b>	131,839	181	7,863	1,014	31,839	109	2,400	72,656	288,000	6,650	1,638
	± 11,610	± 47	± 620	± 152	± 5,794	± 22	± 423	± 7,371	± 52,478	± 1,580	± 614
<b>CH (n=8)</b>	96,900	238	10,157	833	34,822	72	3,009	51,777	294,925	13,473	1,601
	± 18,048	± 58	± 2,274	± 204	± 8,844	± 15	± 779	± 10,580	± 72,845	± 4,507	± 464
<b>Mean</b>	100,837	174	8,069	851	35,098	88	2,122	51,764	298,846	8,161	1,203
	± 14,363	± 40	± 1,337	± 179	± 8,632	± 21	± 452	± 7,450	± 55,975	± 2,347	± 359